

Copyright

By

Kristen Shawn Donnelly

2009

**Influence of Precast Concrete Panel Surface Condition on Behavior of
Composite Bridge Decks at Skewed Expansion Joints**

By

Kristen Shawn Donnelly, B.S.Arch.E.

Thesis

Presented to the Faculty of the Graduate School of

The University of Texas at Austin

In Partial Fulfillment

Of the Requirements

For the Degree of


Master of Science in Engineering

The University of Texas at Austin

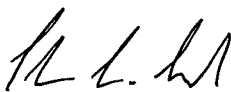
May 2009

**Influence of Precast Concrete Panel Surface Condition on Behavior of
Composite Bridge Decks at Skewed Expansion Joints**

**Approved by
Supervising Committee:**



James O. Jirsa, Supervisor



Sharon L. Wood

Dedication

To my family and friends for their encouragement and love

Acknowledgments

First and foremost, my great appreciation must be expressed to the University of Texas at Austin, the Texas Department of Transportation, and the Center for Transportation Research for providing funding for my graduate studies and allowing me the invaluable opportunity of having a graduate research experience.

For their patience, guidance, and vast knowledge of structural behavior and construction, Dr. James Jirsa, Dr. Sharon Wood, and Dr. Oguzhan Bayrak should receive particular acknowledgement. They certainly have my utmost respect and gratitude for their exemplary dedication to teaching and research.

I would also like to give special recognition to the Ferguson Structural Engineering Laboratory technicians, Dennis Phillip, Blake Stasney, and Andrew Valentine, for their extensive construction knowledge and assistance during specimen fabrication and testing. Bryan Bindrich, a fellow graduate structures student, also deserves recognition for helping me with construction and testing and keeping me entertained on the lab floor.

Finally, I must express my appreciation to my family and friends for motivating me and providing me with endless support.

May 4, 2009

Abstract

Influence of Precast Concrete Panel Surface Condition on Behavior of Composite Bridge Decks at Skewed Expansion Joints

Kristen Shawn Donnelly, M.S.E.

The University of Texas at Austin, 2009

Supervisor: James O. Jirsa

Following development of rectangular prestressed, precast concrete panels (PCP) that could be used as stay-in-place formwork adjacent to expansion joints in bridge decks, the Texas Department of Transportation (TxDOT) initiated a research effort to investigate the use of PCP units at skewed expansion joints. The fabrication of trapezoidal PCP units was studied and the response of skewed panels with 45° and 30° skew angles was obtained. The panels were topped with a 4 in. thick cast-in-place (CIP) slab to complete the bridge deck. Specimens with 45° skew performed well under service and overload levels. The deck failed in diagonal shear at loads well over the design level loads. However, two 30° specimens failed prematurely by delamination between the topping slab and the PCP. The cause of the delamination was insufficient shear transfer

capacity between the PCP and CIP topping slab. For the specimens tested at a square end, the failure mode was punching shear at high loads for all specimens. The surface condition of the PCP was specified to have a “broom finish” and the panel was to have a saturated surface dry (SSD) condition so that PCP units would not leach moisture from the CIP topping slab. Neither of these conditions was satisfied in the two panels that failed prematurely. Although the panels were specified to have a broom finish, the panel surface had regions that were quite smooth.

The objective of this research project was to reinvestigate the response of 30° PCP at an expansion joint following specified procedures for finish and moisture conditions. One specimen was constructed with a rectangular panel placed between two 30° skewed panels. These panels had a much rougher surface texture than the previously tested panels that failed in delamination. The skewed ends of the specimen were subjected to monotonically increasing static loads at midspan of the panel ends. The panels failed in diagonal shear and the response of the tested specimen confirmed that the panel surface roughness, and not the skew angle, caused delamination with the previously tested specimens. While TxDOT does not currently specify a minimum panel surface roughness, a surface roughness of approximately ¼ in. is required in some codes for developing composite action. In addition, wetting the panels to a SSD condition prior to placement of the topping slab further enhances shear transfer between the topping slab and the PCP.

Table of Contents

Chapter 1: Introduction.....	1
1.1 Introduction.....	1
1.2 Background.....	1
1.3 Scope.....	7
Chapter 2: Literature Review.....	8
2.1 Introduction.....	8
2.2 Prestressed Concrete Panels in Perpendicular Bridges.....	8
2.2.1 TxDOT Project 0-4418	8
2.2.1.1 Coselli (2004).....	10
2.2.2 TxDOT Project 0-5367	12
2.2.2.1 Agnew (2007).....	12
2.2.3 Dowell and Smith (2006).....	15
2.2.4 Merrill (2002).....	16
2.2.5 Abendroth (1994).....	17
2.2.6 Barker (1975).....	17
2.3 Prestressed Concrete Panels in Skewed Bridges	18
2.3.1 TxDOT Project 0-5367	18
2.3.1.1 Boswell (2008) and Kreisa (2008)	18
2.3.2 Merrill (2002).....	21
2.3.3 Abendroth (1994).....	21
2.3.4 Barker (1975).....	22
2.4 Research Significance.....	22
Chapter 3: Test Specimen.....	24
3.1 Introduction.....	24
3.2 Design Considerations	26
3.3 Material Properties.....	28

3.3.1	Concrete	28
3.3.2	Steel.....	29
3.3.3	Bedding Strip Material.....	29
3.4	Specimen Construction	31
3.4.1	Support Beams	34
3.4.2	Precast Panels Used in Test Specimen.....	35
3.4.2.1	30° Panels.....	36
3.4.2.2	Rectangular Panel.....	39
3.4.3	Cast-in-Place Topping Slab	41
Chapter 4:	Loading and Instrumentation	44
4.1	Introduction.....	44
4.2	Specimen Loading	45
4.2.1	Loading Setup	45
4.2.2	Load Application	47
4.3	Instrumentation	49
4.3.1	Strain Gages	50
4.3.2	Linear Potentiometers	51
4.3.3	Data Collection	52
Chapter 5:	Measured Response of Test Specimen.....	53
5.1	Introduction.....	53
5.2	Load Tests.....	53
5.3	Measured Response of Specimen P30P3.....	57
5.3.1	Load Applied at Midspan of Skewed End of Panel A.....	58
5.3.2	Load Applied at Midspan of Skewed End of Panel B	67
5.3.3	Load Applied at Midspan of Square End of Panel A.....	76
5.4	Summary	81
Chapter 6:	Discussion of Results	83
6.1	Introduction.....	83

6.2	Summary	83
6.2.1	Load Applied at Midspan of Skewed Ends.....	84
6.2.2	Loads Applied at Midspan of Square End	87
6.3	Recommendations.....	88
Chapter 7: Conclusions and Recommendations		90
7.1	Summary	90
7.2	Conclusions.....	91
Appendix A: Complete Set of Test Data		95
A.1	Panel A.....	95
A.1.1	Load Applied at Midspan of Skewed End	95
A.1.2	Load Applied at Midspan of Square End.....	99
A.2	Panel B	100
Appendix B: Summary of Specimens Tested in TxDOT Project 0-5367.....		105
B.1	Description of Specimens Tested by Boswell (2008) and Kreisa (2008).....	105
B.1.1	Material Properties.....	106
B.1.1.1	Concrete.....	107
B.1.1.2	Bedding Strip Material	107
B.1.2	Specimen Construction	108
B.1.2.1	Precast Panel Conditions Prior to Topping Slab Placement... 108	
B.2	Loading Information for Specimens Tested by Boswell (2008) and Kreisa (2008).....	109
B.3	Measured Response of Specimens Tested by Boswell (2008) and Kreisa (2008).....	112
B.4	Comparison of All Specimens Tested in TxDOT Project 0-5367	114
B.4.1	Load Applied at Midspan of End Adjacent to SEJ	114
B.4.2	Load Applied at Midspan of Square End of Skewed Specimens	117

References.....	119
Vita.....	121

List of Figures

Figure 1.1 – Typical Bridge Construction Prior to Placing Bridge Deck (Agnew 2007)...	2
Figure 1.2 – Typical Bridge Construction during Placement of Precast Panels (Agnew 2007).....	3
Figure 1.3 – Panels and Topping Slab Reinforcement Prior to Casting Topping Slab (Agnew 2007)	3
Figure 1.4 – Comparison of Traditional IBTS Detail at Expansion Joint and Precast Panel System (PCP) at Expansion Joint (Agnew 2007)	4
Figure 1.5 – Temporary Formwork Erected for IBTS Detail (Agnew 2007).....	5
Figure 1.6 – Complex Geometry and Hazardous Work Environment at a Skewed Expansion Joint under Construction (Agnew 2007).....	5
Figure 1.7 – Trapezoidal Gap Adjacent to Skewed Expansion Joint (Agnew 2007)	7
Figure 2.1 – Plan View of First Specimen of TxDOT Project 0-4418 (Ryan 2003)	9
Figure 2.2 – Cross-Sections of the IBTS and UTSE Details of the First Specimen of TxDOT Project 0-4418 (Ryan 2003)	9
Figure 2.3 – Cross-Section of Precast Panel System (PCP) Detail (Coselli 2004).....	10
Figure 2.4 – Plan View of 0° Skew PCP System Specimen (Coselli 2004).....	11
Figure 2.5 – Elevation View of Positive Moment Specimen Subject to Fatigue Loading (Agnew 2007)	13
Figure 2.6 – Plan View of Positive Moment Specimen Subject to Fatigue Loading (Agnew 2007)	13
Figure 2.7 – Elevation View of Negative Moment Specimens Subjected to Fatigue Loading (Agnew 2007).....	14
Figure 2.8 – Plan View of Negative Moment Specimens Subjected to Fatigue Loading (Agnew 2007)	14
Figure 2.9 – Side View of Overall Setup for Bridge Decks Tested in Simple Bending (Dowell and Smith 2006).....	16

Figure 2.10 – Cross-Section of Precast Panel with Strands Parallel to Skewed End (Kreisa 2008)	19
Figure 2.11 – Selected Design Alternatives for Strand Layout in 45° Panels (Kreisa 2008)	19
Figure 2.12 – Trapezoidal Panels for Composite Bridge Deck Systems (Abendroth 1994)	22
Figure 3.1 – HL-93 Design Truck Loads on Bridge Deck (Boswell 2008).....	27
Figure 3.2 – Panel on Bedding Strip (Boswell 2008)	29
Figure 3.3 – TxDOT Bedding Strip Dimensions (TxDOT 2008).....	30
Figure 3.4 – Construction Sequence for Specimen P30P3	33
Figure 3.5 – Configuration of Support Beams, Elastomeric Bearing Pads, and Concrete Blocks for Specimen P30P3.....	34
Figure 3.6 – Alignment of U-bars for Specimen P30P3	35
Figure 3.7 – Definitions of Boundaries for Specimen P30P3.....	36
Figure 3.8 – Skewed Panel Reinforcement for Specimen P30P3	37
Figure 3.9 – Fabrication Process for 30° Panels (Kreisa 2008).....	38
Figure 3.10 – Designed and Actual Alignment of Rectangular and Skewed Panels for Specimen P30P3	39
Figure 3.11 – Backer Rod between Adjacent Panels for Specimen P30P3	40
Figure 3.12 – Concrete Flow-Through on Bottom Surface of Specimen P30P3	40
Figure 3.13 – Cast-in-Place Topping Reinforcement for Specimen P30P3	41
Figure 3.14 – Formwork for Topping Slab in Position.....	41
Figure 3.15 – SEJ Attached to Topping Slab Formwork.....	42
Figure 4.1 – Load Frame for Static Loading of Specimen P30P3	46
Figure 4.2 – Hydraulic Ram, Load Cell, and Load Plate for Specimen P30P3.....	47
Figure 4.3 – Location of Load Plates and Order of Loading for Specimen P30P3	48
Figure 4.4 – Load Plate Position over Square End of Skewed Precast Panel (Boswell 2008)	49

Figure 4.5 – Concrete Strain Gage Locations and Labels for Specimen P30P3.....	51
Figure 4.6 – SEJ Strain Gage Locations and Labels for Specimen P30P3.....	51
Figure 4.7 – Linear Potentiometer Locations and Labels for Specimen P30P3 for Load Applied at Midspan of Skewed Ends.....	52
Figure 4.8 – Linear Potentiometer Locations and Labels for Specimen P30P3 for Load Applied at Midspan of Square End of Panel A.....	52
Figure 4.9 – Data Collection System	56
Figure 5.1 – Rigid Body Movement of Loaded End of Specimen P30P3 (modified from Boswell 2008)	54
Figure 5.2 – Presentation of Strain Gage Data (Boswell 2008).....	57
Figure 5.3 – Measured Displacement Response of Panel A for Load Applied at Midspan of Skewed End	58
Figure 5.4 – Variation of Displacement along Skewed End of Panel A.....	59
Figure 5.5 – Change in Tensile Strain on Bottom of Panel A at Midspan of Skewed End	60
Figure 5.6 – Distribution of Change in Concrete Strain on Bottom of Panel A along Skewed End	61
Figure 5.7 – Compressive Strain at Midspan of SEJ in Panel A	62
Figure 5.8 – Variation of Strain along SEJ of Panel A.....	63
Figure 5.9 – Observed Cracks Conclusion of Static Test of Panel A for Load Applied at Midspan of Skewed End.....	65
Figure 5.10 – Photograph of Skewed End of Panel A at Conclusion of Static Test for Load Applied at Midspan of Skewed End	66
Figure 5.11 – Photograph of Skewed End of Panel A at Conclusion of Static Test for Load Applied at Midspan of Skewed End	66
Figure 5.12 – Measured Displacement Response of Panel B for Load Applied at Midspan of Skewed End	67
Figure 5.13 – Variation of Displacement along Skewed End of Panel B.....	68

Figure 5.14 – Change in Tensile Strain on Bottom of Panel B at Midspan of Skewed End	69
Figure 5.15 – Distribution of Change in Concrete Strain on Bottom of Panel B along Skewed End	70
Figure 5.16 – Compressive Strain at Midspan of SEJ in Panel B.....	71
Figure 5.17 – Variation of Strain along SEJ of Panel B	72
Figure 5.18 – Observed Cracks at Conclusion of Static Test of Panel B for Load Applied at Midspan of Skewed End	74
Figure 5.19 – Photograph of Panel B at Conclusion of Static Test for Load Applied at Midspan of Skewed End	75
Figure 5.20 – Photograph of Panel B at Conclusion of Static Test for Load Applied at Midspan of Skewed End	75
Figure 5.21 - Measured Displacement Response at Midspan of Square End of Panel A	77
Figure 5.22 – Observed Cracks at Conclusion of Static Test of Panel A for Load Applied at Midspan of Square End.....	78
Figure 5.23 – Photograph of Punching Shear Failure under Load Applied at Midspan of Square End of Panel A.....	79
Figure 5.24 – Photograph of Spalled Concrete at Conclusion of Test of Panel A for Load Applied at Midspan of Square End.....	80
Figure 6.1 – Measured Displacement Response for Load Applied at Midspan of Skewed Ends of Specimen P30P3	85
Figure 6.2 – Measured Displacement Responses of Specimen P30P3 Compared to Previously Tested 30° Specimens (Boswell 2008, Kreisa 2008).....	86
Figure 6.3 – Measured Compressive Strains in Specimen P30P3 at Midspan of SEJ Compared to Previously Tested 30° Specimens (Boswell 2008, Kreisa 2008).....	86
Figure 6.4 – Measured Displacement Response of Panel A for Load Applied at Midspan of Square End.....	88

Figure 7.1 – Recommended 30° Skew Panel Ordinary Reinforcing Layout and Detail (modified from TxDOT Report No. FHWA/TX-09/0-5367-1: Recommendations for the Use of Precast Deck Panels at Expansion Joints, 2008)	94
Figure A.1 – Measured Relative Displacements along Skewed End of Panel A	95
Figure A.2 – Measured Support Displacements of Panel A Loaded at Midspan of Skewed End	96
Figure A.3 – Measured Change in Tensile Strains on Bottom of Panel A for Load Applied at Midspan of Skewed End	97
Figure A.4 – Measured Compressive Strains in SEJ of Panel A for Load Applied at Midspan of Skewed End	98
Figure A.5 – Measured Relative Displacements of Panel A for Load Applied at Midspan of Square End.....	99
Figure A.6 – Measured Support Displacements of Panel A for Load Applied at Midspan of Square End.....	100
Figure A.7 – Measured Relative Displacements of Panel B for Load Applied at Midspan of Skewed End	101
Figure A.8 – Measured Support Displacements of Panel B for Load Applied at Midspan of Skewed End	102
Figure A.9 – Measured Change in Tensile Strains on Bottom of Panel B for Load Applied at Midspan of Skewed End	103
Figure A.10 – Measured Compressive Strains in SEJ of Panel B for Load Applied at Midspan of Skewed End	104
Figure B.1 – Location of Load Plates and Order of Loading for Specimens Tested by Boswell (2008) and Kreisa (2008).....	111
Figure B.2 – Measured Displacement Responses of Specimen P30P3 Compared to Previously Tested 0° (Agnew 2007) and 30° Specimens (Boswell 2008, Kreisa 2008).....	114

Figure B.3 – Measured Compressive Strains in Specimen P30P3 at Midspan of SEJ Compared to Previously Tested 0° (Agnew 2007) and 30° Specimens (Boswell 2008, Kreisa 2008).....	115
Figure B.4 – Measured Displacement Responses of Specimen P30P3 Compared to Previously Tested 45° and 30° Specimens (Boswell 2008, Kreisa 2008)	116
Figure B.5 – Measured Compressive Strains in Specimen P30P3 at Midspan of SEJ Compared to Previously Tested 45° Specimens (Boswell 2008, Kreisa 2008).....	116
Figure B.6 – Measured Displacement Response of Panel A for Load Applied at Midspan of Square End.....	117
Figure B.7 – Measured Displacement Responses of All Skewed Specimens Loaded at Midspan of Square End.....	118

List of Tables

Table 3.1 – Characteristics of Skewed Test Specimen	25
Table 3.2 – Support Beam and Topping Slab Concrete Mixture Design (Boswell 2008)	28
Table 3.3 – Timeline of Construction and Testing	43
Table 4.1 – Applied Loads to Test Specimen	45
Table 4.2 – Instrumentation Quantities for Specimen P30P3.....	50
Table 5.1 –Loads Corresponding to HL-93 Design Truck (Boswell 2008)	56
Table 5.2 - Initial Stiffness and Apparent Cracking Load of Panel A for Load Applied at Midspan of Skewed End	64
Table 5.3 – Initial Stiffness and Apparent Cracking Load of Panel B for Load Applied at Midspan of Skewed End	73
Table 5.4 - Summary of Response of Specimen P30P3	82
Table B.1 – Characteristics of Skewed Specimens Tested by Boswell (2008) and Kreisa (2008).....	106
Table B.2 – Concrete Cylinder Strengths for Topping Slabs at 21-days (Boswell 2008, Kreisa 2008).....	107
Table B.3 – Average Overall Slab Depth at Midspan of Skewed End (Boswell 2008, Kreisa 2008).....	108
Table B.4 – Panel Surface Roughness and Wetness before Topping Slab Placement (Boswell 2008, Kreisa 2008)	109
Table B.5 – Timeline of Specimen Construction and Testing (Boswell 2008, Kreisa 2008)	109
Table B.6 – Applied Loads to Specimens Tested by Boswell (2008) and Kreisa (2008)	110
Table B.7 – Summary of Response of Specimens Tested by Boswell (2008) and Kreisa (2008).....	113

Chapter 1: Introduction

1.1 INTRODUCTION

The introduction of precast concrete panels as stay-in-place formwork has improved the efficiency, quality, and economy of bridge construction in Texas. Fabricating prestressed bridge deck panels at a precast plant allows for better concrete quality control, as well as increased construction speed on site. In addition, utilizing the panels as stay-in-place formwork eliminates much of the cost associated with bridge deck formwork. Currently, the Texas Department of Transportation (TxDOT) does not allow the use of precast panels at expansion joints, where the panels would have an unsupported free end. Furthermore, where bridges have skewed expansion joints, the standard rectangular precast panels leave an unresolved geometry. At these locations, TxDOT has traditionally used a thickened cast-in-place slab that requires additional formwork and material. For these reasons, several research projects have been conducted using rectangular and skewed precast panels at expansion joints to determine if an entirely precast panel system would perform as well as the conventional system with the thickened slab detail. This chapter presents background information essential to understand the purpose of this investigation in Section 1.2, followed by the scope of this research in Section 1.3.

1.2 BACKGROUND

TxDOT began using precast concrete panels (PCPs) in bridge deck construction in 1983. Since then, the large majority of bridges built in Texas have used precast panels as stay-in-place formwork, resulting in faster construction, better economy, and an overall safer work environment on site. While the bridge girders are being placed to span between bridge supports (Figure 1.1), the panels are fabricated at a precast yard, then transported to the construction site and lifted into place, spanning from girder to girder along each span of the bridge (Figure 1.2). Because half of the 8 in. deep bridge deck is

comprised of 4 in. thick precast panels, the amount of deck reinforcement that must be tied on site, as well as the volume of cast-in-place concrete needed for the deck, is roughly cut in half (Figure 1.3). Once the 4 in. thick cast-in-place slab has been placed, the result is an 8 in. deep composite bridge deck.

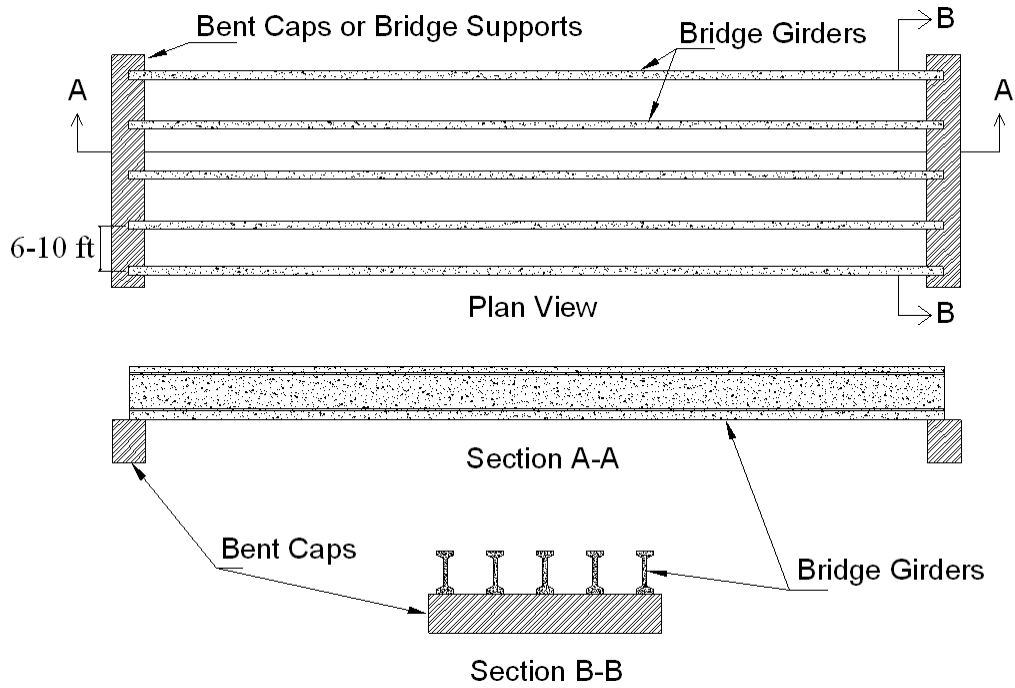


Figure 1.1: Typical Bridge Construction Prior to Placing Bridge Deck (Agnew 2007)

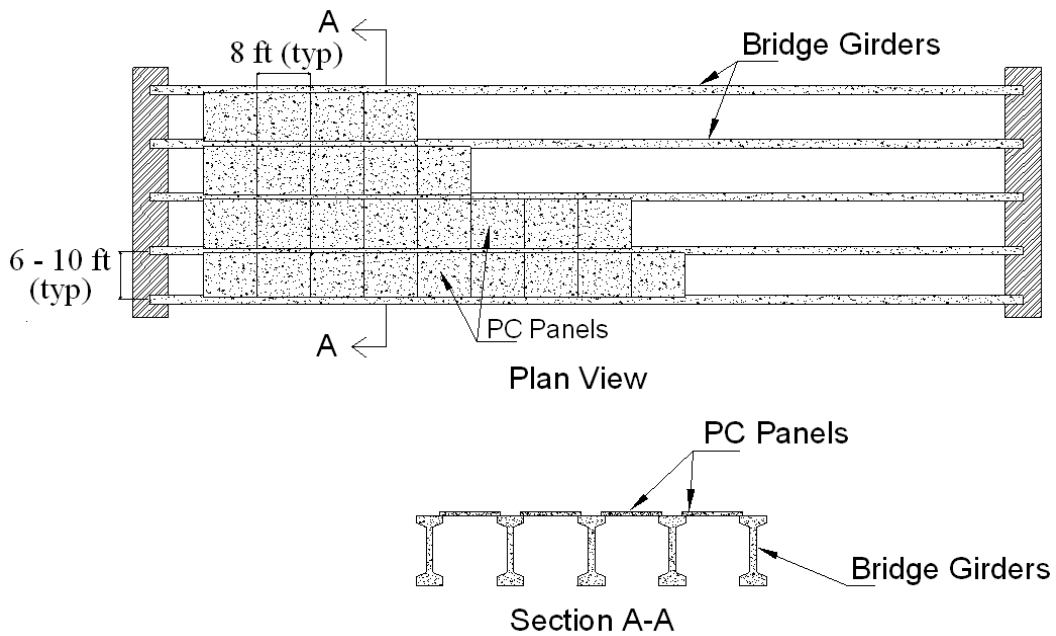


Figure 1.2: Typical Bridge Construction during Placement of Precast Panels
(Agnew 2007)



Figure 1.3: Panels and Topping Slab Reinforcement Prior to Casting Topping Slab
(Agnew 2007)

Expansion joints are placed along the bridge to allow for thermal expansion and contraction of the structure as the ambient temperature fluctuates. Traditionally, TxDOT has required the precast panel forming to terminate 4 ft. from the expansion joint, where formwork is erected to create a 10 in. deep, cast-in-place thickened slab, known as an I-Beam Thickened Slab (IBTS) detail. Adjacent to the expansion joint, the IBTS section was designed to be thicker than the composite panel section to ensure adequate stiffness at the unsupported end of the deck (Figure 1.4). The formwork for the IBTS detail is constructed on site, prior to the placement of the topping slab, when there are voids where no panels are present, high above the ground (Figure 1.5). For this reason, safety wires must be used to keep construction workers from falling through the voids (Figure 1.6). Formwork construction is further complicated at IBTS sections where the expansion joint is skewed (Figure 1.6), resulting in a potentially unsafe work environment and increased cost and time due to complicated formwork geometries.

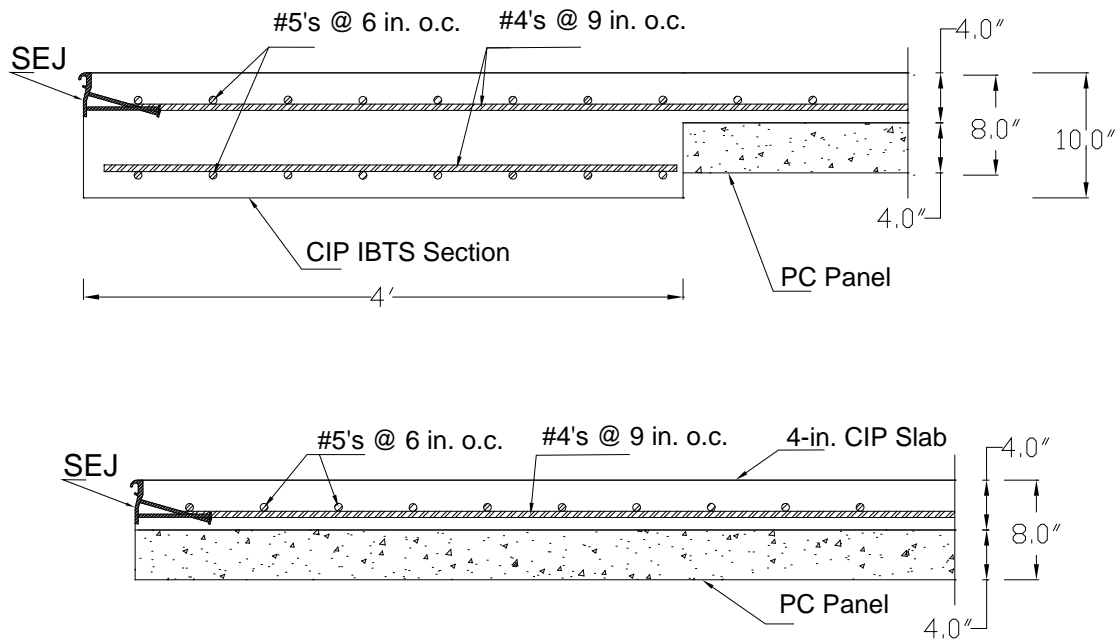


Figure 1.4: Comparison of Traditional IBTS Detail at Expansion Joint (top) and Precast Panel System (PCP) at Expansion Joint (bottom) (Agnew 2007)

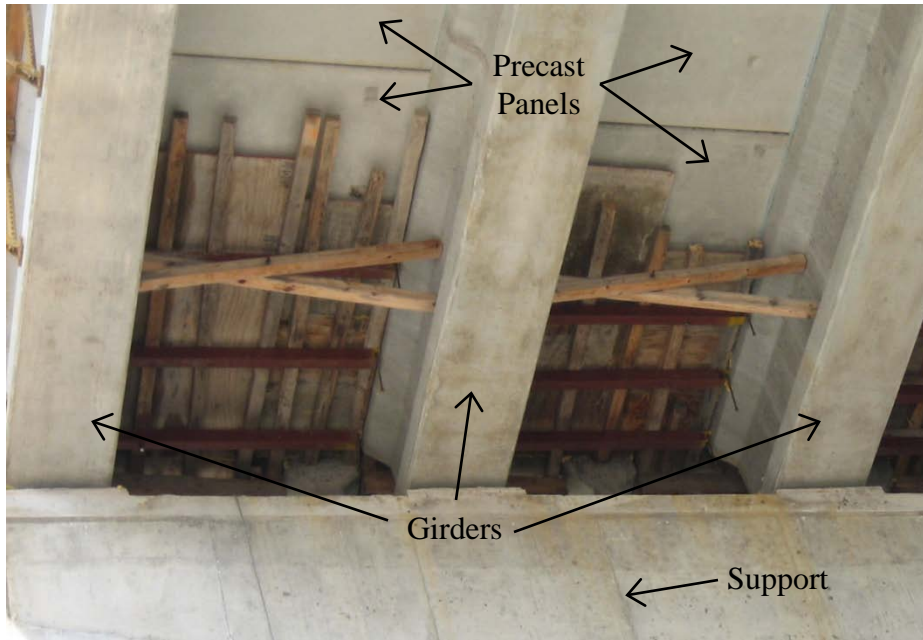


Figure 1.5: Temporary Formwork Erected for IBTS Detail (Agnew 2007)



Figure 1.6: Complex Geometry and Hazardous Work Environment at a Skewed Expansion Joint under Construction (Agnew 2007)

In an effort to resolve the expense, timing, and safety issues associated with the IBTS detail, TxDOT sponsored two research projects to be conducted at the University of Texas at Austin. In TxDOT project 0-4418, the performance of the traditional IBTS detail was compared to the performance of a system in which precast panels were continued all the way to the expansion joint, resulting in a uniform 8 in. deep composite section. The project was conducted at the Ferguson Structural Engineering Laboratory (FSEL), where a full-scale bridge deck specimen with a 0° skew angle at the expansion joints was constructed. The specimens were constructed to have the conventional IBTS detail at one end and the proposed PCP detail at the other end of the span. The results of testing indicated that the entirely precast panel system provided adequate strength and stiffness with reduced construction costs and timing, as well as improved worker safety, when compared to the traditional IBTS detail (Figure 1.4).

The findings and recommendations of Project 0-4418 initiated a second series of investigations, TxDOT Project 0-5367, which was completed in three phases. In the first phase, the fatigue response of the PCP detail in bridges with 0° skew at the expansion joint was evaluated. Because precast panels are typically rectangular, bridge decks with skewed expansion joints leave an unresolved geometry in which a trapezoidal gap is left in the bridge deck, adjacent to the expansion joint (Figure 1.7). To utilize the precast panels at skewed expansion joints, the second phase of this project was initiated to evaluate the use of trapezoidal precast panels at expansion joints in bridge decks with 45° and 30° skew angles. Issues arising from the testing of the 30° precast panels led to the third phase of the project, and the basis of this thesis, in which further testing of 30° panels at expansion joints was conducted. A more in-depth discussion of both projects is discussed in Chapter 2 of this thesis.

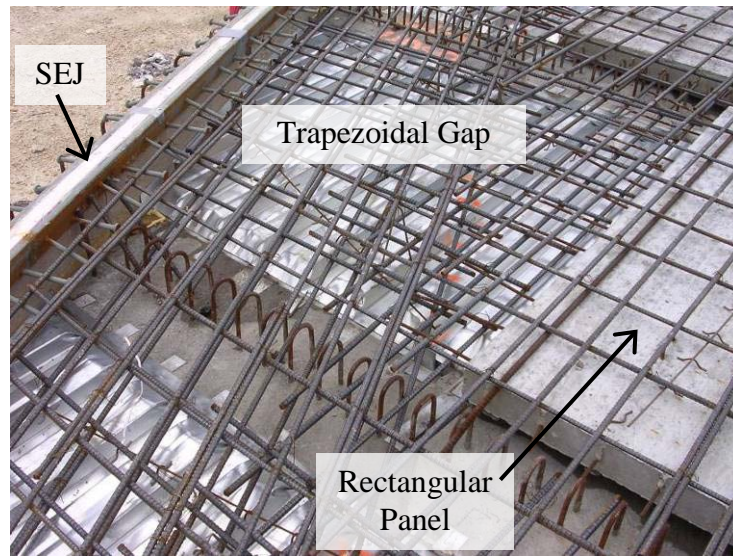


Figure 1.7 – Trapezoidal Gap Adjacent to Skewed Expansion Joint (Agnew 2007)

1.3 SCOPE

The focus of this phase of the investigation was to ensure that adequate strength and stiffness can be achieved with 30° precast panels adjacent to skewed expansion joints. In this thesis, the response of the 30° PCP detail in bridge decks under a point load at midspan was studied. Midspan loading has been shown to be the critical load condition from analyses of bridge deck pattern loading and from the earlier tests of full-scale bridge decks. Issues critical to composite performance of the PCP decks, such as panel surface roughness and moisture content prior to placement of the topping slab, are also discussed in this thesis.

One specimen was constructed according to TxDOT specifications, using sealed expansion joints (SEJs) and full-scale precast panels with 30° skew angles. Each specimen was subject to static loading at midspan until failure was achieved. The results of each test, as well as recommendations for the use of precast panels in bridge deck construction, are presented in this thesis.

Chapter 2: Literature Review

2.1 INTRODUCTION

Simple and inexpensive to produce, prestressed concrete panels are plant-cast, rather than cast on site, resulting in a more durable product, since admixtures and lower water-cementitious materials ratios can be used under controlled conditions. In addition, the use of precast panels in bridge deck construction eliminates much of the formwork necessary adjacent to expansion joints, saving time and material cost on site and improving worker safety. For these reasons, the use of prestressed concrete panels in bridge deck construction continues to grow in the state of Texas. This chapter discusses previous research related to precast concrete panel use in bridge decks. Concentrating on precast panel systems in which a structural cast-in-place topping slab is included, the discussion begins with rectangular panels, with an emphasis on panel surface roughness and moisture content prior to topping slab placement, followed by panels with skewed ends, and finally the significance of previous research.

2.2 PRESTRESSED CONCRETE PANELS IN PERPENDICULAR BRIDGES

In this section, the findings of six studies in which rectangular precast concrete panels were used are summarized. The Texas Department of Transportation (TxDOT) sponsored two of these investigations at the University of Texas. One study was a report on construction practices for precast panel decks and the remaining three studies were conducted outside of Texas.

2.2.1 TxDOT Project 0-4418

In an effort to reduce forming costs and improve the speed and safety of bridge construction, TxDOT sponsored Project 0-4418, in which the performance of a proposed Uniform Thickness Slab End (UTSE) was compared to that of the traditional I-Beam Thickened Slab (IBTS) detail at expansion joints in bridge decks (Figures 2.1 and 2.2). After the results of testing indicated that the UTSE detail provided sufficient strength and

stiffness when compared to the IBTS detail, another phase of the project was initiated to investigate the use of a fully precast panel (PCP) system. The PCP system proposed the use of precast panels as stay-in-place formwork all the way to the expansion joint, which would further optimize the bridge deck construction process. The final phase of Project 0-4418 pertains to bridge decks with PCP expansion joint detail that have 0° skew.

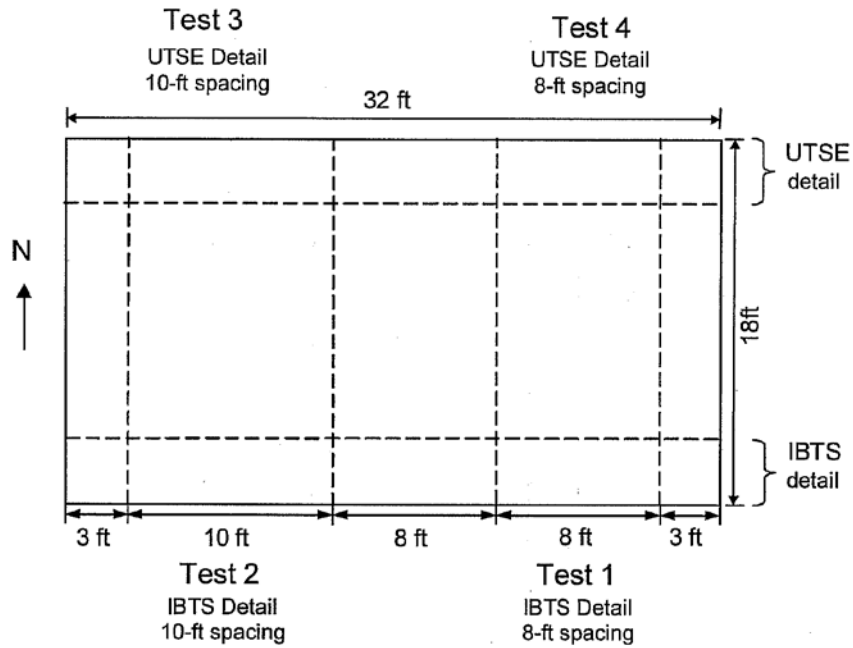


Figure 2.1: Plan View of First Specimen of TxDOT Project 0-4418 (Ryan 2003)

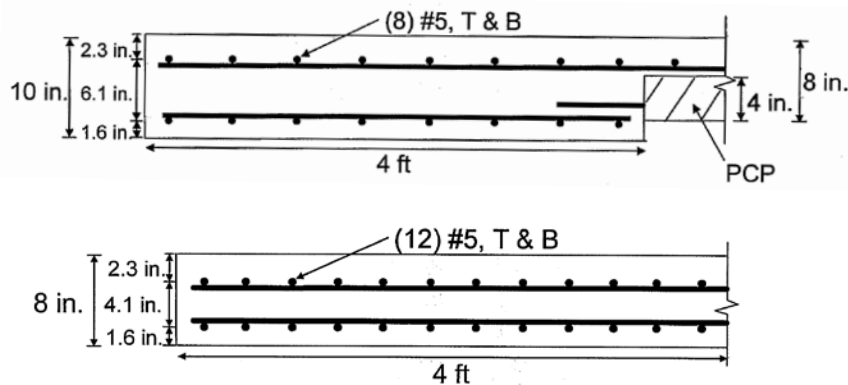


Figure 2.2: Cross-Sections of the IBTS (top) and UTSE (bottom) Details of the First Specimen of TxDOT Project 0-4418 (Ryan 2003)

2.2.1.1 Coselli (2004)

To evaluate the constructability and behavior of the proposed PCP detail, a full-scale bridge deck was constructed with a 0° skew at each end. In place of the traditional IBTS detail, each end of the specimen was built to utilize the cost-saving alternative design of the proposed PCP system detail (Figure 2.3) by continuing the precast concrete panels (PCPs) with cast-in-place (CIP) topping slab all the way to the ends of the specimen. Consisting of one 10 ft. wide bay and two 8 ft. wide bays, the test specimen was a 32 ft. by 18 ft. composite bridge deck with a total of six test locations (Figure 2.4).

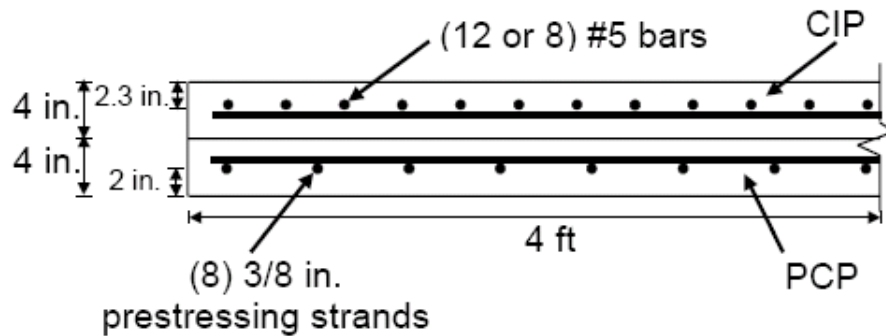


Figure 2.3: Cross-Section of Precast Panel System (PCP) Detail (Coselli 2004)

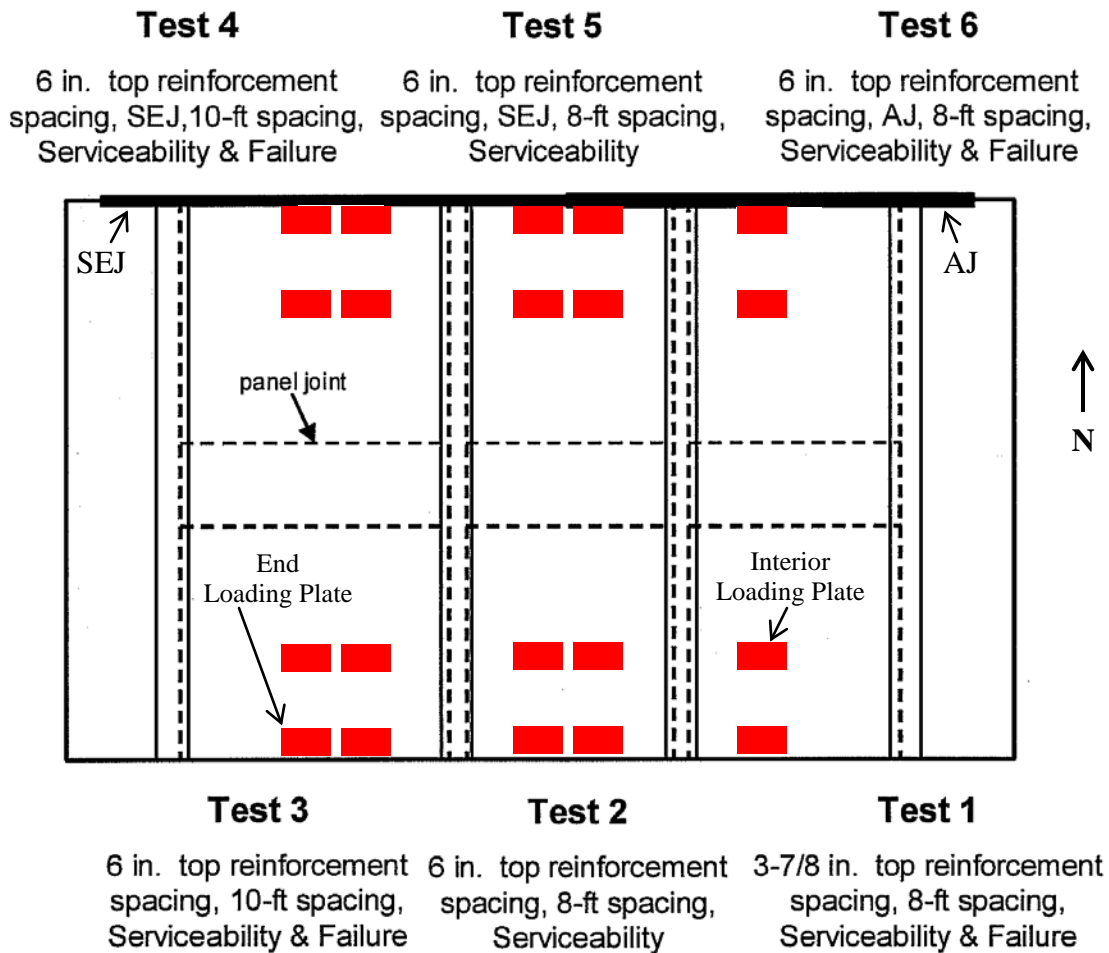


Figure 2.4: Plan View of 0° Skew PCP System Specimen (Coselli 2004)

Coselli investigated the influence of the presence and type of expansion joint armor on the composite member’s performance. The eastern half of the middle bay and the entire eastern bay of the specimen used an armor joint (AJ) at the northern end of the spans. The western half of the middle bay and the entire western bay used a sealed expansion joint (SEJ) at the northern end of each span. On the southern end of the specimens, all three bays were constructed without any expansion joint (Figure 2.4).

In an effort to prevent one test region from influencing subsequent test regions, each test area was first loaded to service level loads, as prescribed by the American Association of State Highway and Transportation Officials (AASHTO) Bridge

Specifications for the HS-20 Design Tandem truck. To produce maximum positive moment (tests 3 and 4), loads were placed at mid-span of the 10 ft. wide (western) bay, whereas maximum negative moments (tests 1, 2, 5, and 6) were produced by centering loads over the interior girders (Figure 2.4). After cracking patterns were observed, four of the test areas (1, 3, 4, and 6) were loaded to failure.

All of the tested areas demonstrated excellent performance under service level loads. In fact, no cracking was observed in any of the tests until load was at least twice the design level load. The ends of the specimen that included expansion joint armor experienced less deflection and failed at loads 20-25% higher than the ends without any armor. For the areas loaded to failure, the ultimate load was 5.4 to 7 times the design level load and the mode of failure was punching shear. In summary, the results of the tests conducted by Coselli indicated that both ends of the deck behaved comparably under service loads and that the reserve capacity of the PCP detail was more than adequate for bridge deck design.

2.2.2 TxDOT Project 0-5367

Based on the results of the tests conducted by Coselli (2004), TxDOT initiated Project 0-5367 in an effort to better understand the behavior of precast concrete panels (UTSE detail) adjacent to expansion joints. The first phase of Project 0-5367 pertains to bridge decks with precast panel forming and expansion joints that have 0° skew.

2.2.2.1 Agnew (2007)

In the first phase of project 0-5367, completed by Agnew (2007), the fatigue response of composite bridge deck (UTSE detail) specimens with 0° skew at the expansion joints was evaluated. Four full-scale specimens were constructed, two of which were tested in positive moment, and two of which were tested in negative moment. Each single-bay positive moment specimen measured 8 ft. by 11 ft. and was built using a single, rectangular precast panel (Figure 2.5). Agnew (2007) developed a finite element model for the positive moment specimens and determined that the HL-93 Design Truck

produced larger stresses at the end of the specimen, when compared to the stresses produced by the HL-93 Design Tandem. For this reason, positive moment specimens were subjected to a single point load at midspan of the end with the SEJ; the point load represented a wheel load from the HL-93 Design Truck (Figure 2.6).

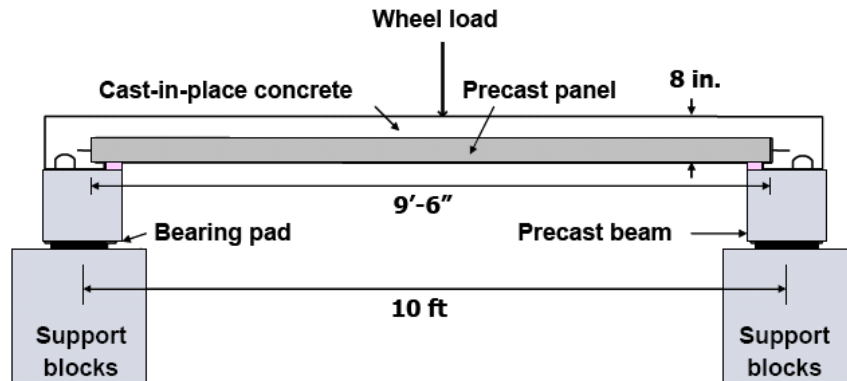


Figure 2.5: Elevation View of Positive Moment Specimen Subject to Fatigue Loading (Agnew 2007)

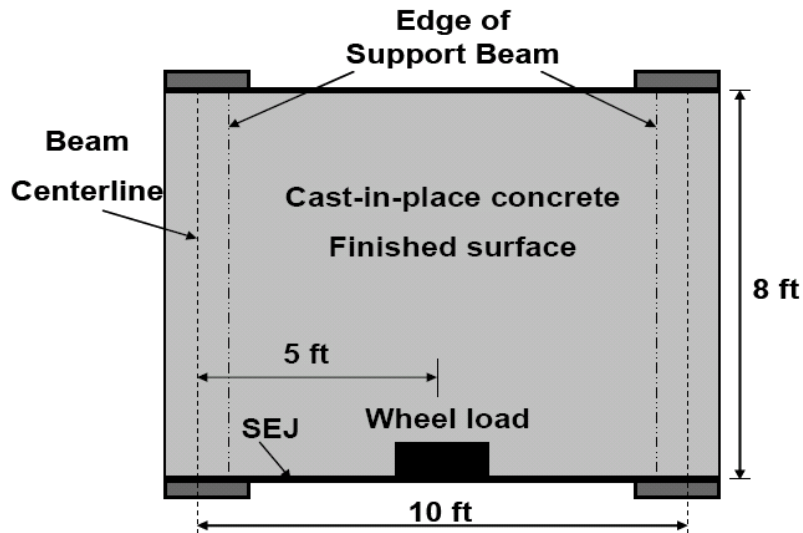


Figure 2.6: Plan View of Positive Moment Specimen Subject to Fatigue Loading (Agnew 2007)

Each two-bay negative moment specimen measured 8 ft. by 21 ft. and was constructed using two rectangular precast panels (Figure 2.7). To create maximum

negative moment in the specimen, two point loads, spaced 6 ft. apart, were centered over the interior beam using a spreader beam so that only one actuator could be used for all tests (Figure 2.8). This two-point loading represented the wheel load from the HL-93 Design Truck, with the 6-ft. spacing being the width of the axle of the truck.

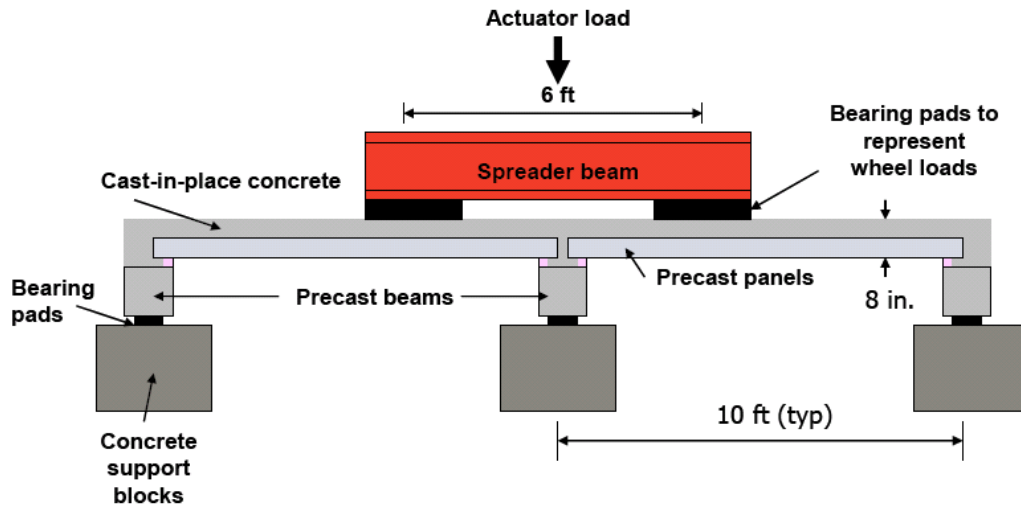


Figure 2.7: Elevation View of Negative Moment Specimens Subjected to Fatigue Loading (Agnew 2007)

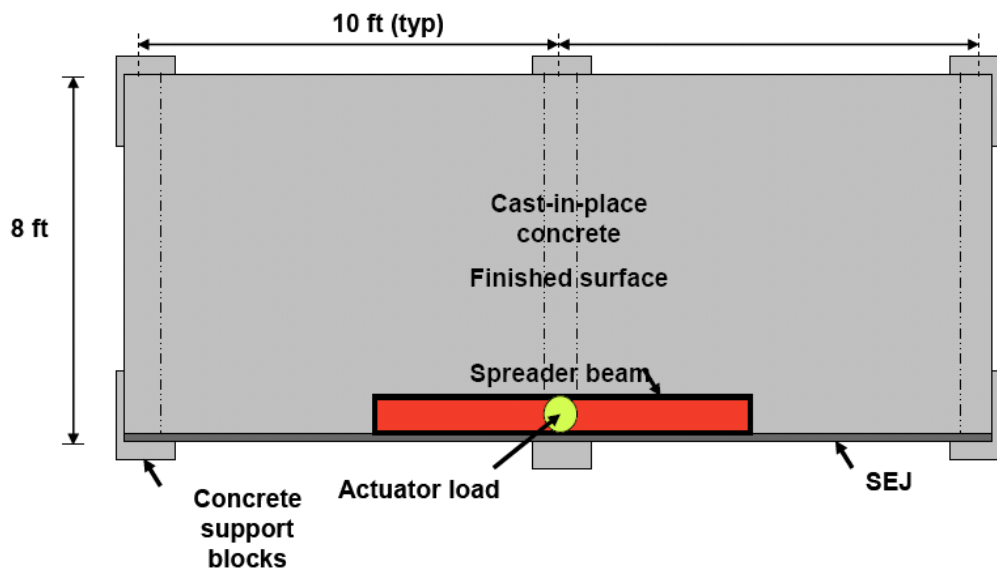


Figure 2.8: Plan View of Negative Moment Specimens Subject to Fatigue Loading (Agnew 2007)

Each of the four specimens was subjected to design level fatigue loads for a few million cycles, during which the stiffness of each composite slab remained essentially constant. Next, each specimen was subjected to a static overload test, which resulted in some decrease in stiffness. Fatigue loading was then resumed for several more million cycles; during the second fatigue load testing, there was no further decrease in stiffness. Finally, each specimen was statically loaded to failure, which occurred in punching shear at a minimum of 4.1 times the design wheel loads. Test data also showed that the SEJ did not yield before a static loading of 3.5 times the design wheel loads.

The results of testing indicated that increased cyclic loading of the precast panel system adjacent to the expansion joint did not result in any deterioration of the composite slab and that the PCP detail provided adequate fatigue performance for use in bridge deck design.

2.2.3 Dowell and Smith (2006)

Since the precast panel system with topping slab does not contain shear studs or any mechanical means of transferring horizontal shear between the precast panel and the topping slab, the surface roughness of the precast panel is the sole means of transferring horizontal shear stresses from the topping slab to the precast panel. In fact, the system can only act as a composite slab if this shear transfer is maintained. To study the relationship between horizontal shear transfer and panel surface roughness in such composite systems, Dowell and Smith (2006) constructed tests specimens with 3¼ in. thick precast panels and 4¼ in. thick cast-in-place topping slabs. Each specimen was simply supported with a single point load located at midspan (Figure 2.9). To achieve variable surface roughness on the precast panel surfaces, “coarse broom,” “medium broom,” and “carpet drag” finishes were applied to the precast panels before the concrete cured.

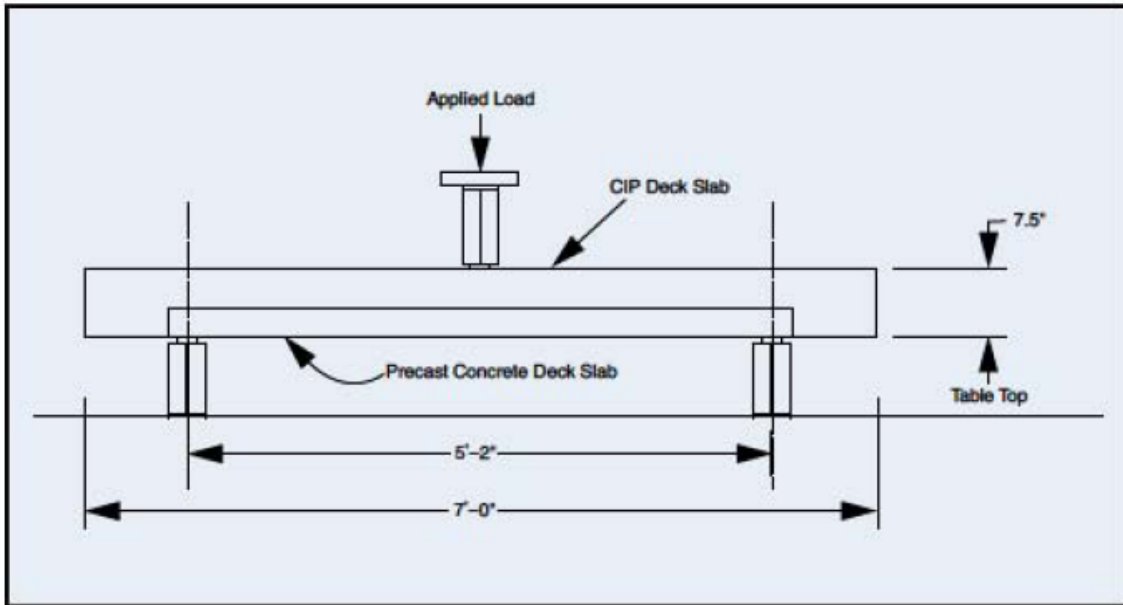


*Figure 2.9: Side View of Overall Setup for Bridge Decks Tested in Simple Bending
(Dowell and Smith 2006)*

Upon the conclusion of testing, Dowell and Smith (2006) found that all of the applied finishes provided enough horizontal shear strength to prevent slip between the topping slab and precast panel. Results of their testing indicated that as long as sufficient panel surface roughness is provided and maintained through curing, the precast panel and topping slab will act as a truly composite section.

2.2.4 Merrill (2002)

Investigating the use of rectangular precast concrete panels as stay-in-place forming for bridge deck construction in Texas, Merrill (2002) discussed specific aspects of the construction process, such as precast panel fabrication and deck construction issues. One such issue was the consolidation of cast-in-place topping slab underneath the sides of the precast panels and at the ends with the expansion joint. Adequate consolidation of concrete under the sides and at the ends of the precast panels is essential to provide a uniform bearing surface and true composite action at all locations of the system. Merrill

(2002) also paid particular attention to the moisture content of the precast panels immediately prior to placement of the topping slab, noting that panels may leach moisture from the freshly placed concrete if they are not moistened to a saturated, surface dry (SSD) condition prior to placement of the topping slab. Merrill (2002) concluded that precast panel forming allowed for a very efficient bridge deck system, provided that close attention is paid to construction details that ensure composite action, such as adequate consolidation of concrete and sufficient moisture content of the panels prior to topping slab placement.

2.2.5 Abendroth (1994)

To evaluate the degradation of bond between the topping slab and precast panels in composite bridge deck systems subject to HS-20 wheel loads, Abendroth (1994) constructed and tested specimens with 2½ in. thick precast panels and 5½ in. cast-in-place topping slabs. Each precast panel was roughened with a rake before the concrete cured. After testing, Abendroth (1994) concluded that the first interface slip between the topping slab and precast panel occurred at loads greater than twice the design wheel load amplified for impact (20.8 kips). After this initial slip, the specimens demonstrated a significant amount of reserve strength, indicating that the rake finish provided adequate surface roughness to allow horizontal shear transfer between the topping slab and precast panels.

2.2.6 Barker (1975)

To compare the performance of fully cast-in-place bridge decks with that of a proposed system that uses stay-in-place forming, Barker (1975) investigated three bridge forming techniques: removable wood formwork, stay-in-place steel forms, and stay-in-place precast panels. For the systems involving precast panels, some of the panels were constructed to have shear studs protruding from the top surface of the panels, while other panels had raked surface finishes. After reviewing various test results, Barker (1975) reported that adequate panel surface roughness provided sufficient shear transfer,

eliminating the need for shear reinforcement between the panel and the topping slab. In addition, it was found that the performance of the precast panel system was not affected by the joints between the precast panels. Barker (1975) concluded that bridge deck construction could be streamlined without compromising structural capacity by utilizing precast panel forming.

2.3 PRESTRESSED CONCRETE PANELS IN SKEWED BRIDGES

To date, four research studies regarding the use of precast concrete panels in skewed bridge deck construction have been reported. Particular emphasis is paid to the research conducted by Boswell (2008) and Kreisa (2008), which immediately preceded, and lead to the topic of, this thesis.

2.3.1 TxDOT Project 0-5367

TxDOT Project 0-5367 was initiated to better understand the behavior of precast panels (PCP detail) adjacent to square expansion joints. The second phase of the project pertains to bridge decks with precast panel forming and skewed expansion joints.

2.3.1.1 Boswell (2008) and Kreisa (2008)

The second phase of Project 0-5367 investigated the PCP detail with expansion joint skew angles of 45° and 30°. Single-bay test specimens were constructed, using 4 in. thick precast panels (Figure 2.10) and 4 in. thick cast-in-place topping slab. Load was applied at midspan of the skewed end. Kreisa (2008) focused on skewed panel fabrication and constructability issues, such as prestressing strand layout (Figure 2.11), whereas Boswell (2008) concentrated on the structural performance of the skewed panel system. In depth discussions on the construction of skewed precast panels and their structural capacities can be found in Kreisa (2008) and Boswell (2008), respectively.

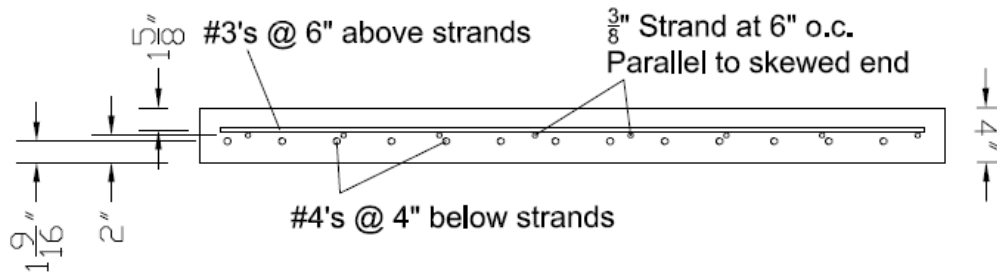


Figure 2.10: Cross-Section of Precast Panel with Strands Parallel to Skewed End
(Kreisa 2008)

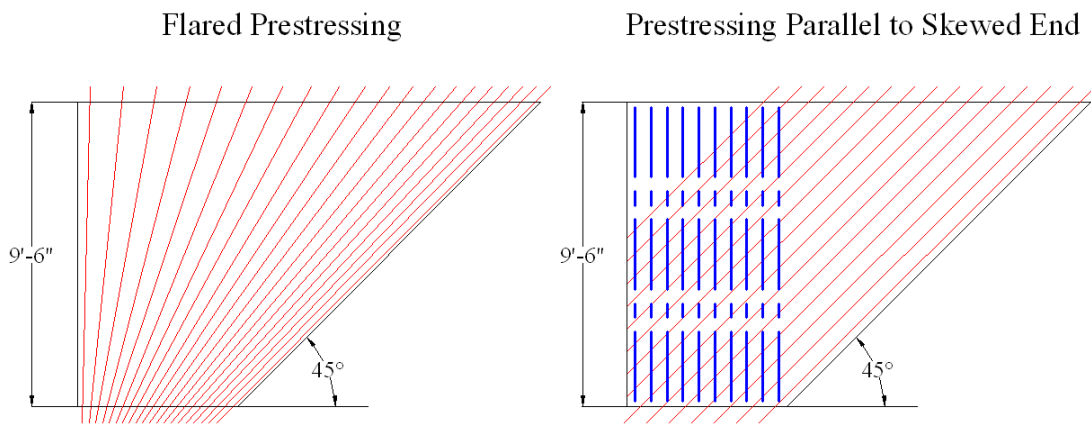


Figure 2.11: Selected Design Alternatives for Strand Layout in 45° Panels
(Kreisa 2008)

All of the specimens were first loaded to failure at midspan of the skewed end, which was adjacent to the SEJ, and some of the specimens were then loaded at midspan of the square end, which did not include an SEJ. When loaded at midspan of the skewed end, the 45° specimens demonstrated excellent behavior, failing in diagonal shear at the short side support. That behavior coincided with the rectangular specimens tested by Agnew (2007). The load-displacement data for the skewed specimens (see Appendix B) showed that the initial stiffness of the skewed composite systems were also very similar to those of the rectangular specimens tested by Agnew (2007). On the other hand, when the 30° panels were loaded at midspan of the skewed end, failure occurred suddenly at significantly lower loads, as the topping slab “unzipped” from the precast panel. This

mode of failure is known as delamination, in which horizontal shear stresses cannot effectively be transferred from the topping slab to the precast panel. When delamination occurs, the topping slab and precast panel no longer act as a composite member and the ultimate capacity of the system is significantly decreased, when compared to a system in which the composite action is maintained up to failure (discussed further in Chapter 6 and Appendix B).

After being loaded to failure at midspan of the skewed ends, some of the specimens were then loaded at midspan of the square end. As all but one of the skewed panels had prestressing strands running parallel to the skew, these panels had a corner on the square end in which strands were too short to develop the prestressing force and were therefore debonded. This raised a concern that the capacity of the section might be limited at that corner where strands were not prestressed. Testing of the square end resulted in much greater capacities than were seen in the skewed-end tests and the mode of failure was always punching shear when loaded at the square end (Chapter 6 and Appendix B). Therefore, the capacity was not limited by the corner with the debonded strands.

Boswell (2008) and Kreisa (2008) concluded that using skewed precast panel forming in bridge deck construction provided an efficient composite system with ample reserve capacity, provided that delamination was avoided. Kreisa (2008) found that using prestressing strands parallel to the skew angle resulted in easier fabrication. The non-prestressed corner performed well when compared to panels that used a fanned strand pattern. Boswell (2008) concluded that composite systems with skewed panels had initial stiffnesses similar to systems with rectangular panels, and suggested that further investigation be done on 30° panels with a rougher surface texture to provide additional horizontal shear transfer. Delamination, and not the skew angle, was likely the limiting factor on capacity. To evaluate that premise, the third phase of Project 0-5367, and the basis of this thesis, was initiated.

2.3.2 Merrill (2002)

As discussed in Section 2.2.4, Merrill (2002) investigated the use of precast panels as stay-in-place forming for bridge deck construction in Texas. Aside from the evaluation of rectangular bridges, Merrill (2002) also considered skewed bridges, concluding that the unresolved geometry introduced the need for complex forming adjacent to the expansion joint.

2.3.3 Abendroth (1994)

Aside from the tests conducted on rectangular bridge deck specimens, which are presented in Section 2.2.5, Abendroth (1994) also investigated the use of precast panels in skewed bridge decks. Specimens consisted of 2½ in. thick precast panels with a 5½ in. thick topping slab. The precast panels were trapezoidal in shape, fabricated to have 15°, 30°, and 45° skew angles and prestressing strands that remained parallel to the perpendicular end for all of the panels (Figure 2.12). The skewed end of each panel was supported by a diaphragm, while the sides were supported by “girders.” The results of testing indicated that the trapezoidal panels performed well under design level loads and significant reserve strength was observed beyond the design level loads. It was noted that presence of the diaphragm support under the skewed end, along with the shape of the panel, caused uplift at the acute corner of the trapezoidal panels.

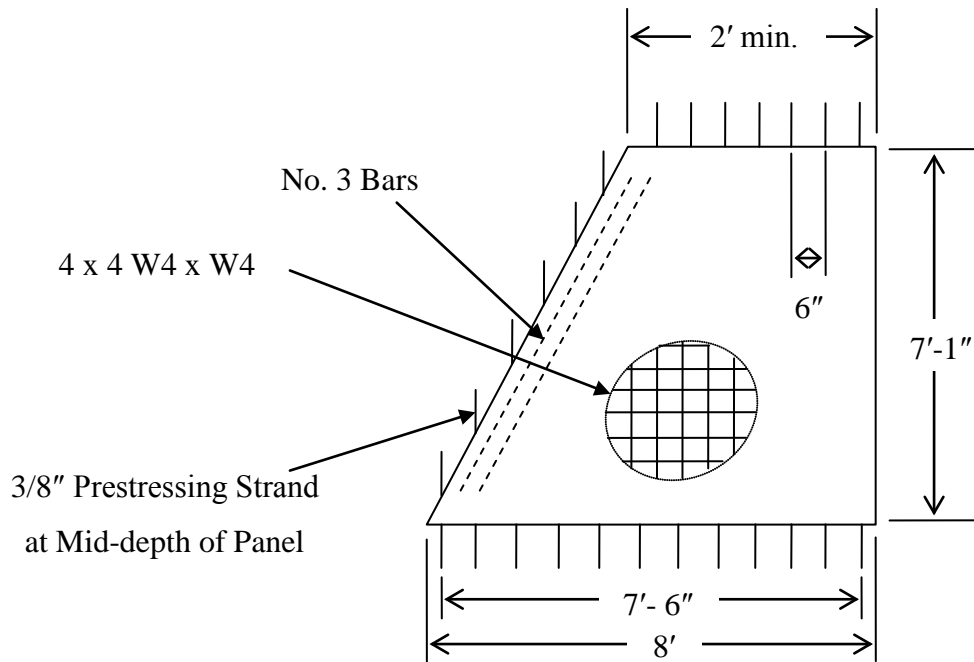


**Figure 2.12 - Trapezoidal Panels for Composite Bridge Deck Systems
(Abendroth 1994)**

2.3.4 Barker (1975)

Barker (1975) studied several projects that used precast panel forming in bridge deck construction, as previously discussed in Section 2.2.6. With regard to the unresolved geometry associated with skewed bridges, Barker (1975) saw-cut one end of a rectangular precast panel so that it had the same skew angle as the bridge. Diaphragms were then used to support the skewed ends of the modified panels.

2.4 RESEARCH SIGNIFICANCE

Prestressed precast panels have been used as stay-in-place formwork for bridge deck construction in Texas for nearly three decades, resulting in a faster and less expensive construction process and safer work environment. While the behavior of rectangular panels, which are simple and inexpensive to produce, has been widely studied, few investigations of trapezoidal panels at skewed expansion joints have been conducted.

Furthermore, diaphragms are typically used to support panel ends at expansion joints, so little research has been done to investigate the behavior of unsupported, skewed precast panel ends. While the first phase of TxDOT Project 0-5367 indicated that unsupported, rectangular precast panels at expansion joints perform very well under design loads, and the second phase of the project suggested that skewed panels also perform well under the same conditions, the delamination experienced in the second phase raised concerns about the effect of fabrication and construction practices on structural capacity and mode of failure. The purpose of this research is to study the behavior of unsupported skewed ends of precast panels adjacent to the expansion joint when strict panel fabrication and deck construction requirements are enforced.

Chapter 3: Test Specimen

3.1 INTRODUCTION

In this phase of the investigation, one specimen was constructed at Ferguson Structural Engineering Laboratory to study the behavior of skewed prestressed concrete panels under static loading when used adjacent to the expansion joint. The specimen consisted of one rectangular panel placed between two skewed panels. The three precast panels spanned transversely between longitudinal support beams, and were topped with a cast-in-place slab. Design considerations, material properties, specimen construction, and testing procedures are summarized in this chapter.

To facilitate comparison with previously tested specimens in Project 0-5367, the specimen was identified using the notation developed by Agnew (2007):

ABCD

where

A can either be “P” or “N” for the test specimens investigated in TxDOT Project 0-5367. When the panel was tested in positive moment, “P” was used, whereas “N” was used for panels tested in negative moment. In this phase of the investigation, the specimen was only subjected to positive moment.

B is the angle of the skew. Agnew (2007) tested four panels with 0° skew. Boswell (2008) and Kreisa (2008) tested three panels with 45° skew and two panels with 30° skew. In this phase of the investigation, both ends of the specimen were skewed 30° with respect to the longitudinal beams.

C was “P” for all specimens tested in Project 0-5367 and refers to the precast deck system.

D refers to the sequence of testing for each family of skew angles. The specimen tested herein was the third to have 30° skew angles.

Thus, the specimen tested in this phase of Project 0-5367 was labeled “specimen P30P3” and consisted of two panels, which are simply referred to as “panel A” and “panel B.” The characteristics of specimen P30P3 are summarized in Table 3.1. For comparison, the characteristics of the specimens tested by Boswell (2008) and Kreisa (2008) are provided in Table B.1 of Appendix B.

Table 3.1 – Characteristics of Skewed Test Specimen

	Specimen P30P3
Skew Angles	30°
No. of Panels	3
Skewed Panel Strand Pattern	Parallel to Skew
Skewed Panel Fabrication Site	Off-Site
Long Beam Length	18' - 0"
Long Beam Cross Section	12" x 12"
Short Beam Length	18' - 0"
Short Beam Cross Section	12" x 12"
Beam Clear Spacing	9' - 0"
Bedding Strip Type	Dow Styrofoam Highload 60
Bedding Strip Strength	60 psi

3.2 DESIGN CONSIDERATIONS

To represent prestressed concrete bridges in Texas, design of the test specimen was based on the following assumptions: centerline spacing between “girders,” or support beams, was assumed to be 10 ft.; and the thicknesses of the prestressed concrete panels and the cast-in-place topping slab were both 4 in., creating an overall bridge deck depth of 8 in.

Loads imposed on the specimen represented the design vehicle rear axle load. In TxDOT Project 0-4418 the HL-93 Design Truck was used for all tests. Subsequently, Boswell (2008) and Kreisa (2008) also chose to use the HL-93 Design Truck to test their skewed specimens. For this reason, the HL-93 Design Truck was also used to test the specimen in this phase of the investigation.

The HL-93 Design Truck axle arrangement, as well as three possible ways that axle loads could be applied to the bridge deck, are shown in Figure 3.1. Since the HL-93 Design Truck axles are far enough apart, deck behavior is only influenced by the axle directly over it. Whereas axle position A produces the largest positive moment in the bridge deck, axle position C results in the greatest negative moment. Previously, both negative and positive moment were considered for specimens with 0° skew (Agnew 2007). Agnew (2007) developed finite element models of a full bridge deck and an idealized test specimen that consisted of one precast panel, two side beams, and a topping slab. Model analysis indicated that the greatest moments were induced when a point load was applied at midspan of the end along the sealed expansion joint (Figure 3.1). Thus, the skewed specimens tested by Boswell (2008) and Kreisa (2008), as well as the one tested in this phase of the investigation, were loaded using a single wheel load at midspan to create positive moment.

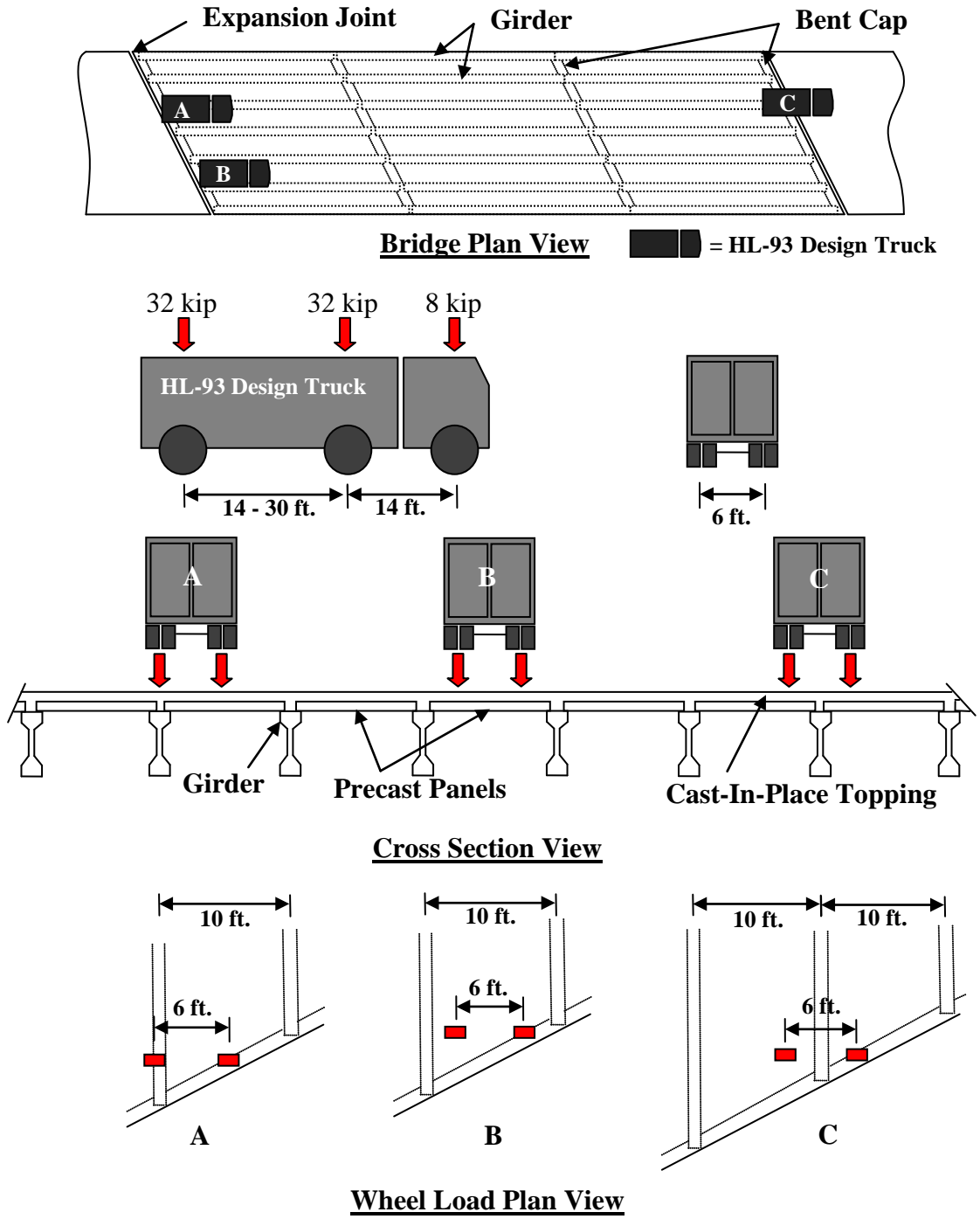


Figure 3.1 – HL-93 Design Truck Loads on Bridge Deck (Boswell 2008)

3.3 MATERIAL PROPERTIES

3.3.1 Concrete

The concrete mixture design used to construct the support beams and topping slab was different from the concrete used to construct the precast panels.

In the previous phase of the investigation, the precast panels with 45° skew were produced at the Ferguson Structural Engineering Laboratory (FSEL), while the 30° panels were produced at a precast yard (Boswell 2008, Kreisa 2008). The 30° panels tested within this phase of the investigation were also fabricated at a precast yard, and thus no information is available about the mixture design or the concrete strength. For the 45° panels produced at FSEL, a detailed description of panel construction is provided by Kreisa (2008).

Constructed at FSEL, the support beams and topping slab were cast using TxDOT specifications for Class “S” Structural Concrete, which was provided by a local ready-mix concrete plant. Class “S” Structural Concrete has a specified strength of 4000 psi. Mixture proportions are given in Table 3.2. Currently, TxDOT provisions require cast-in-place bridge decks to remain free of load for 21 days after concrete placement. The concrete strength of the specimen tested in this phase of the investigation was just over 4880 psi at 21 days. For comparison, the 21-day concrete strengths of the specimens tested by Boswell (2008) and Kreisa (2008) are provided in Table B.2 of Appendix B.

Table 3.2 – Support Beam and Topping Slab Concrete Mixture Design (Boswell 2008)

Cement	SSD Fine Aggregate	SSD Coarse Aggregate	Water	Fly Ash
lb/yd ³	lb/yd ³	lb/yd ³	lb/yd ³	lb/yd ³
479	1350	1857	250	85

3.3.2 Steel

Grade 60 mild reinforcement was used to construct the support beams and topping slab. In addition, the precast panels were prestressed using grade 270, 3/8 in. diameter seven-wire strand.

Fabricated from A36 steel, the sealed expansion joint (SEJ) was shown to have a yield strength of 48 ksi by mill reports. In keeping with previously conducted tests, an SEJ-A section was used, with 3.5 in. vertical leg and 6 in. deep studs spaced at 6 in. on center.

3.3.3 Bedding Strip Material

Consisting of continuous strips of foam, the bedding strips are placed on the top face of the support beams, followed by the precast panels. The panels are placed such that the sides of the panels extend beyond the bedding strips; this allows the topping slab concrete to flow underneath the panel sides, which provides a uniform bearing surface for the panels (Figure 3.2).

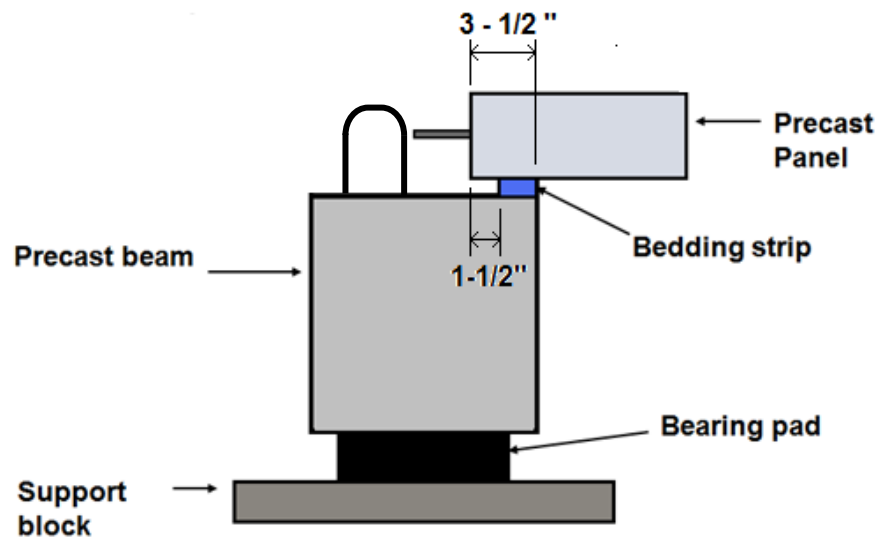


Figure 3.2 – Panel on Bedding Strip (Boswell 2008)

In practice, the height of the bedding strips varies along the length of the support beam to account for camber in the prestressed girder. Since the support beams

constructed for the investigation did not have camber, continuous 2 in. by 2 in. strips of foam were used for all test specimens. TxDOT specifies requirements on bedding strip dimensions, as well as the minimum overhang of the precast panel over the bedding strip (Figure 3.3). The minimum 1½ in. overhang was used for all test specimens in the investigation.

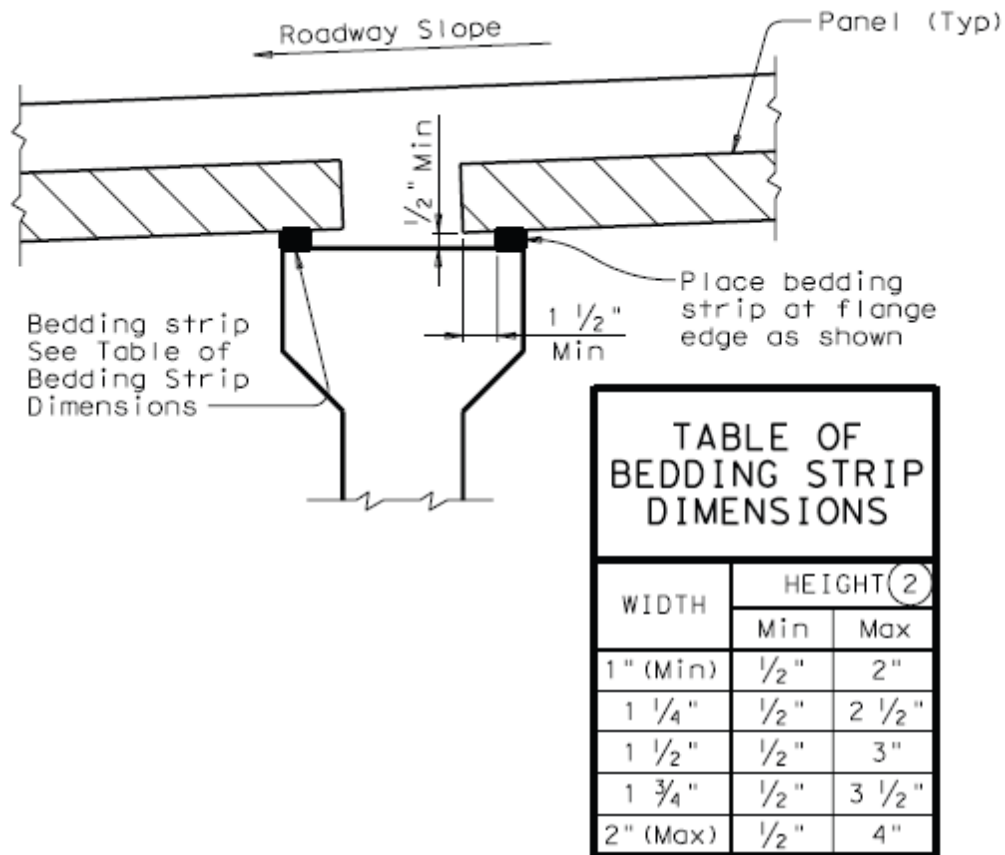


Figure 3.3 – TxDOT Bedding Strip Dimensions (TxDOT 2008)

Throughout the various phases of the investigation, two different types of foam were used for bedding strips. Initially, Agnew (2007) constructed all of the 0° specimens using Foamular Rigid Foam Insulation, which is not a structural building material and has a compressive strength of about 25 psi. In keeping with previous testing, Bowell (2008) and Kreisa (2008) used Foamular foam board to construct the first skewed specimen, P45P1. Because Foamular foam board is only 3/4 in. thick, three 2 in. wide strips were cut

and glued together to form a 2-¼ in. by 2 in. bedding strip along the length of the support beam. After the skewed panel was placed on the Foamular bedding strip, the foam compressed excessively and floor jacks were required to lift the panel in an attempt to achieve the desired topping slab thickness. Despite the floor jacks, movement of the panels occurred during placement of the topping slab, resulting in an overall bridge deck thickness that was larger than desired. For this reason, it was decided that subsequent specimens would be constructed using another type of foam for bedding strips.

For the bedding strips of the successive specimens, Boswell (2008) and Kreisa (2008) decided to use Dow Styrofoam Highload 40, which has a compressive strength of about 40 psi and is commonly used in TxDOT bridge construction. While the Foamular foam board compressed more, compression still occurred in the Highload 40 foam, with the largest compression observed under the short side of the skewed panel. This is due to the trapezoidal shape of the skewed panels, which causes the stresses under the short side to be larger than those under the long side. Additional information regarding bedding strip compression at the short side support is given in Kreisa (2008).

In this phase of the investigation, Dow Styrofoam Highload 60 was used for the bedding strips of specimen P30P3. With a compressive strength of approximately 60 psi, the foam only slightly compressed at the short side of the skewed ends. This resulted in an overall bridge deck thickness that was 8 in. thick throughout. A summary of the overall slab depth at midspan of the skewed end of each of the specimens tested by Boswell (2008) and Kreisa (2008) is given in Table B.3 for comparison.

3.4 SPECIMEN CONSTRUCTION

Specimen P30P3, which consists of two test panels, was constructed following the sequence shown in Figure 3.4. While TxDOT currently limits the transverse centerline spacing of precast girders to 10 ft. - 0 in., a spacing of 8 ft. – 0 in. is more typical. This centerline spacing of girders will increase with the implementation of new cross-sectional shapes for prestressed I-beams used in Texas, although the clear spacing between I-beam

top flanges will remain at 9 ft. – 0 in. Thus, the support beams were placed with a clear spacing of 9 ft. – 0 in. between them. Bedding strips were placed along the length of the support beams, followed by the 4 in. thick precast panels and then the cast-in-place topping slab was placed to connect the components. The dimensions and details of these elements are summarized in Table 3.1. Table B.1 contains details of the components for the specimens tested by Boswell (2008) and Kreisa (2008).

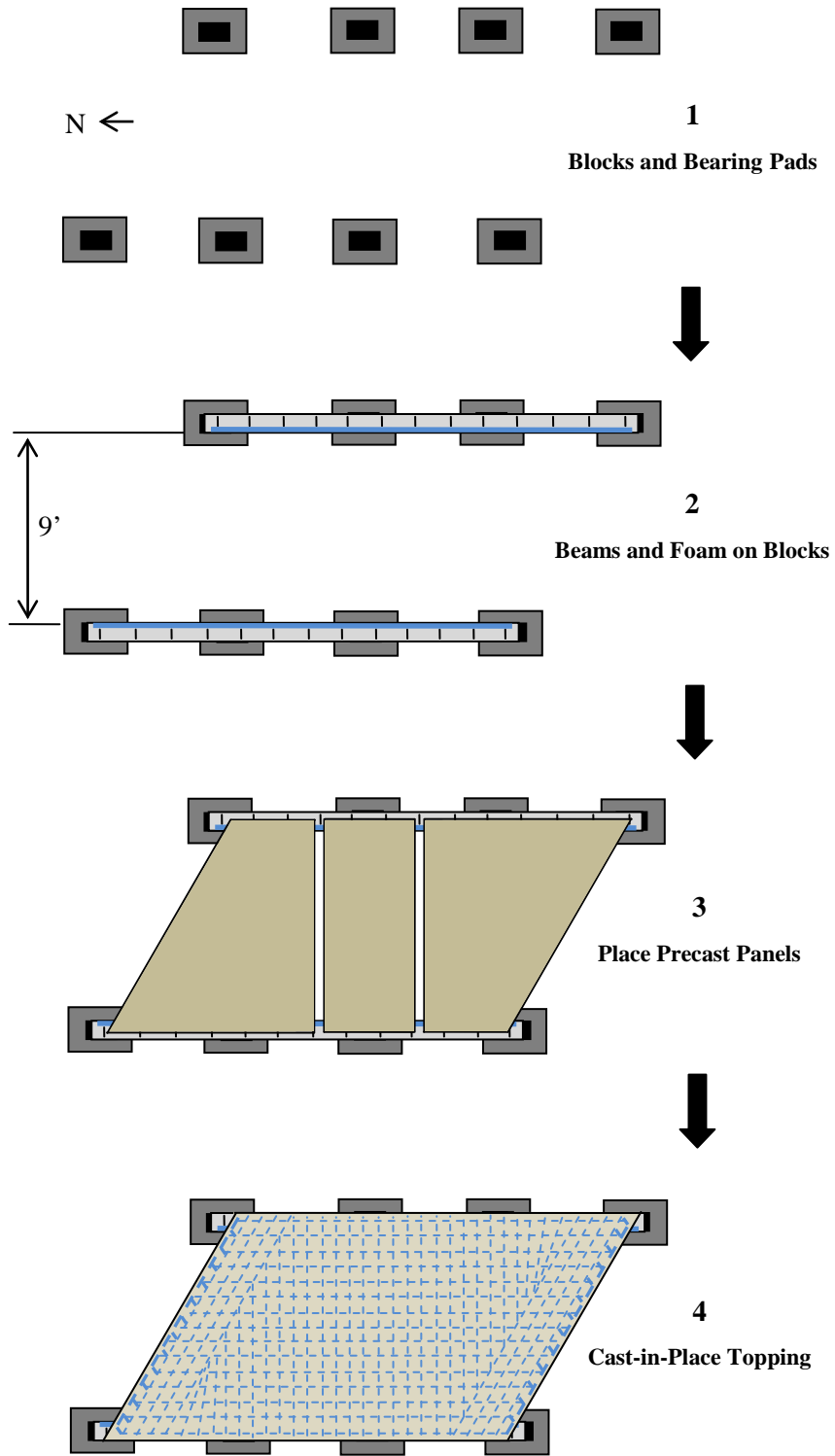


Figure 3.4 – Construction Sequence for Specimen P30P3

3.4.1 Support Beams

The precast panels described in Section 3.4.2 were supported by longitudinal, reinforced concrete beams. The two support beams had the same length and cross-section. Each longitudinal beam was supported by elastomeric bearing pads resting on concrete blocks, simulating the support for prestressed girders in typical TxDOT bridge construction. The elastomeric bearing pads measured 9 in. by 13 in. by 2½ in. Four concrete blocks were used to support each beam, with one block supporting each end of the beam and two blocks spaced evenly in between (Figure 3.5).

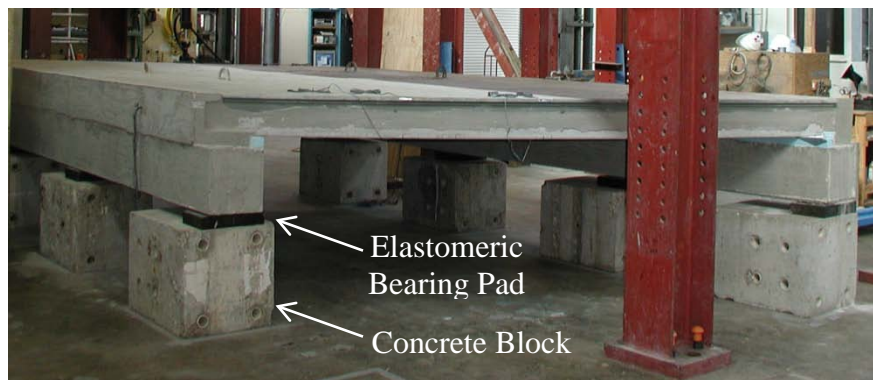


Figure 3.5 – Configuration of Support Beams, Elastomeric Bearing Pads, and Concrete Blocks for Specimen P30P3

In order to provide shear transfer and continuity between the deck and the supporting “girders,” transverse reinforcement extended above the top surface of the beam so that when the topping slab is placed, composite action is developed. In earlier phases of the investigation, these U-bars were oriented perpendicular to the longitudinal axis of the beam, as illustrated in Figure 3.2. This caused difficulty during construction, as the U-bars interfered with the placement of the topping slab reinforcement, and it was decided to rotate the U-bars by 90° to better accommodate placement of both the prestressed panels and the topping slab reinforcement (Figure 3.6).

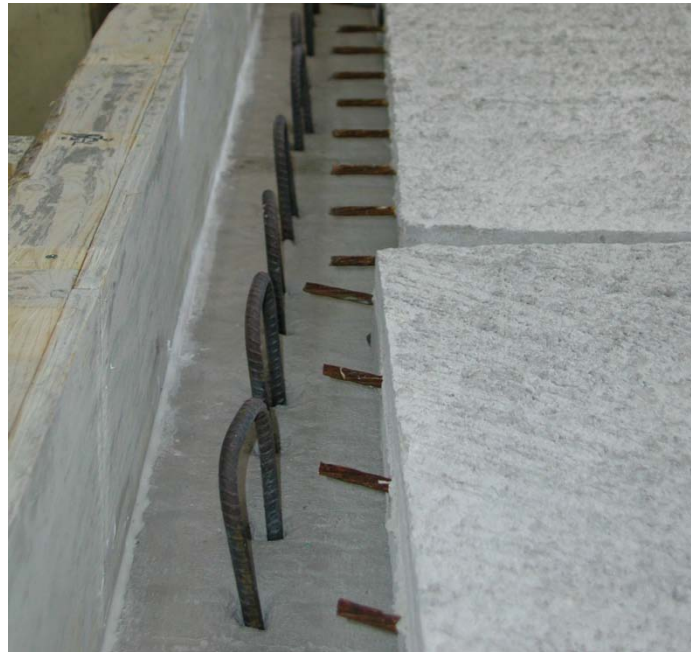


Figure 3.6 – Alignment of U-bars for Specimen P30P3

3.4.2 Precast Panels Used in Test Specimen

As 92% of all skewed bridges in Texas have a skew of 45° or less (Van Landuyt 2006), Boswell (2008) and Kreisa (2008) tested specimens with 30° and 45° skew angles in the previous phase of the investigation. The results of their tests indicated that the 45° specimens had capacities close to the rectangular specimens tested previously by Agnew (2007). However, the 30° panels failed suddenly at much lower loads, due to delamination between the precast panels and cast-in-place topping slab (Boswell 2008). Delamination is thought to have occurred because the precast panels lacked adequate surface roughness. For this reason, two more 30° panels were constructed and tested in this phase of the investigation to demonstrate that the surface roughness, and not the skew angle, was the factor that limited capacity.

Specimen P30P3 was constructed using a rectangular panel sandwiched by two 30° panels (Figure 3.7). The 30° panels and rectangular panel are discussed further in Sections 3.4.2.1 and 3.4.2.2, respectively. All three panels were fabricated at an

independent precast yard and more information on the production is provided in Kreisa (2008).

As references will be made to the boundaries of the trapezoidal panels, the labeling of the boundaries is discussed herein. The boundaries of the panels that are supported by the longitudinal beams are labeled the “sides” of the panel, whereas boundaries that are not supported by the beams are called the “ends” of the panel (Figure 3.7). Due to the trapezoidal shape of the skewed panels, each panel has a “long” side associated with the “acute corner” and a “short” side with the “obtuse corner.” Each 30° panel also has a skewed end, which corresponds to the location of the SEJ, and a square end that is adjacent to the rectangular panel.

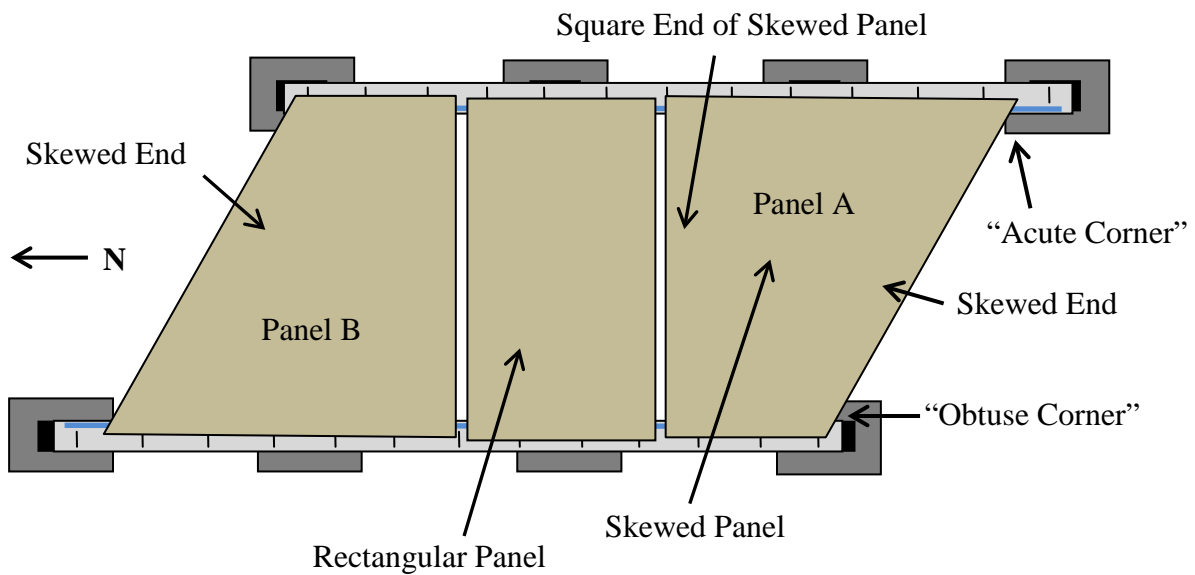


Figure 3.7 – Definitions of Boundaries for Specimen P30P3

3.4.2.1 30° Panels

The panels were designed to have an overall depth of 4 in. with prestressing strands placed parallel to the skew at mid-depth and mild reinforcement provided in the corner where no prestressing strands were present, as illustrated in Figure 3.8.

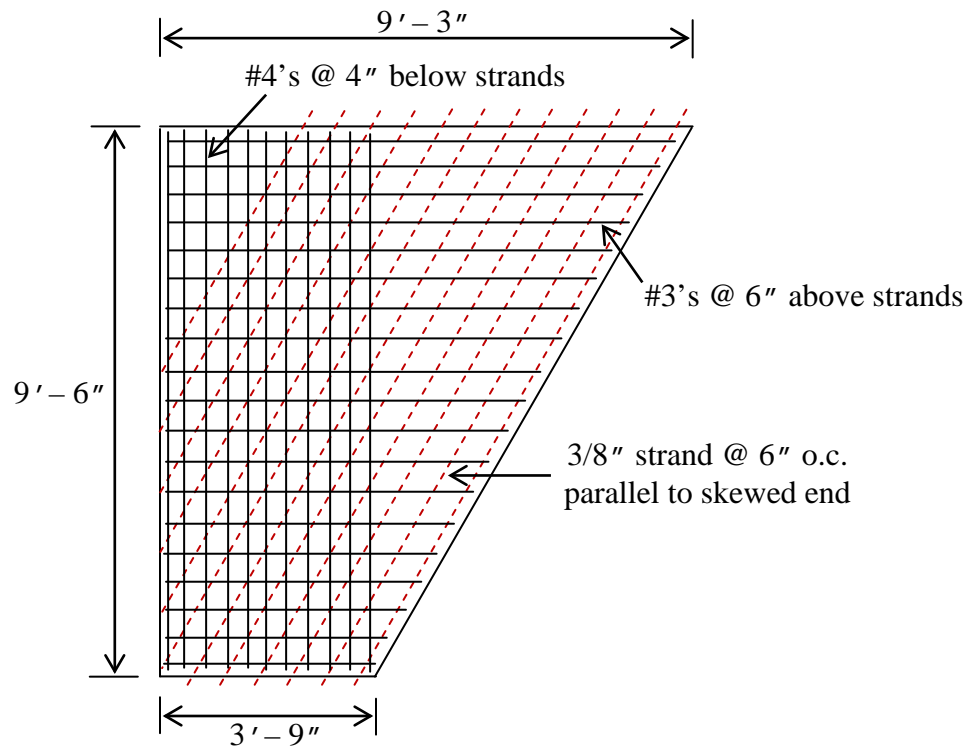


Figure 3.8 – Skewed Panel Reinforcement for Specimen P30P3

To construct the 30° panels, the supplier placed formwork within the 8 ft. wide prestressing bed, laid out the additional mild reinforcement as specified, placed the concrete, and brushed the surface to create the desired surface roughness. This construction process is shown in Figure 3.9. Previously tested 30° panels were broom-brushed and then the prestressing bed was flooded to promote curing. Because a rougher surface was desired in this phase of the investigation, the panels appeared to be finished with a rake to create a surface roughness of approximately 1/4 in.

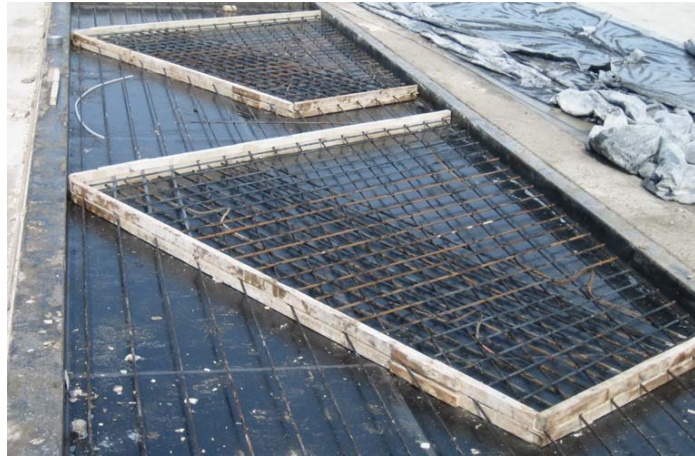


Figure 3.9 – Fabrication Process for 30 °Panels (Kreisa 2008)

3.4.2.2 Rectangular Panel

In specimen P30P3, the strands ran parallel to the skewed end, leaving the corner bounded by the long side and square end without prestressing. To address concerns about the transfer of loads in this region, a 4 ft. rectangular panel was placed between the two skewed panels, as shown in Figure 3.10. The rectangular and trapezoidal panels were intended to have a $\frac{3}{4}$ in. gap between them. Gaps allow contractors to have some placement tolerance in the field. While placing the panels, it became apparent that the square ends of the 30° panels were not perpendicular to the sides. To retain the 30° skew, the trapezoidal panels were rotated slightly, resulting in gaps between the rectangular and skewed panels that varied from about $\frac{1}{2}$ in. on one side to $1\frac{1}{2}$ in. on the other side (Figure 3.10).

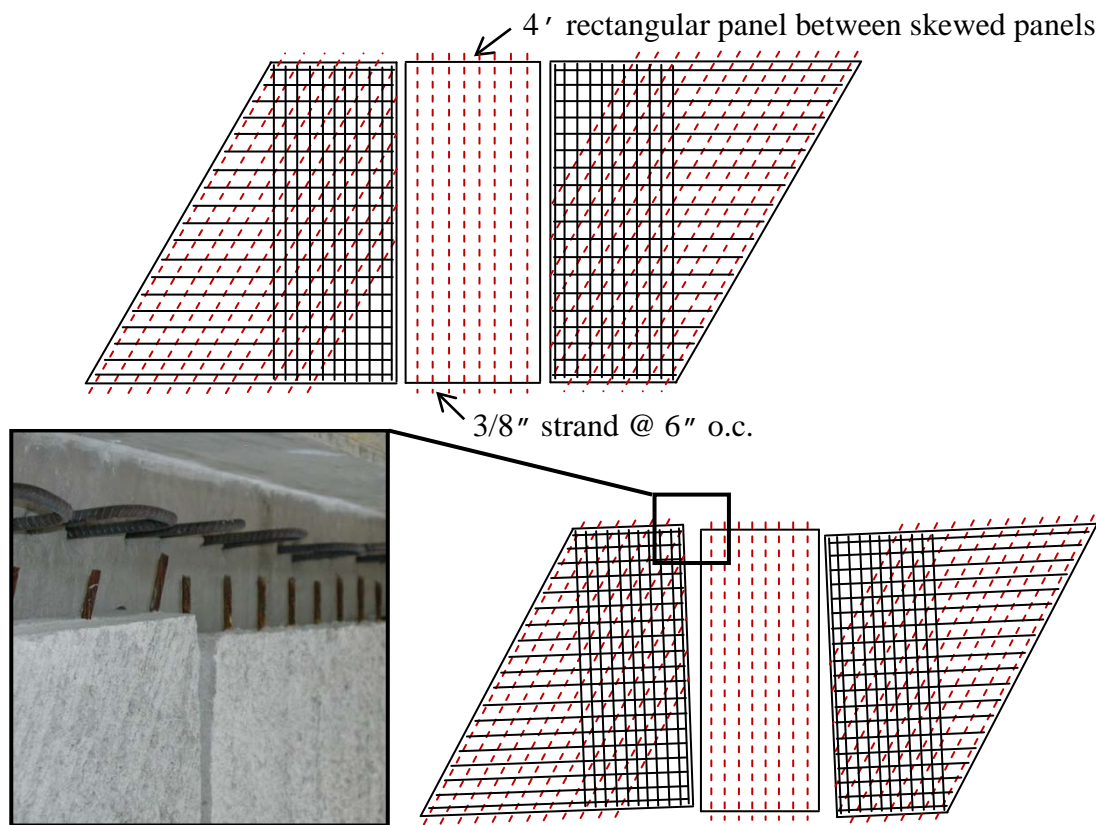


Figure 3.10 – Designed (top) and Actual (bottom) Alignment of Rectangular and Skewed Panels for Specimen P30P3 (gaps exaggerated)

Once the precast panels were placed, the gaps between them were filled with backer rod to limit concrete from flowing through the gaps during placement (Figure 3.11). Due to the variation in width of the gaps from one side to the other, several sizes of backer rod were needed to fill the gaps. Concrete did flow through some of the wider gaps between panels (Figure 3.12).



Figure 3.11 – Backer Rod between Adjacent Panels of Specimen P30P3

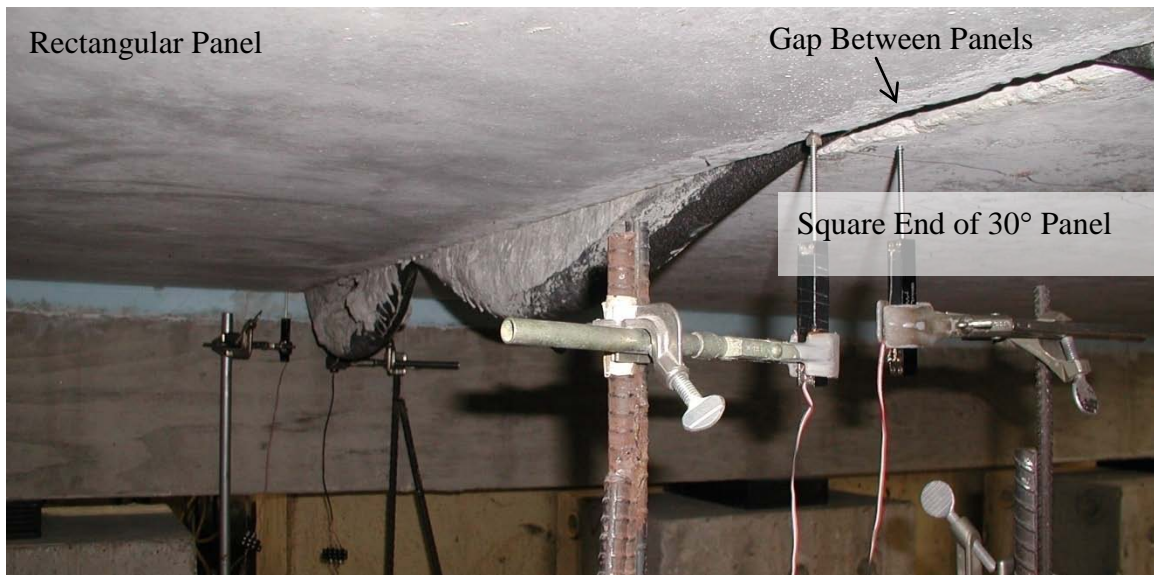


Figure 3.12 – Concrete Flow-Through on Bottom Surface of Specimen P30P3

3.4.3 Cast-in-Place Topping Slab

After the panels were placed on the support beams, the topping slab reinforcement was laid out and tied as specified in standard TxDOT details (Figure 3.13). Formwork was constructed around the perimeter of the specimen so that the topping slab would be 4 in. deep over the precast concrete panels (PCPs) and 10 in. deep over the support beams, resulting in an 8" deep deck (Figure 3.14).

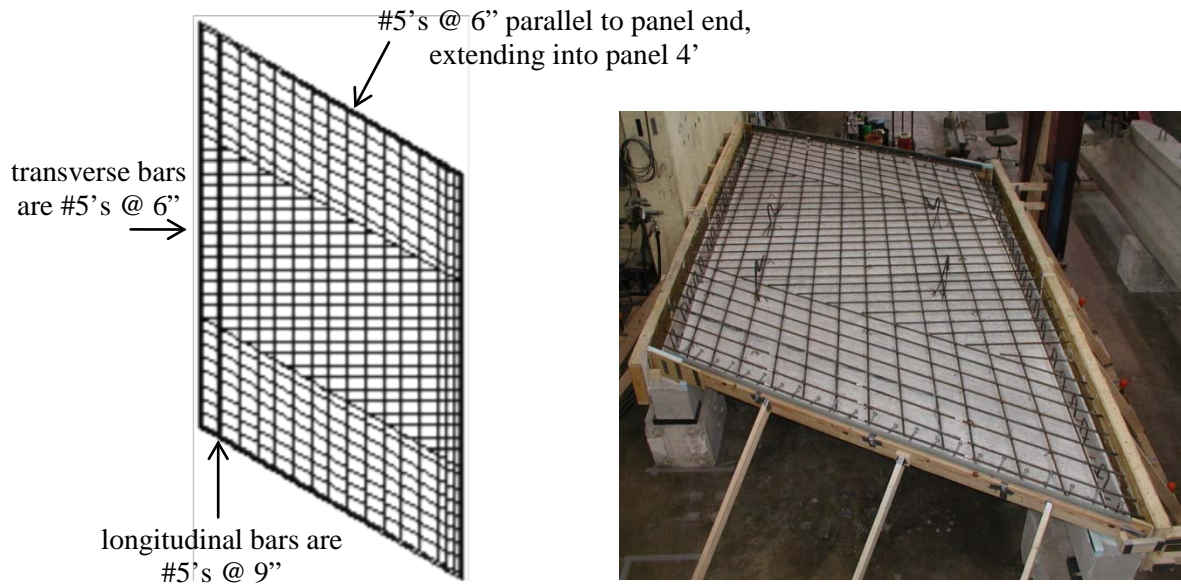


Figure 3.13 – Cast-in-Place Topping Reinforcement for Specimen P30P3

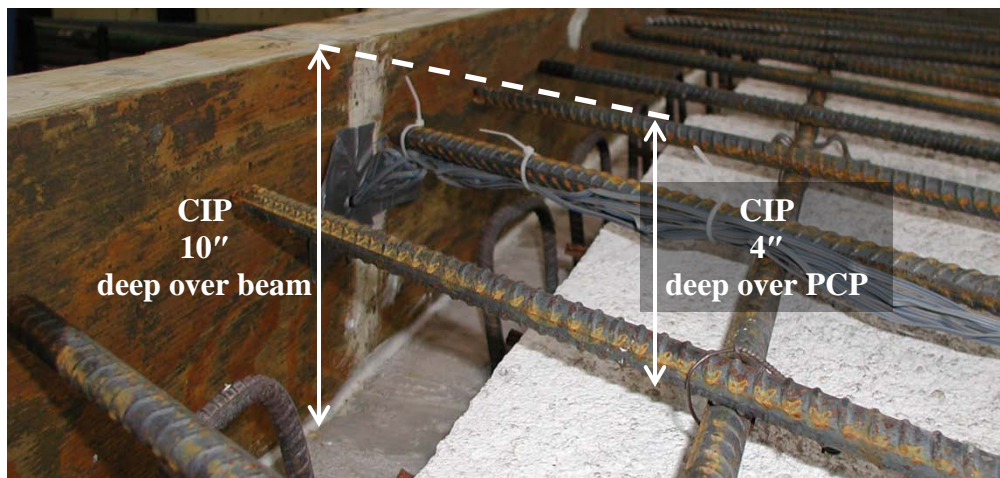


Figure 3.14 – Formwork for Topping Slab in Position

To attach the sealed expansion joint (SEJ) to the formwork, holes were drilled at matching locations in the vertical leg of the SEJ and the formwork along the skewed end so that the top of the SEJ would be flush with the top of the finished slab. The vertical leg of the SEJ was then placed on the interior side of the formwork, flat against the formwork so that the holes lined up, and bolts were used to fasten the SEJ in place (Figure 3.15).

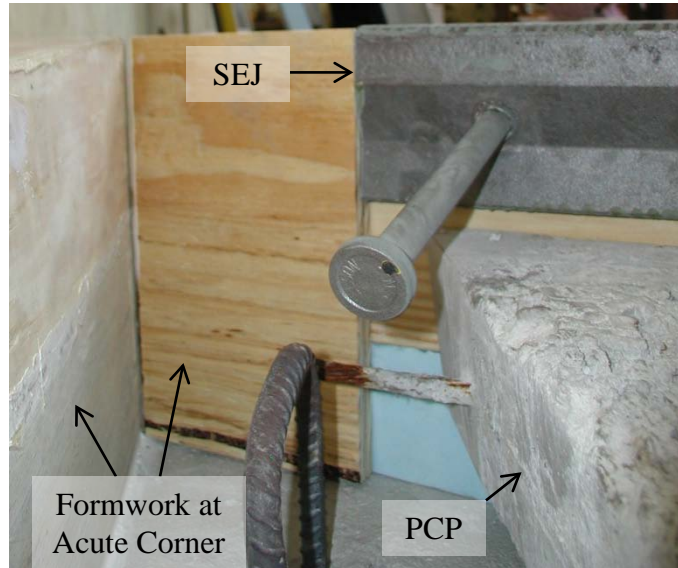


Figure 3.15 – SEJ Attached to Topping Slab Formwork

Prior to placement of the cast-in-place topping slab, the top faces of the panels were moistened to a saturated surface dry (SSD) condition to help prevent the dry precast panels from leaching moisture out of the freshly placed topping slab concrete. In previous phases of the investigation, this was not always done.

During placement, vibrators were used to consolidate the concrete, taking extra care over the support beams to ensure proper flow of the concrete under the sides of the panels, so that the precast panels would have a uniform bearing area along the length of the support beams. Interaction between the topping slab and precast panels is also greatly affected by the surface roughness of the precast panels. While current panel specifications in Texas do not stipulate a required level of surface roughness, the panels tested in this phase of the investigation were produced to have a rough surface texture, to

avoid an undesirable failure by delamination as was experienced by Boswell (2008) and Kreisa (2008) upon testing panels with rather smooth surfaces. After the initial set of the concrete, the top surface of the 30° panels tested by Boswell (2008) and Kreisa (2008) were brushed with a broom and then flooded with water to promote curing. For the panels investigated in this phase of the investigation, it is thought that the top surface was rake-finished to create a much rougher surface (¼ in. typical). For comparison, the characteristics of the panels tested by Boswell (2008) and Kreisa (2008) are given in Table B.4.

As TxDOT specifications currently require that cast-in-place bridge decks remain free of load for at least 21 days after placement, specimen P30P3 was covered with a sheet of heavy plastic immediately after finishing the freshly placed concrete and was left to cure for 21 days before testing (Table 3.3). For comparison, construction and testing dates for the specimens tested by Boswell (2008) and Kreisa (2008) are given in Table B.5.

Table 3.3 – Timeline of Construction and Testing

	Specimen P30P3
Date Panel Cast	1/3/2008
Date Deck Cast	7/23/2008
Date of First Test (Skewed End of Panel A)	8/13/2008
Date of Second Test (Skewed End of Panel B)	8/14/2008
Date of Third Test (Square End of Panel A)	9/04/2008

Chapter 4: Loading and Instrumentation

4.1 INTRODUCTION

In the second phase of TxDOT Project 0-5367, one specimen was subjected to fatigue loading at midspan of the skewed end, prior to being statically loaded to failure at the same location (Boswell 2008, Kreisa 2008). The test results indicated that the fatigue loading did not significantly influence the stiffness of the specimen. For this reason, the specimen tested in this phase of the investigation was subjected only to static loading; a summary of the tests conducted on each specimen is given in Table 4.1. For comparison, a summary of the tests performed by Boswell (2008) and Kreisa (2008) is provided in Table B.6.

As the purpose of testing was to study the behavior of skewed panels adjacent to expansion joints in bridge deck systems, loads were applied to the ends of the skewed panels. Panel A was loaded at midspan of the skewed end and then at midspan of the square end, whereas panel B was loaded only at midspan of the skewed end. In this chapter, loading equipment and locations, as well as the instrumentation used to measure the response of the specimen to the applied load are discussed.

Table 4.1 – Applied Loads to Test Specimen

	Specimen P30P3
No. of Tests	3
Test 1 Location	Southern Skewed End (Panel A)
Test 1 Type	Static
Test 2 Location	Northern Skewed End (Panel B)
Test 2 Type	Static
Test 3 Location	Square End (Panel A)
Test 3 Type	Static
Date of Test 1	8/13/2008
Date of Test 2	8/14/2008
Date of Test 3	9/04/2008

4.2 SPECIMEN LOADING

4.2.1 Loading Setup

Monotonically increasing static loads were applied to the test specimen. To apply load to the test specimen, a simple portal frame was constructed using two columns and two cross beams (Figure 4.1). The columns were bolted to the laboratory strong floor. Consisting of two modified W-sections, the cross beams were lifted into place and bolted to the flanges of the columns using a pneumatic impact wrench. A 60-ton hydraulic ram was bolted to a steel plate, which was then clamped to the bottom flanges of the cross beams. To measure the applied load, a 100-kip load cell was placed below the ram on top of steel load plate and elastomeric bearing pad, which together simulate the bearing area of a wheel from the rear axle of the HL-93 Design Truck (Figure 4.2). To assure uniform load distribution, a spherical head was placed between the load cell and ram. A steel

spacer was then placed between the load cell and steel load plate to preserve the stroke of the ram for testing.

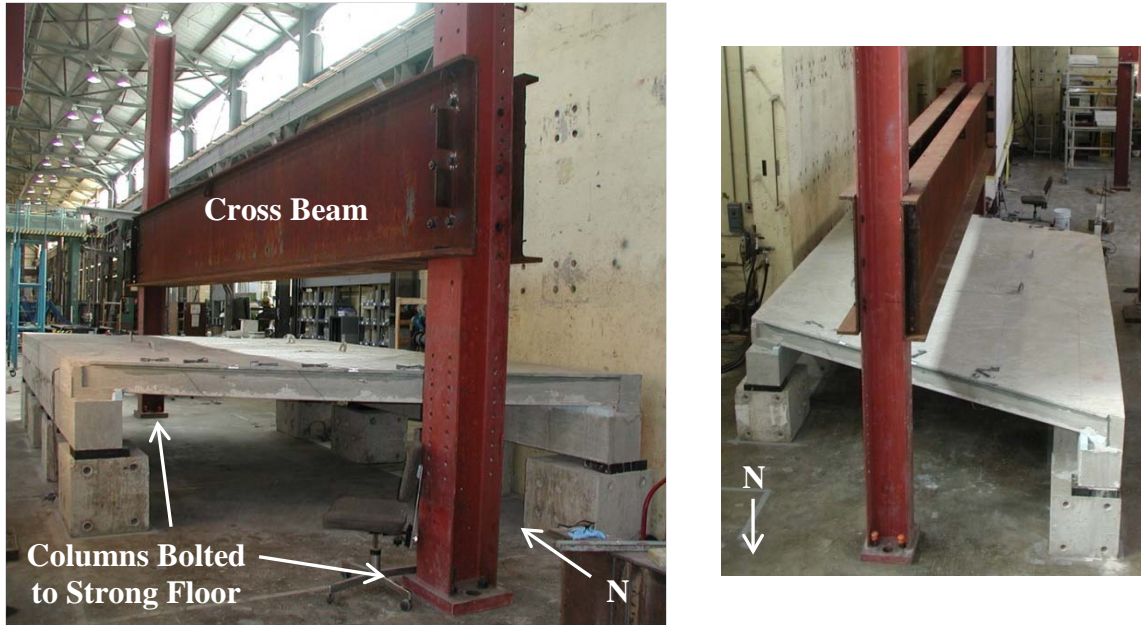


Figure 4.1 – Load Frame for Static Loading of Specimen P30P3

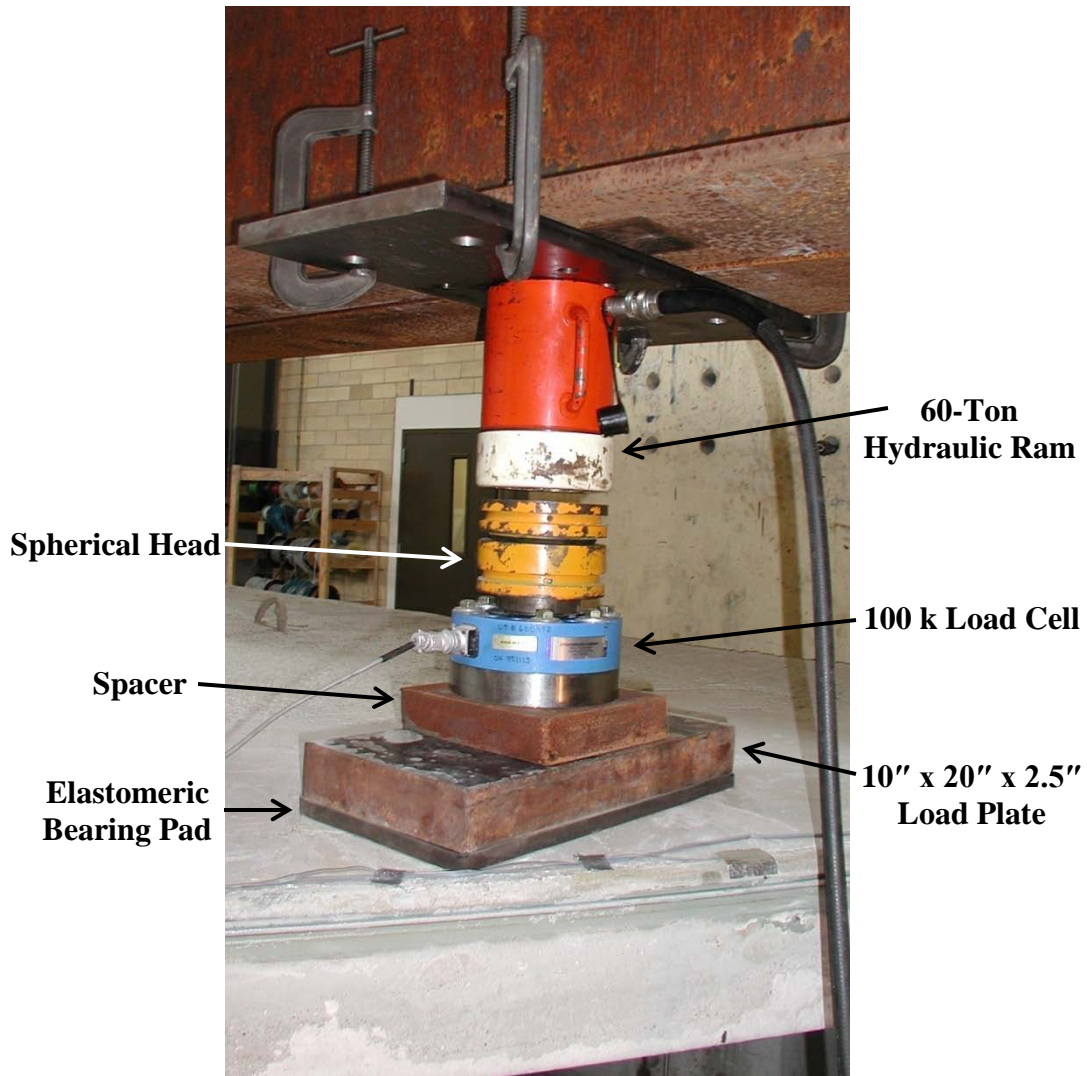


Figure 4.2 – Hydraulic Ram, Load Cell, and Load Plate for Specimen P30P3

4.2.2 Load Application

Static load was applied to the specimen in small increments (approximately 5 to 10 kips) at the locations shown in Figure 4.3. Testing locations for the specimens tested by Boswell (2008) and Kreisa (2008) are provided in Figure B.1 for comparison. For loads applied at midspan of the skewed end, the load plate was located adjacent to the SEJ, positioned so that it did not overlap the SEJ and rested only on concrete. When load was applied to the square end of panel A, the load plate was located at midspan of the

square end, 4 in. from the gap between the rectangular and skewed panels (Figure 4.3). The reason for placing the load plate 4" from the square end was to avoid loading the rectangular panel adjacent to the skewed panel. It was previously estimated that the effective width of the load would increase linearly with depth below the load plate; since the topping slab was 4 in. thick, the load plate was located 4 in. away from the gap between the panels (Figure 4.4).

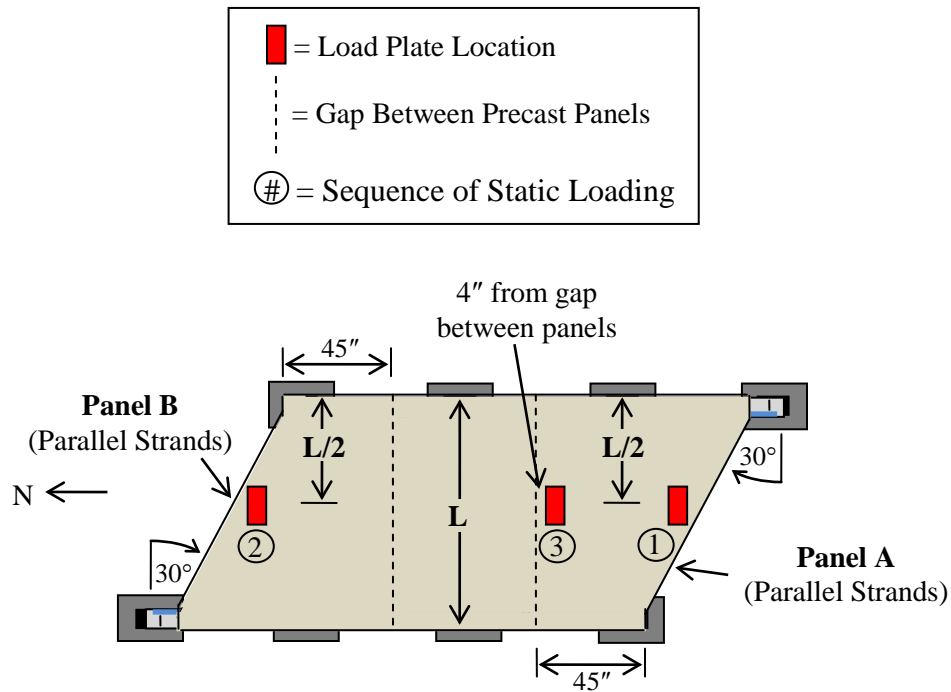


Figure 4.3 – Location of Load Plates and Order of Loading for Specimen P30P3

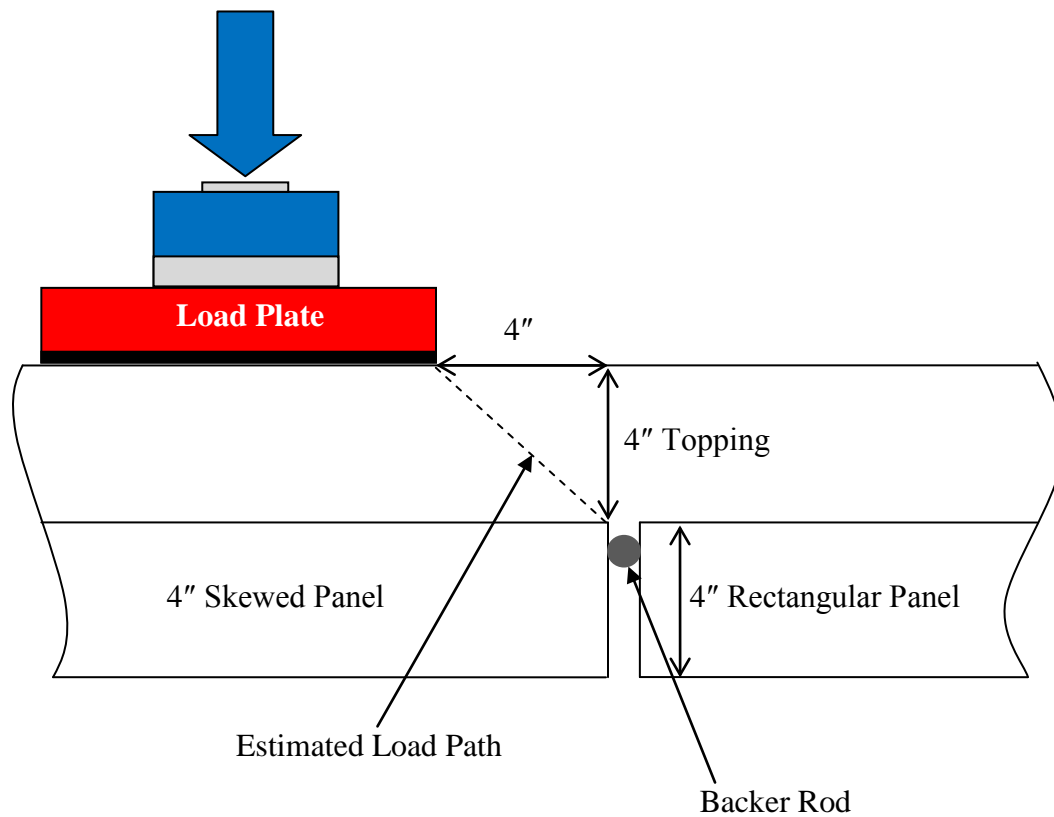


Figure 4.4 – Load Plate Position over Square End of Precast Panel
(Boswell 2008)

4.3 INSTRUMENTATION

To measure the response of the test specimen to applied loads, several types of instrumentation were used. Concrete strain gages were used to measure the changes in tensile strain on the bottom surface of the concrete panels. Compressive strains in the top surface of the SEJ were also measured using strain gages. Linear potentiometers were employed to measure overall vertical deflections. Table 4.2 summarizes the number of each type of instrumentation used for each test.

Table 4.2 – Instrumentation Quantities for Specimen P30P3

	Panel A		Panel B
	Load at Skewed End	Load at Square End	Load at Skewed End
Concrete Strain gages	3	0	3
SEJ Strain Gages	3	0	3
Linear Potentiometers	5	6	5

4.3.1 Strain Gages

In the previous phase of the investigation, some of the skewed panels were instrumented with strain gages on the strands and rebar during construction of the panels. Since the panels tested in this phase of the investigation were fabricated at a precast yard, no strain gages were installed on the prestressing strands or the mild reinforcement. To measure the change in tensile strain of the concrete, the bottom of each skewed precast panel was instrumented with three 60-mm strain gages along the skewed end (Figure 4.5). The top surface of each SEJ was instrumented with three 5-mm strain gages to measure the compressive strain in the SEJ (Figure 4.6). These strain gages measured the response of the specimen when loaded at midspan of the skewed ends. Since the square end of panel A was tested last, significant cracking had already occurred on the bottom surface of the specimen, so strain gages would not have yielded useful information.

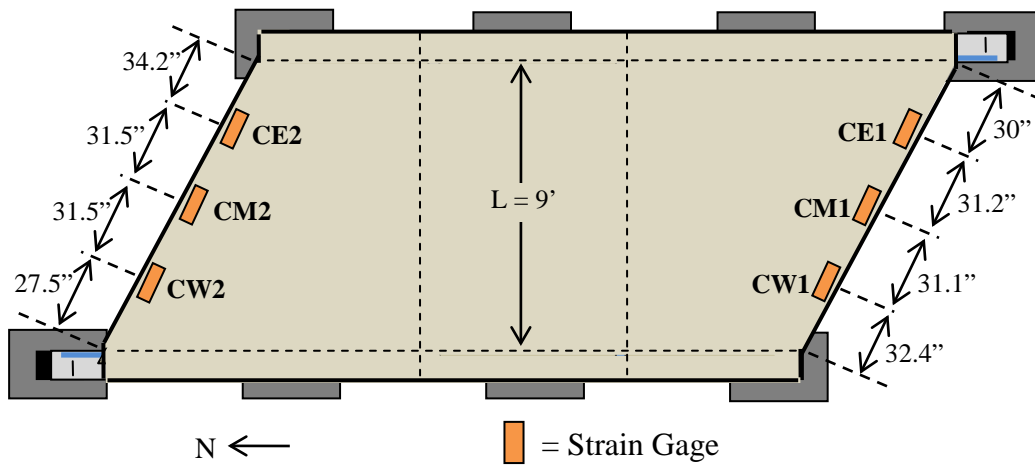


Figure 4.5 – Concrete Strain Gage Locations and Labels for Specimen P30P3

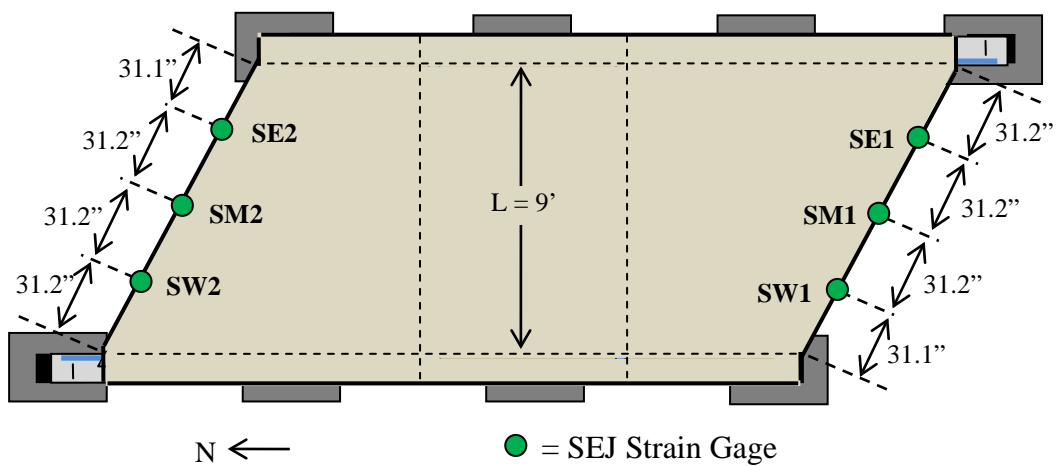


Figure 4.6 – SEJ Strain Gage Locations and Labels for Specimen P30P3

4.3.2 Linear Potentiometers

For load applied at midspan of each skewed end, five linear potentiometers were used to measure the overall vertical deflection response of each panel. When load was applied to midspan of the square end of panel A, six linear potentiometers were used to measure the deflection response. Figures 4.7 and 4.8 illustrate the locations and labels of

the linear potentiometers for load applied to the skewed ends and square end, respectively.

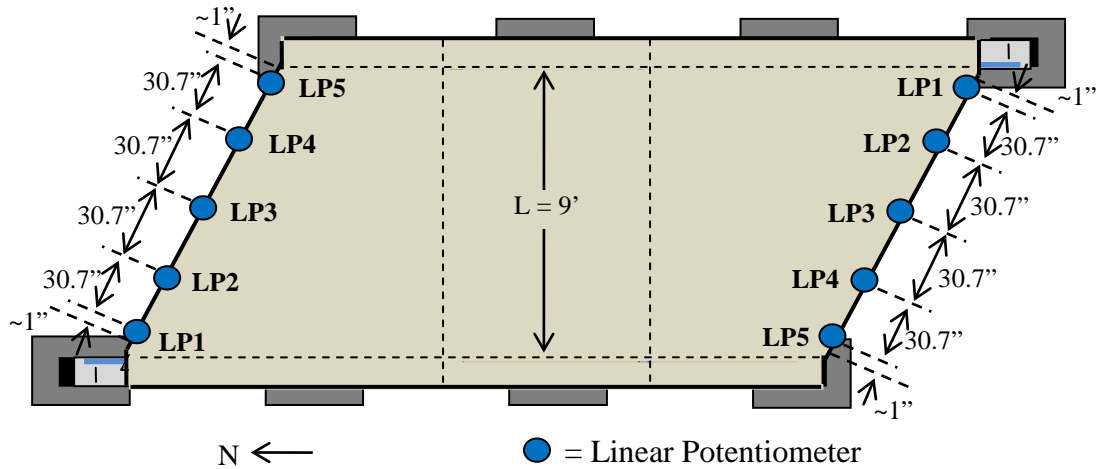


Figure 4.7 – Linear Potentiometer Locations and Labels for Specimen P30P3 for Load Applied at Midspan of Skewed Ends

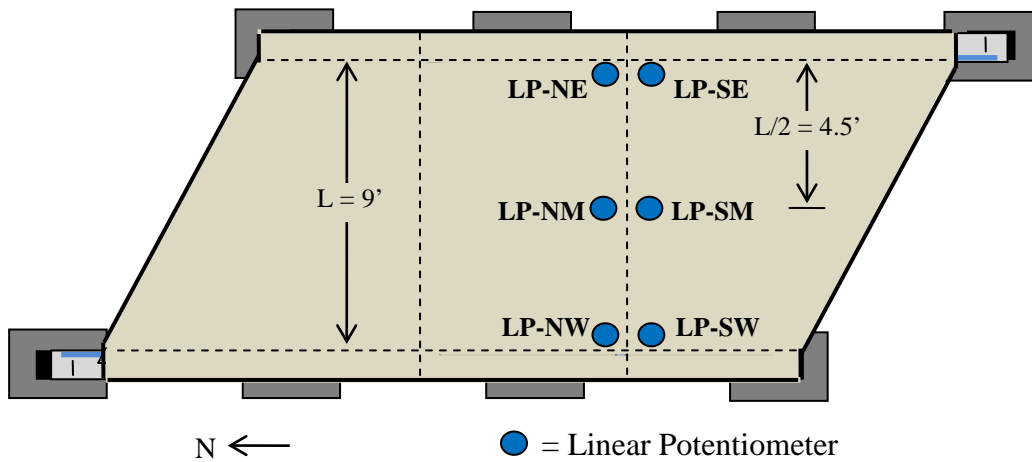


Figure 4.8 – Linear Potentiometer Locations and Labels for Specimen P30P3 for Load Applied at Midspan of Square End of Panel A

4.3.3 Data Collection

During testing, load data, deflections, and strains were collected using a digital data acquisition system and processed to produce graphs that provided information about the behavior of the specimen.

Chapter 5: Measured Response of Test Specimen

5.1 INTRODUCTION

The behavior of skewed prestressed concrete panels used adjacent to expansion joints was studied using the procedures presented in the previous chapters. The response of the specimen is presented in this chapter. Specific issues necessary to understand the presentation of the data are discussed in Section 5.2. The measured and observed response in each test is presented in Section 5.3 in the order of testing.

5.2 LOAD TESTS

As discussed in Chapter 4, three static tests were conducted, and consisted of vertical load applied at midspan of one end of a skewed precast panel. The response in each test is evaluated in this chapter using the measured deflections and strains. While Appendix A provides all measured data from the tests, the key data and observations necessary to understand response are presented in this chapter. For each test, overall deflections were measured along the end of the panel where the load was applied. The overall deflections were then adjusted to account for the relative displacement of the deck due to compression of the bearing pads and bedding strips. The idealized rigid body movement of the loaded end of the deck is illustrated in Figure 5.1. To determine the deflection (δ_x) at any location x along the loaded end, a linear relationship (Equations 5.1 and 5.2) was developed by Boswell (2008) using the displacements (δ_L and δ_S) at the supports. Once the rigid body displacement was calculated for each linear potentiometer location, the relative displacement response of the loaded panel was found by subtracting the rigid body movement from the overall deflection measured by the linear potentiometer.

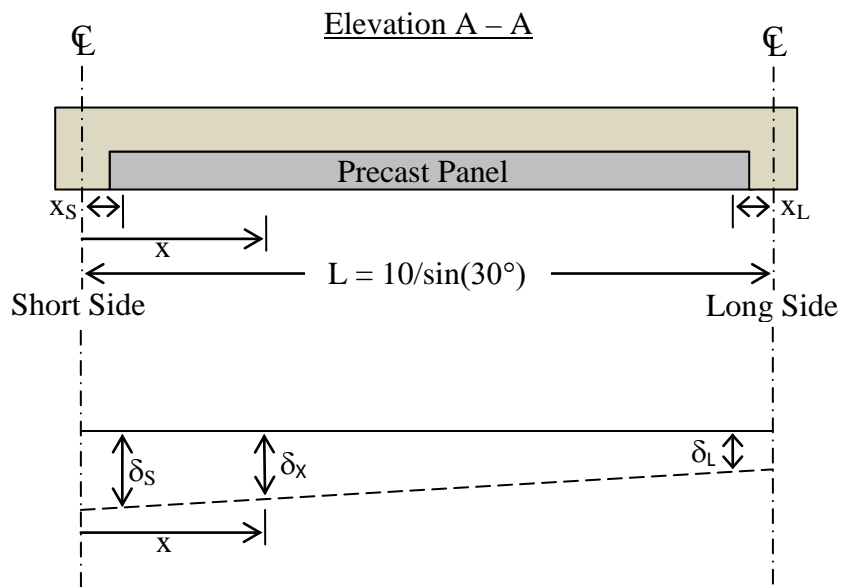
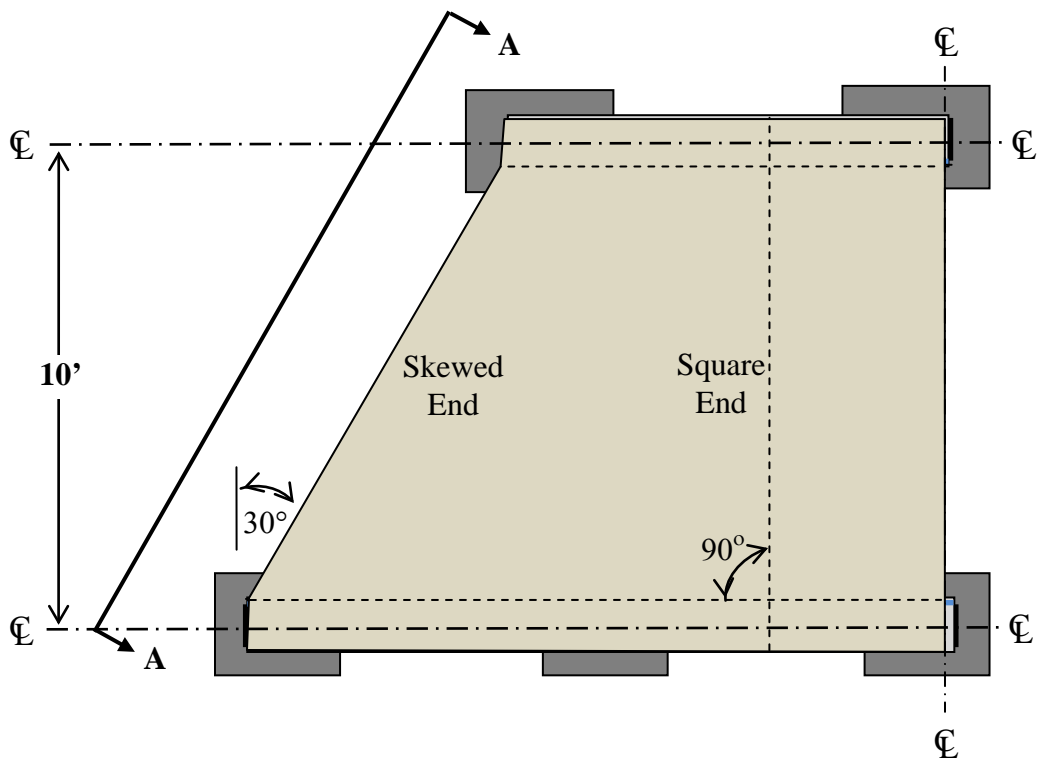


Figure 5.1 – Rigid Body Movement of Loaded End of Specimen P30P3 (modified from Boswell 2008)

$$\Delta(x) = \Delta_m(x) - \delta_x \quad (\text{Equation 5.1})$$

$$\delta_x = \left(\frac{\delta_L - \delta_S}{L - (x_L + x_S)} \right) x + \delta_S \quad (\text{Equation 5.2})$$

$\Delta(x)$ = Relative displacement at location x

$\Delta_m(x)$ = Measured displacement at location x

δ_x = Rigid-body Movement at location x

δ_L = Measured displacement near long support (LP1)

δ_S = Measured displacement near short support (LP5)

L = Length along displaced end from centerline to centerline of supports

x_L = Distance from centerline of long side support to LP1

x_S = Distance from centerline of short side support to LP5

x = Distance from centerline of short side support to location x

Since the prestressed panels of specimen P30P3 were fabricated at a precast yard, no data are available for changes in strand strain due to shrinkage and creep that occurred between the time of release of the strands in the precast panels and the time of testing. Independent production also prohibited the instrumentation of strain gages on the prestressing strands within the panels. In addition, the complicated geometry of the 30° panels prevented the precise calculation of precompression in the concrete caused by the act of prestressing. Thus, strain was not measured in the strands during testing and the reported values of strain measured on the bottom surface of the panels were live load induced strains due to the application of load. Strain data was primarily used to indicate changes in stiffness of the specimen under applied load.

When discussing the response of the specimen, several loads are used for comparison. For the HL-93 Design Truck in particular, three loads are considered, as defined in Table 5.1. The Service Wheel Load (P_w) is one half of the rear axle load for

the truck. The Design Wheel Load (P_L) relates to the Service Wheel Load amplified for impact, where $I = 0.33$. The Factored Wheel Load (P_U) is the product of the Design Wheel Load and live load factor.

Table 5.1 –Loads Corresponding to HL-93 Design Truck (Boswell 2008)

Load	Designation	Expression	Numerical Value
Service Wheel Load	P_W	P_W	16 kips
Design Wheel Load	P_L	$(1 + I) P_W$	21.3 kips
Factored Wheel Load	P_U	$1.75 P_L$	37.3 kips

During testing, the response of the specimen changed at different stages of loading. The load at which visible cracks formed on the surface of the specimen is referred to as the “apparent cracking load,” whereas “cracking load” denotes the load at which the instrumentation measured an appreciable change in the system stiffness. Finally, each specimen experienced failure at the “maximum applied load.”

Collected strain data indicate that some of the concrete strain gages were damaged during testing when the formation of a crack coincided with the location of a strain gage on the bottom surface of the panels. Data beyond the point at which the crack formed are unreliable and an “X” denotes the load at which this damage occurred. Figure 5.2 illustrates unaffected and damaged strain gages and how the data are displayed for each case.

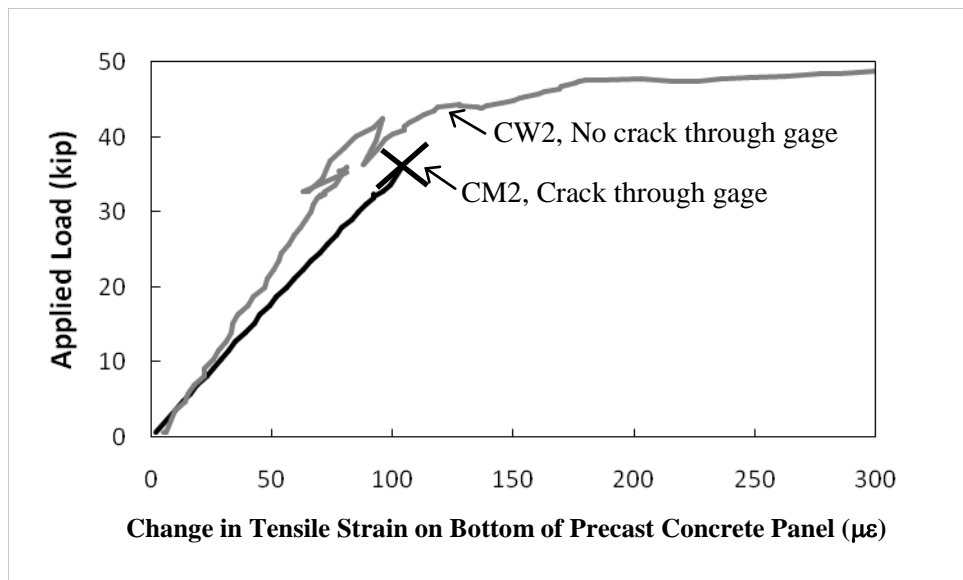
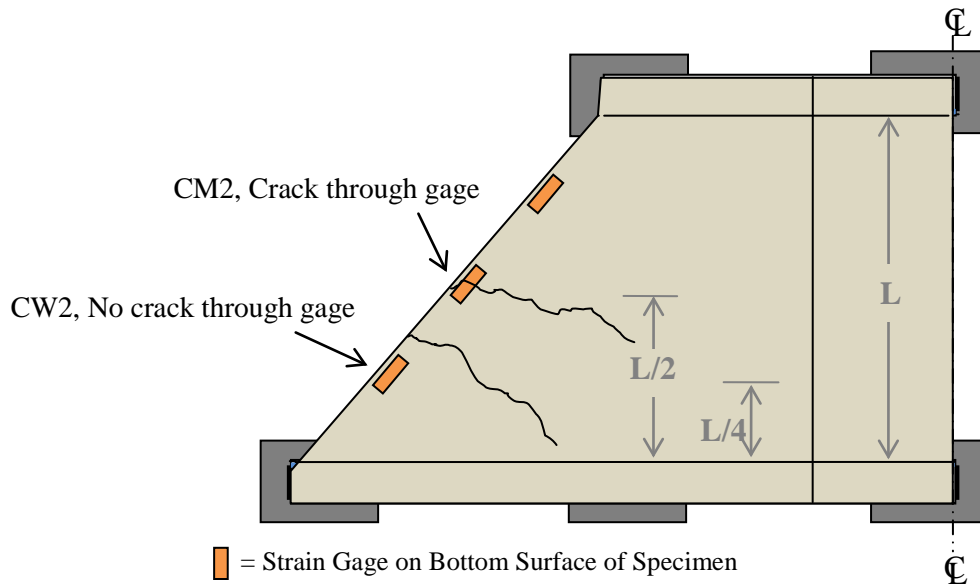


Figure 5.2 – Presentation of Strain Gage Data (Boswell 2008)

5.3 MEASURED RESPONSE OF SPECIMEN P30P3

Specimen P30P3 was tested monotonically to failure three times, first at midspan of the skewed end of panel A, next at midspan of the skewed end of panel B, and finally at midspan of the square end of panel A. In this section, data measured during each test,

including relative deflections along the loaded end, compressive strain on the top surface of the SEJ, and tensile strain on the bottom of the precast panel are presented.

5.3.1 Load Applied at Midspan of Skewed End of Panel A

As load was monotonically applied to the skewed end of panel A, visible cracks formed at about 20 kips. Shown in Figure 5.3, the measured displacement response indicates a cracking load of approximately 20 kips, with stiffness decreasing gradually for further loading. Failure of the specimen occurred at an ultimate load of 79 kips. The distribution of relative displacements along the skewed end is given in Figure 5.4.

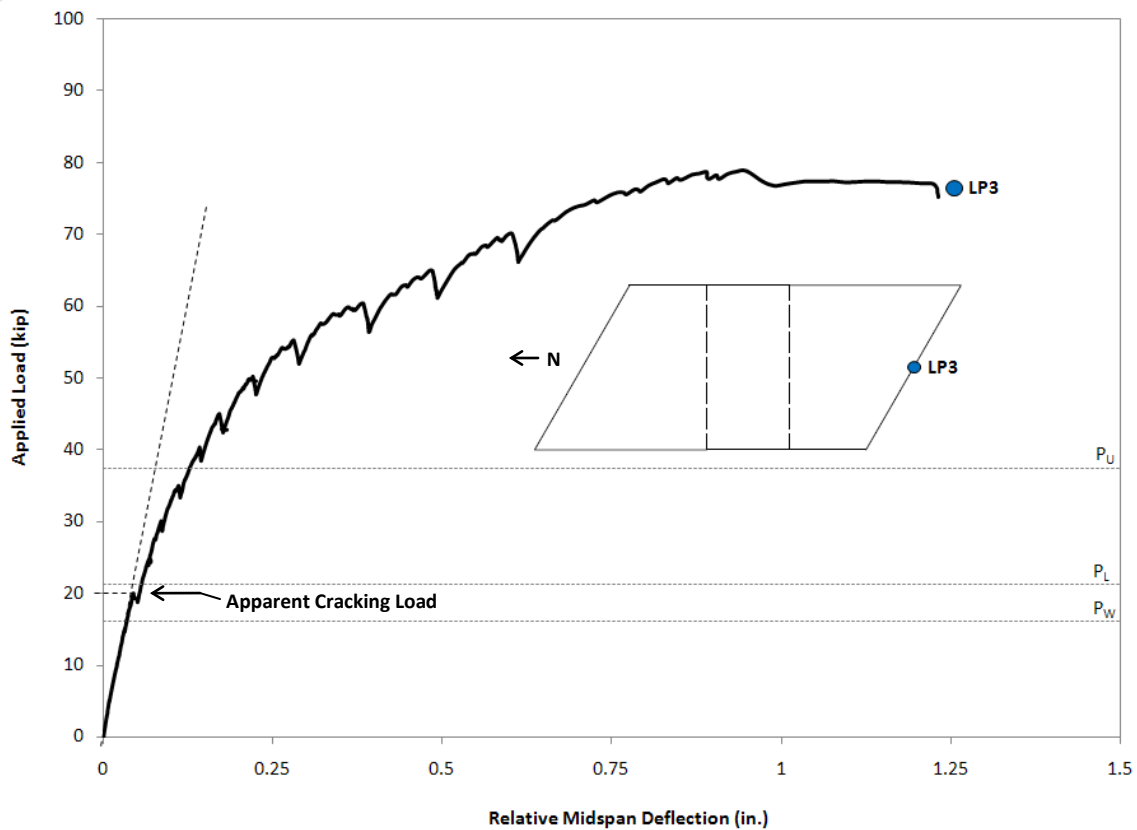


Figure 5.3 – Measured Displacement Response of Panel A for Load Applied at Midspan of Skewed End

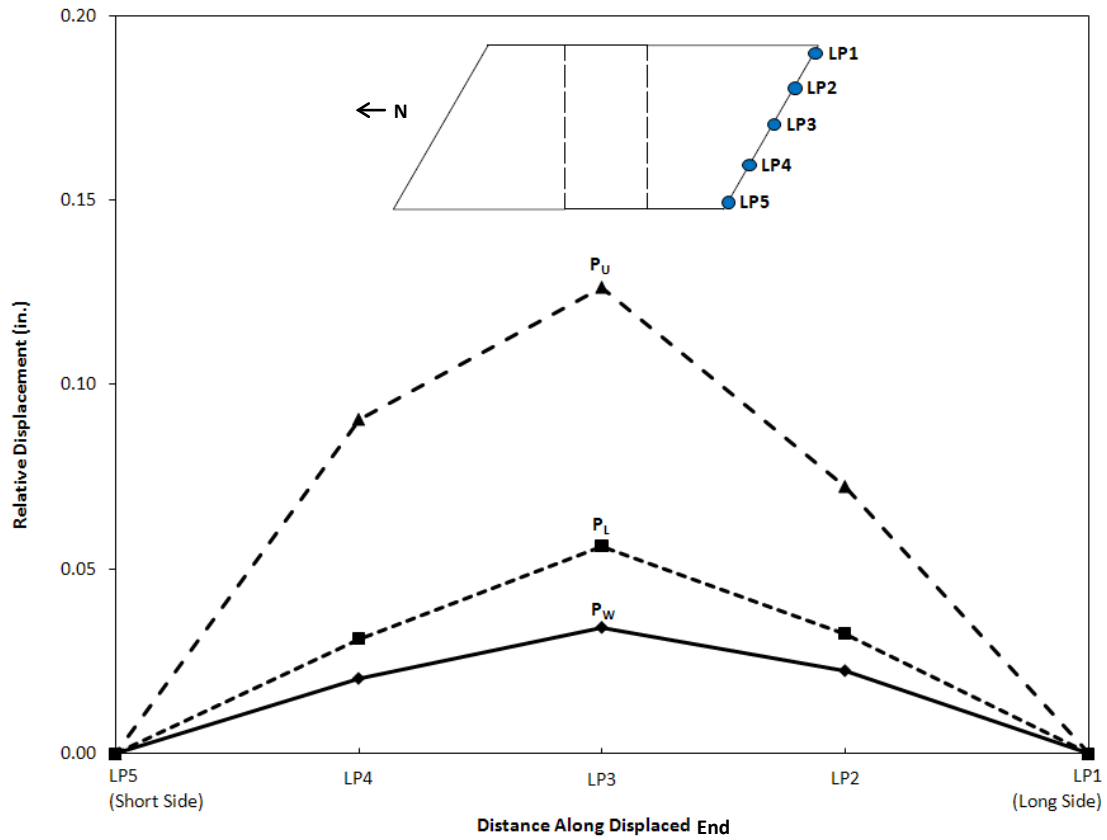


Figure 5.4 - Variation of Displacement along Skewed End of Panel A

The change in tensile strain data (Figure 5.5) from the bottom surface of the precast panel at midspan of the skewed end indicate that the strain gage was damaged at a load of about 25 kips. Since no change in stiffness can be observed from this concrete strain data, a cracking load could not be inferred. Variation of tensile strain on the bottom surface of the panel along the skewed end is shown in Figure 5.6.

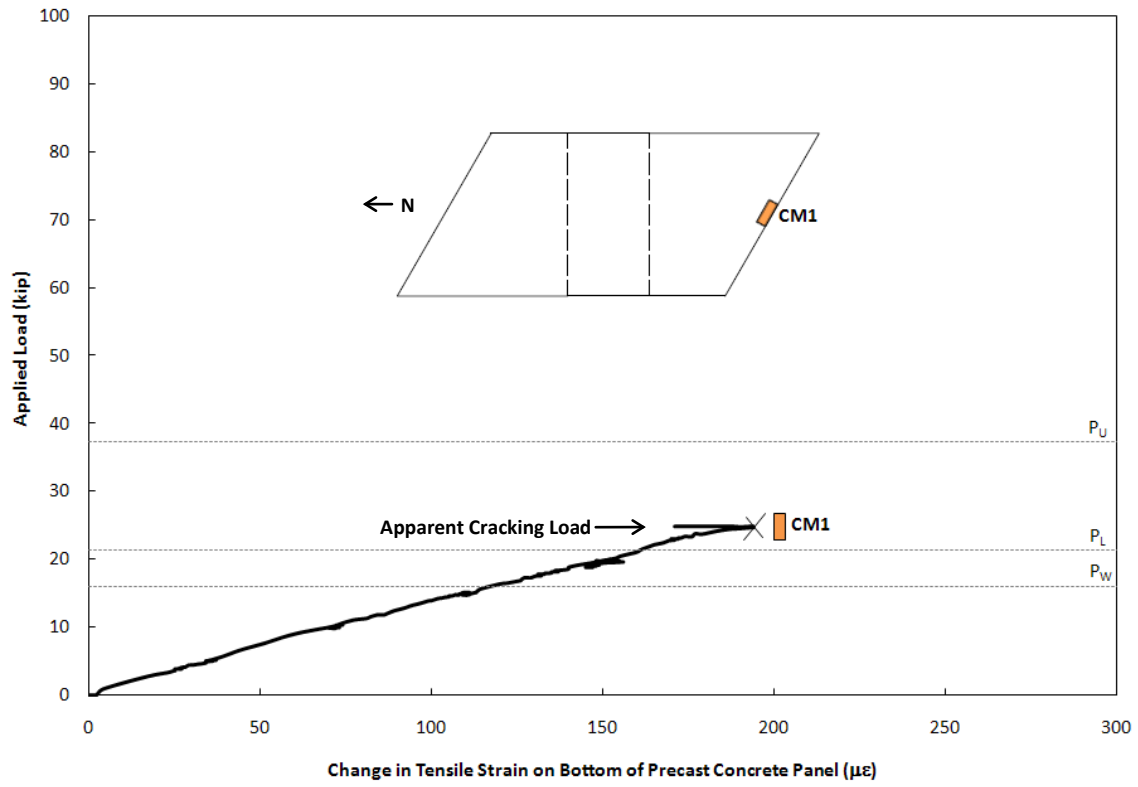


Figure 5.5 – Change in Tensile Strain on Bottom of Panel A at Midspan of Skewed End

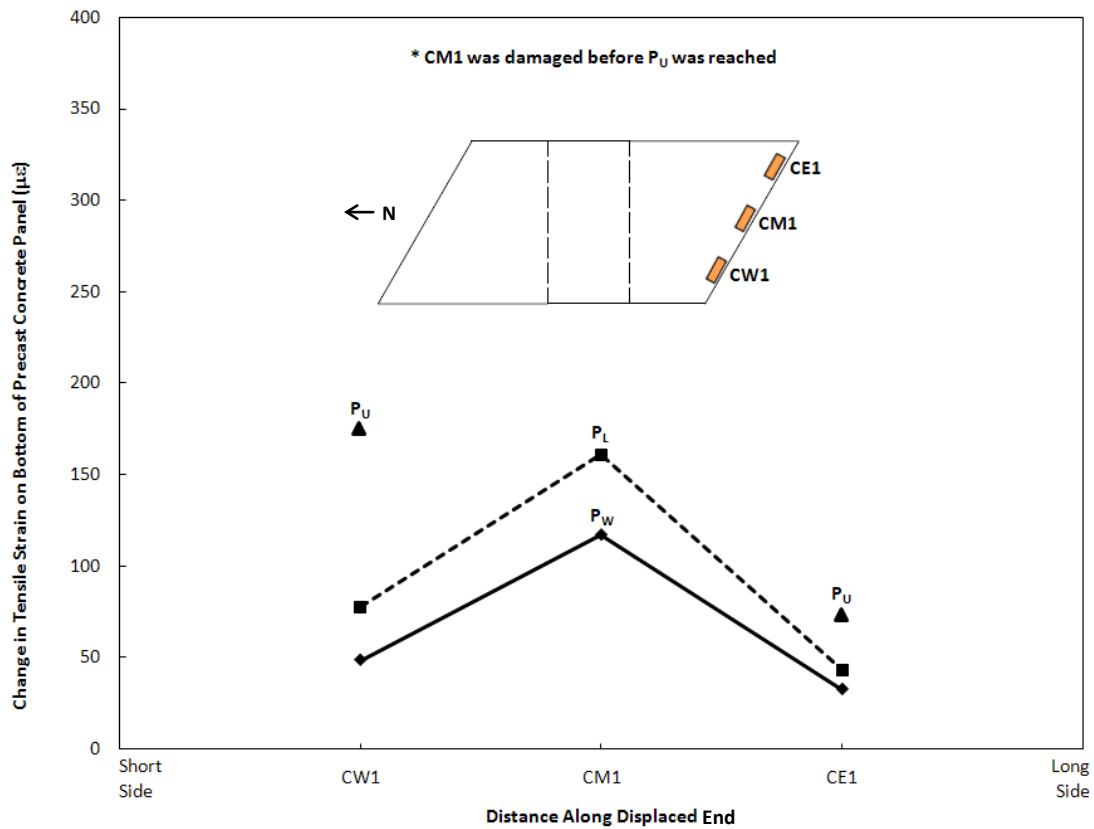


Figure 5.6 – Distribution of Change in Concrete Strain on Bottom of Panel A along Skewed End

Compressive strain data measured at midspan of the SEJ indicate a change in system stiffness, or cracking load of the specimen, at approximately 24 kips (Figure 5.7). Variation of compressive strain along the SEJ in panel A is given in Figure 5.8.

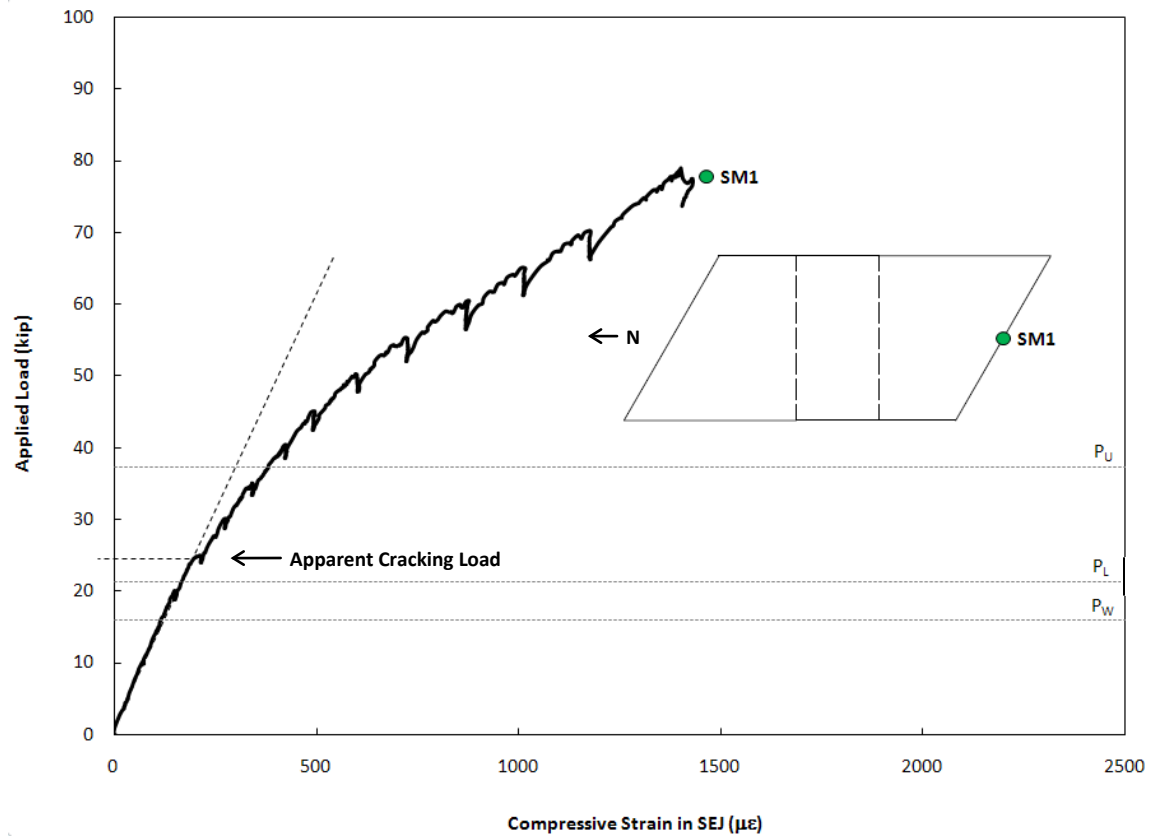


Figure 5.7 – Compressive Strain at Midspan of SEJ in Panel A

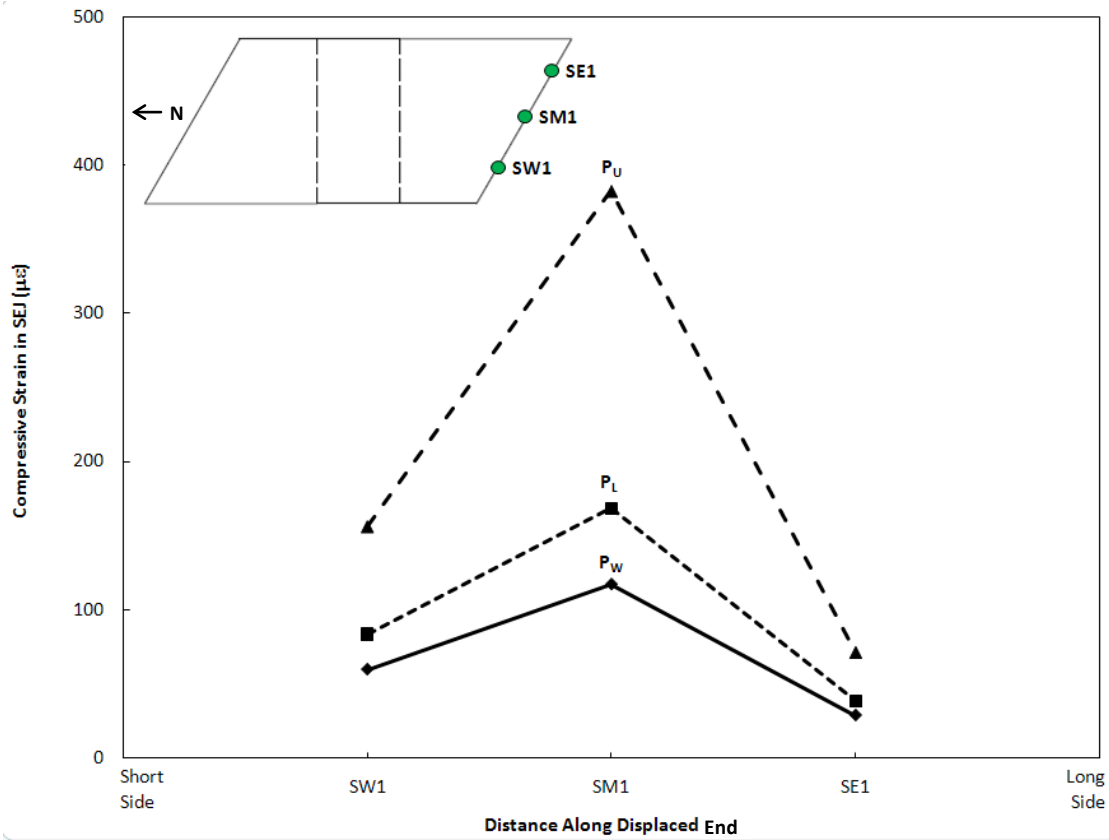


Figure 5.8 - Variation of Strain along SEJ of Panel A

Table 5.2 provides a summary of the apparent cracking loads from visual inspection and from instrumentation for testing of panel A along the skewed end.

Table 5.2 – Initial Stiffness and Apparent Cracking Load of Panel A for Load Applied at Midspan of Skewed End

	Initial Stiffness (k/in, k/ $\mu\epsilon$)	Apparent Cracking Load (kip)
Displacement	372.8	20
Concrete Strain on Bottom of Panel	0.143	-
SEJ Strain	0.124	24
Apparent Cracks	-	20

At the conclusion of the static test to failure, cracks on the top and bottom surfaces of panel A were recorded (Figure 5.9). Unlike the 30° specimens tested by Boswell (2008) and Kreisa (2008), no delamination between the panel and topping slab was observed at the maximum applied load. Rather, the failure mechanism for the skewed end of panel A was a shear failure that occurred at the short side support. Photographs of the specimen at the conclusion of the test are provided in Figures 5.10 and 5.11.

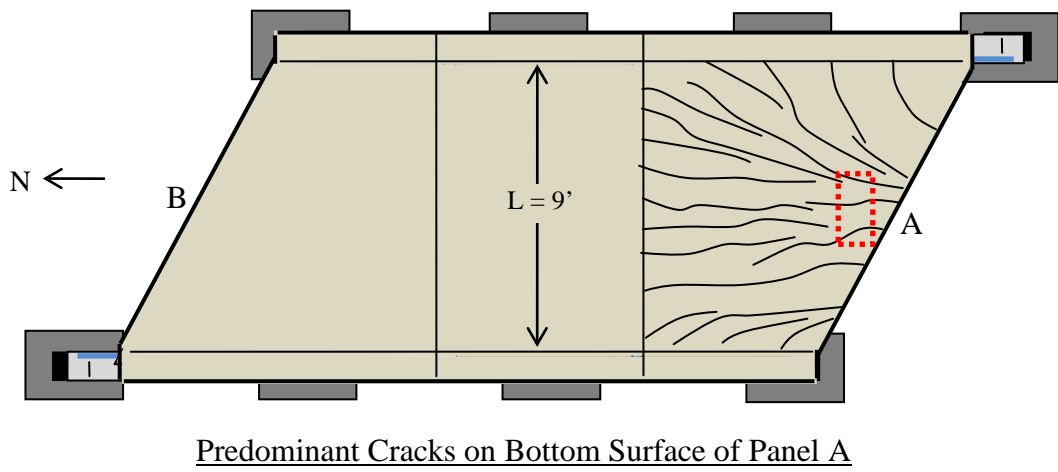
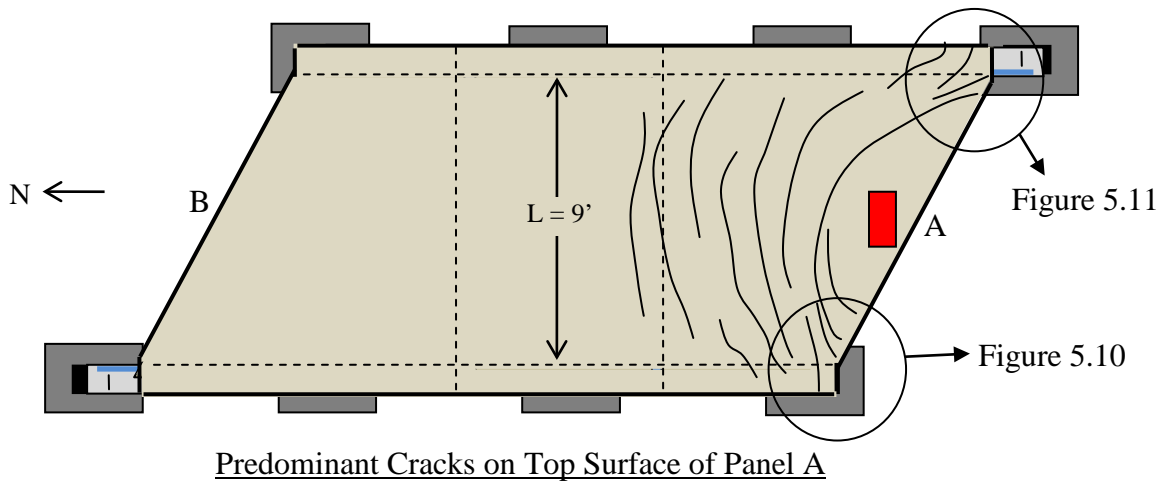


Figure 5.9 – Observed Cracks at Conclusion of Static Test of Panel A for Load Applied at Midspan of Skewed End

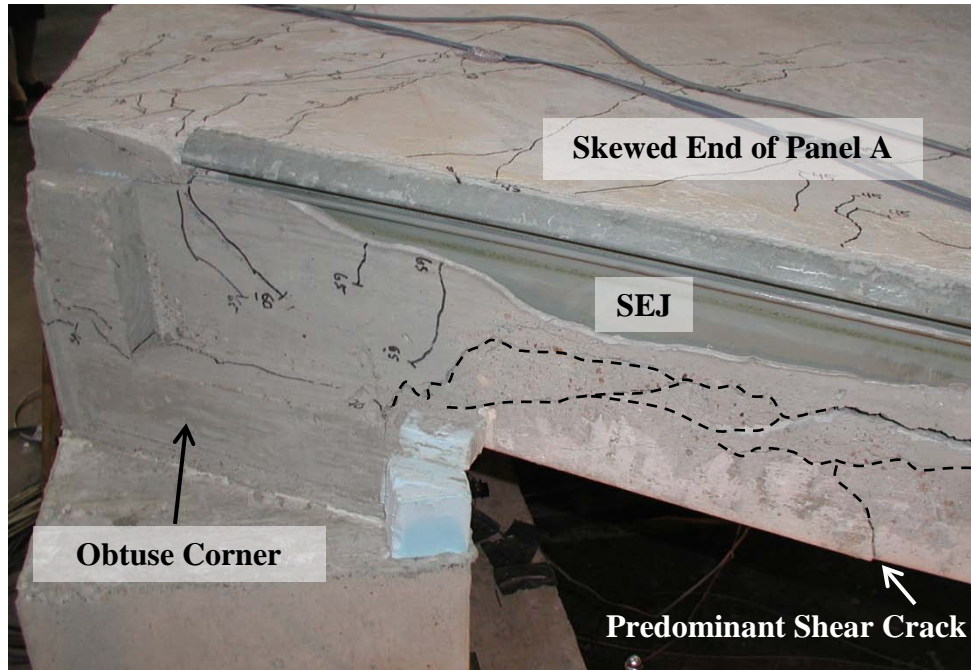


Figure 5.10 – Photograph of Skewed End of Panel A at Conclusion of Static Test for Load Applied at Midspan of Skewed End

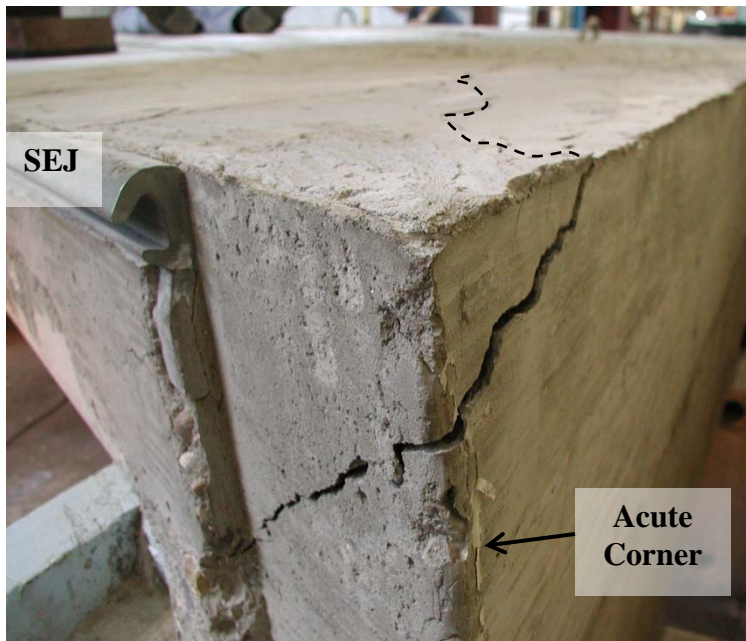


Figure 5.11 – Photograph of Skewed End of Panel A at Conclusion of Static Test for Load Applied at Midspan of Skewed End

5.3.2 Load Applied at Midspan of Skewed End of Panel B

The second test conducted on specimen P30P3 was static loading at midspan of the skewed end of panel B. As load was applied, cracks became visible at approximately 20 kips. The measured displacement response at midspan (Figure 5.12) indicates a slightly lower cracking load of about 18 kips, with gradually decreasing system stiffness upon further loading. Variation of the relative displacements along the skewed end is provided in Figure 5.13.

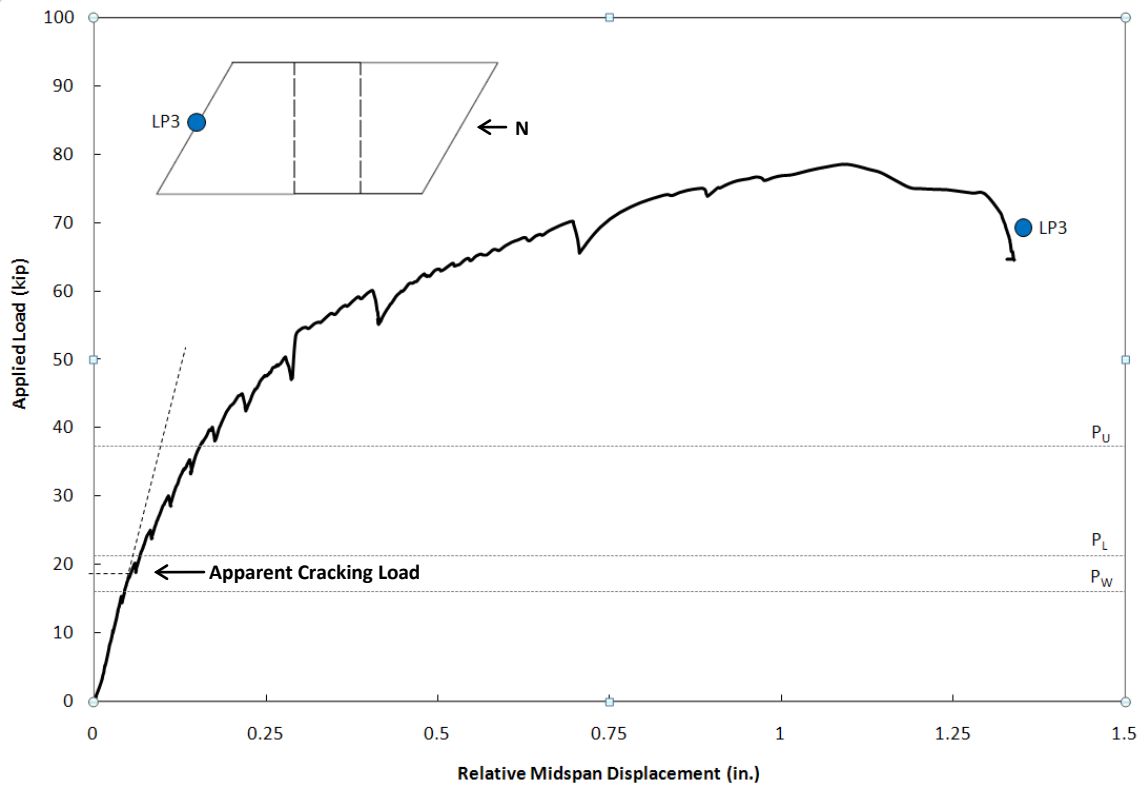


Figure 5.12 – Measured Displacement Response of Panel B for Load Applied at Midspan of Skewed End

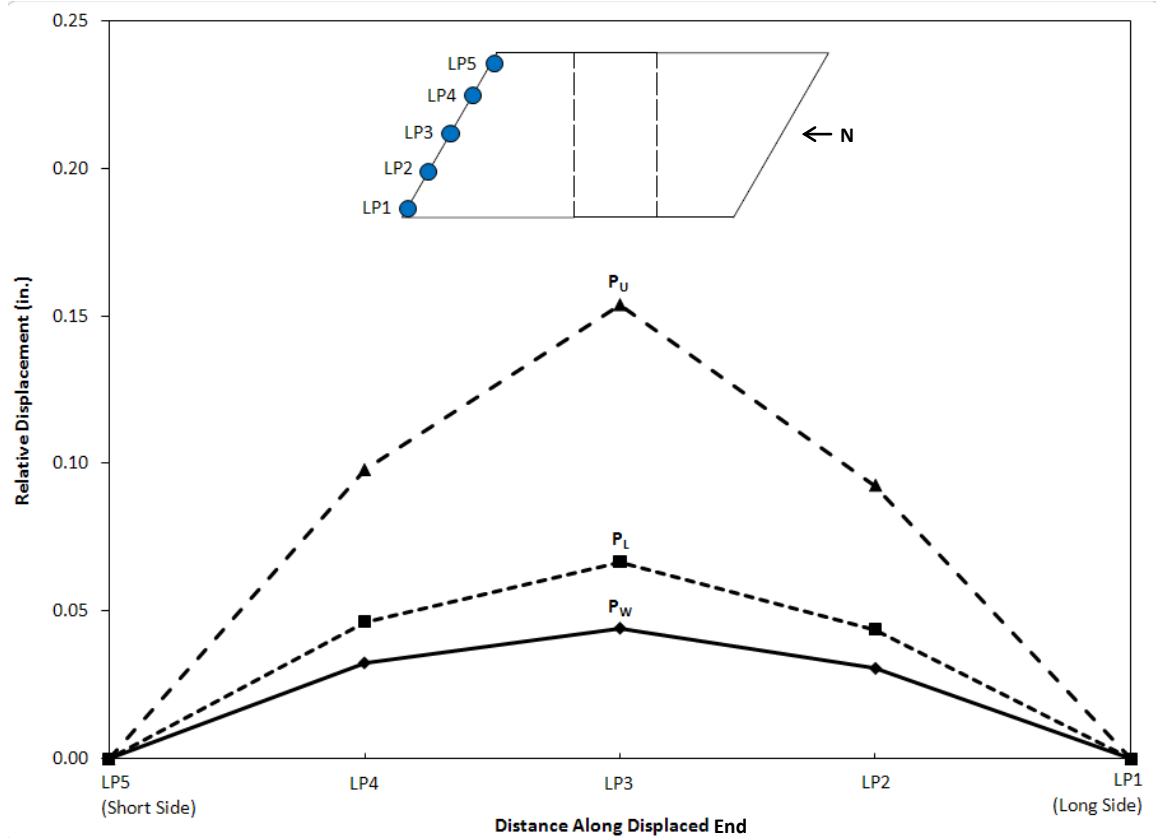


Figure 5.13 - Variation of Displacement along Skewed End of Panel B

The change in tensile strain on the bottom surface of the precast panel at midspan of the skewed end indicates a cracking load of about 16 kips. Variation of tensile strain on the bottom surface of the panel along the skewed end is shown in Figure 5.15.

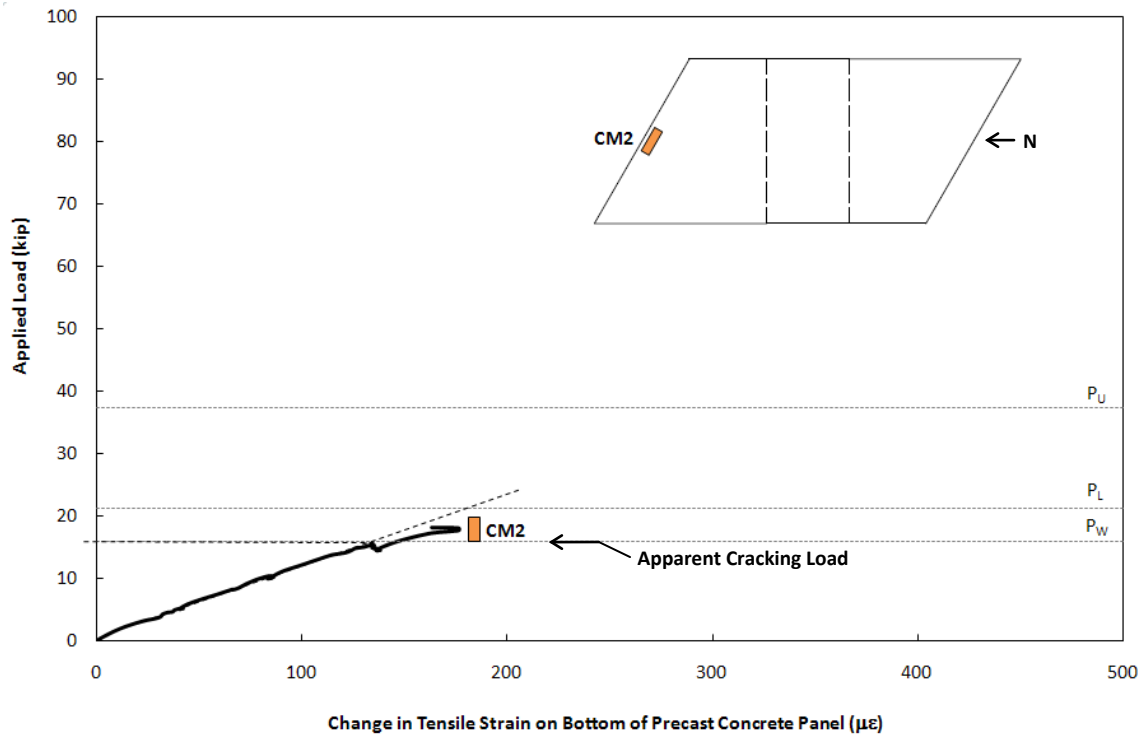


Figure 5.14 – Change in Tensile Strain on Bottom of Panel B at Midspan of Skewed End

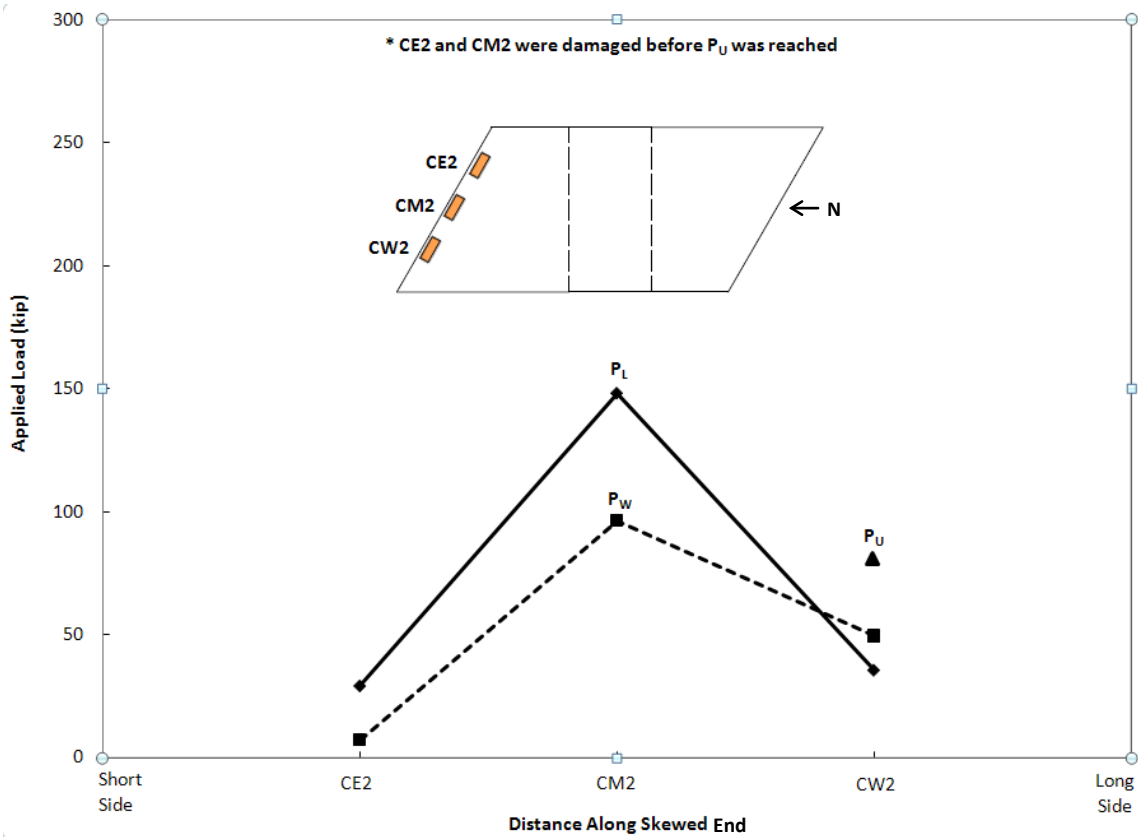


Figure 5.15 – Distribution of Change in Concrete Strain on Bottom of Panel B along Skewed End

Compressive strain data at midspan of the SEJ (Figure 5.16) indicates a cracking load for panel B of about 17 kips. Variation of strain along the top surface of the SEJ is provided in Figure 5.17.

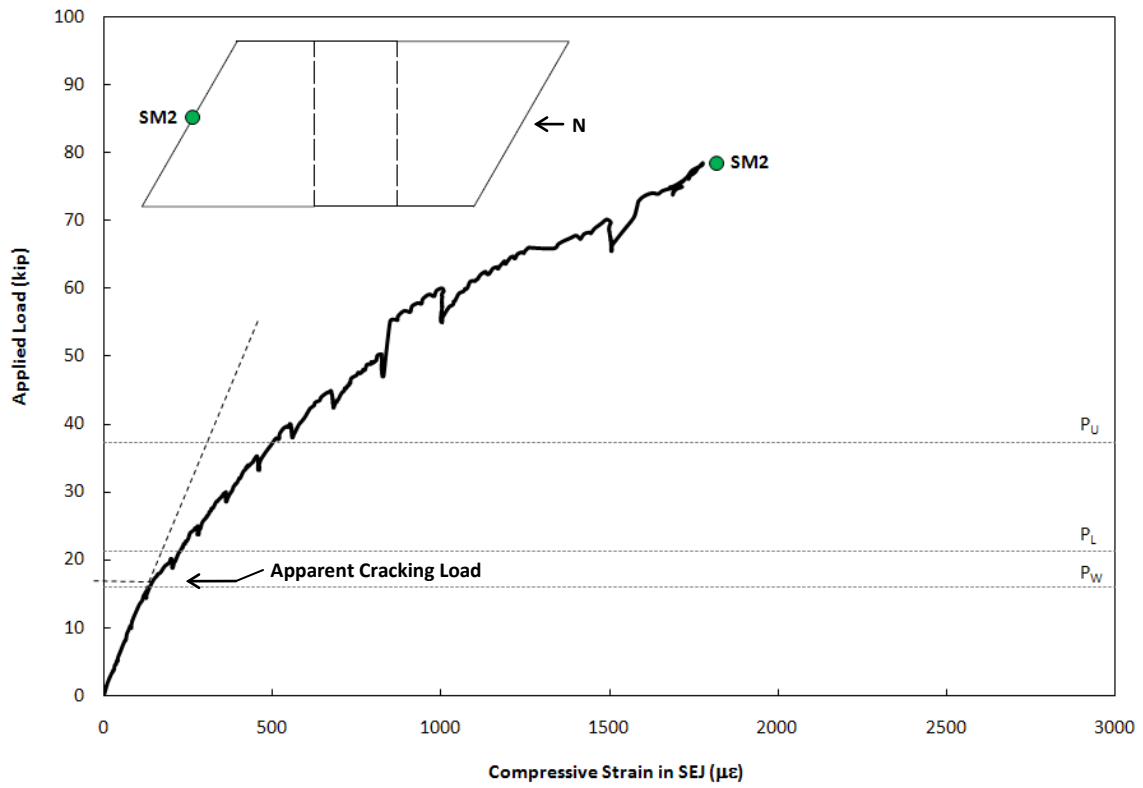


Figure 5.16 – Compressive Strain at Midspan of SEJ in Panel B

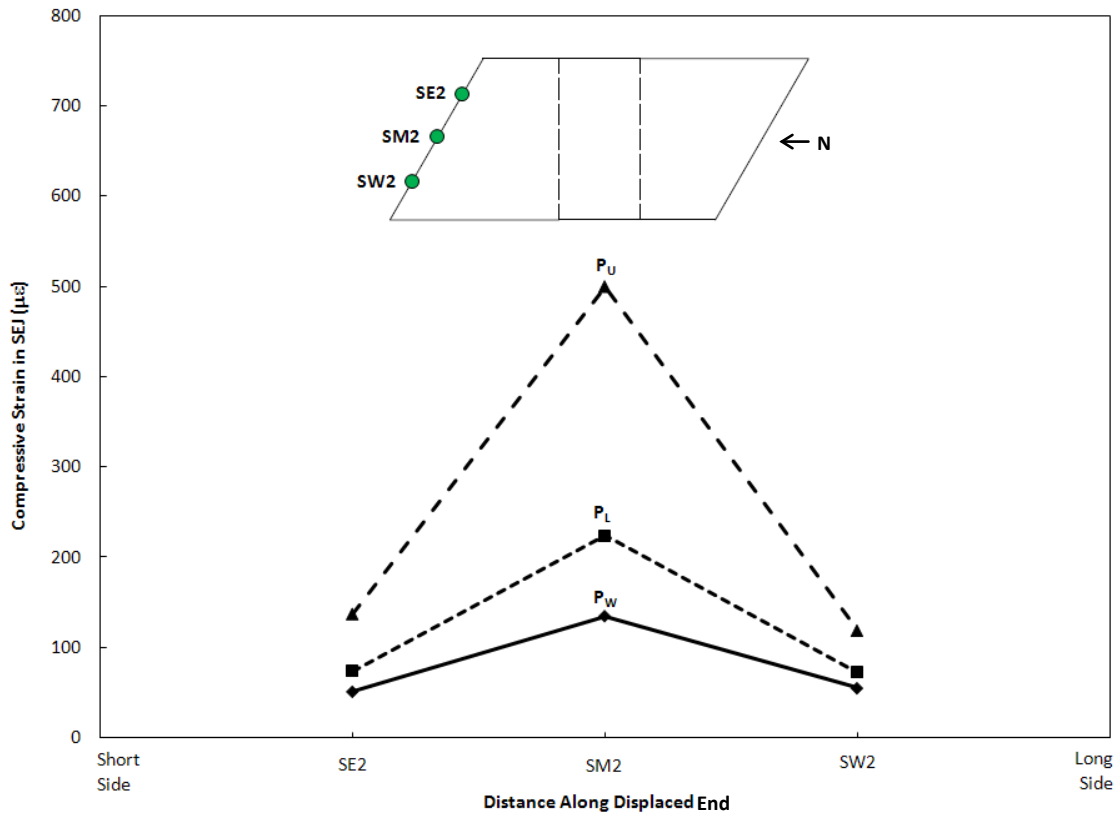


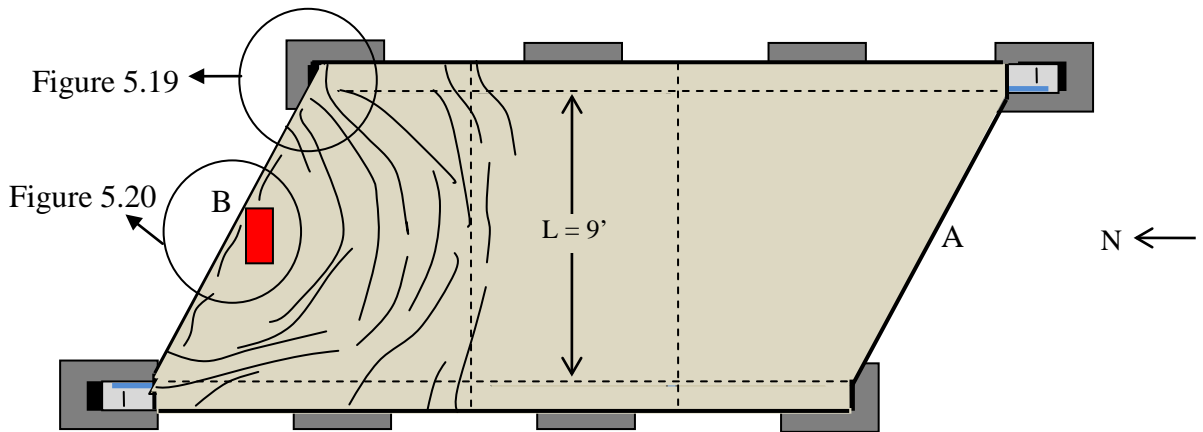
Figure 5.17 - Variation of Strain along SEJ of Panel B

Table 5.3 provides a summary of the cracking loads inferred from instrumentation data and the apparent cracking load for panel B when load was applied at midspan of the skewed end.

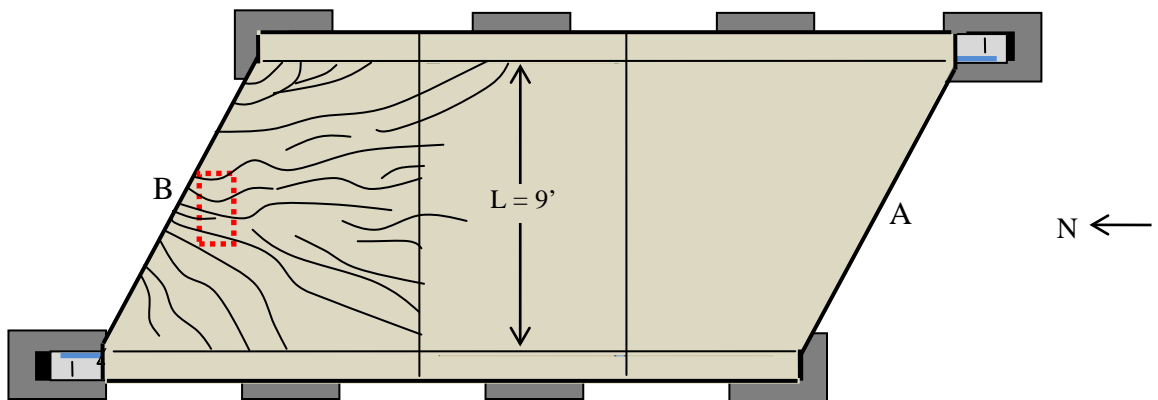
Table 5.3 – Initial Stiffness and Apparent Cracking Load of Panel B for Load Applied at Midspan of Skewed End

	Initial Stiffness (k/in, k/ $\mu\epsilon$)	Apparent Cracking Load (kip)
Displacement	386.4	18
Concrete Strain on Bottom of Panel	0.119	16
SEJ Strain	0.117	17
Apparent Cracks	-	20

Shear failure occurred at the short side support of panel B at a maximum applied load of approximately 79 kips. As with the first test, no delamination was observed between the panel and topping slab. At the conclusion of the static test to failure, observed cracks on the top and bottom surfaces of the specimen were recorded (Figure 5.18) and photographs were taken (Figures 5.19 and 5.20).



Predominant Cracks on Top Surface of Panel B



Predominant Cracks on Bottom Surface of Panel B

Figure 5.18 – Observed Cracks at Conclusion of Static Test of Panel B for Load Applied at Midspan of Skewed End

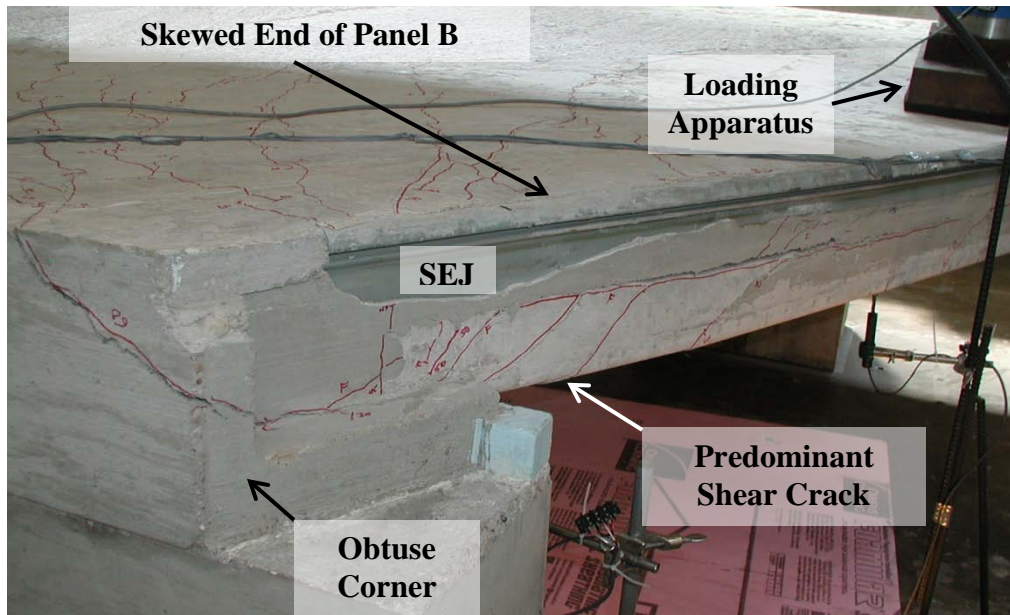


Figure 5.19 – Photograph of Panel B at Conclusion of Static Test for Load Applied at Midspan of Skewed End

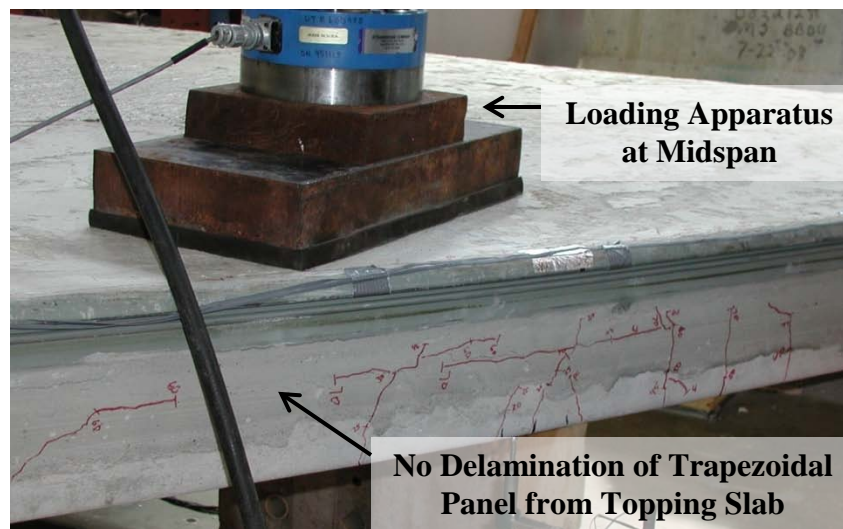


Figure 5.20 – Photograph of Panel B at Conclusion of Static Test for Load Applied at Midspan of Skewed End

5.3.3 Load Applied at Midspan of the Square End of Panel A

After the skewed ends of specimen P30P3 had been monotonically tested to failure, panel A was loaded at midspan of the square end. Since significant cracking had occurred during the first two tests of the member, it was not possible to determine the load at which new cracks appeared during the third test.

Measured displacement responses at midspan of the square ends of both the rectangular and skewed panels of panel A are shown in Figure 5.21. As the skewed panel had experienced significant cracking during the first test along the skewed end, it demonstrated a lower initial stiffness than the rectangular panel. Whereas data from the rectangular panel indicates a cracking load of approximately 42 kips, the skewed panel data implies a change in system stiffness at only 25 kips. The displacement data shows that the linear potentiometers were removed from the test setup at about 70 kips to avoid damage to them, although the specimen was subjected to further loading. At around 115 kips, panel A failed due to punching shear in the topping slab.

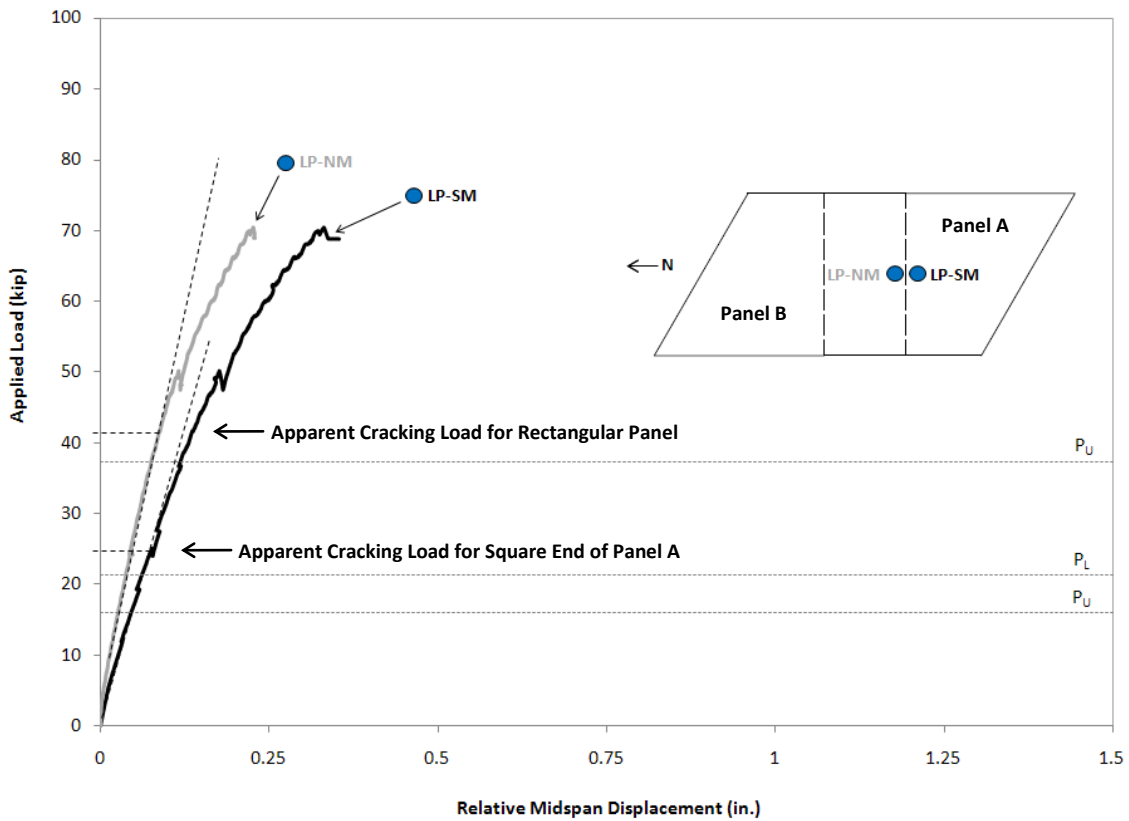
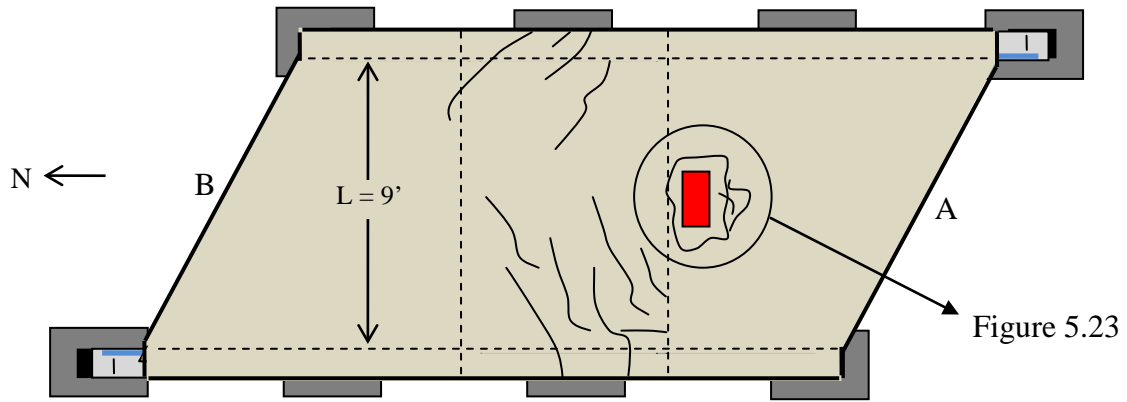
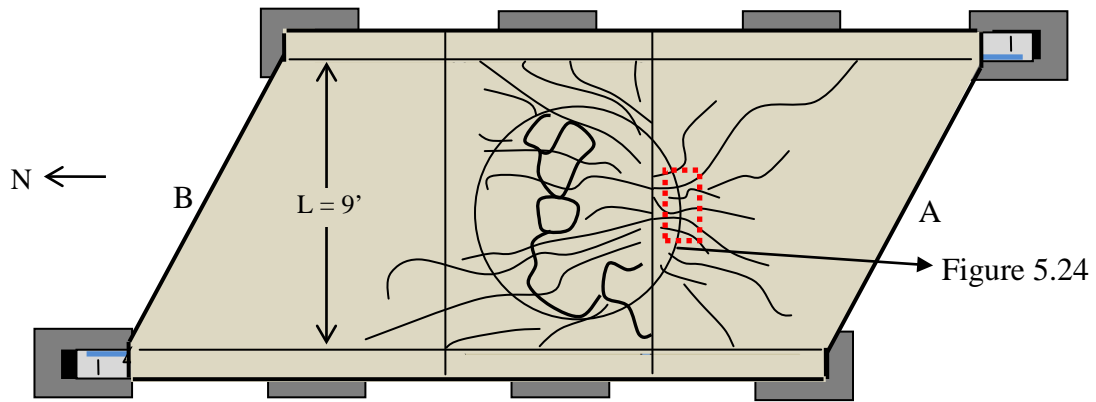


Figure 5.21 – Measured Displacement Response at Midspan of Square End of Panel A

Upon conclusion of test on the square end of specimen A, the observed cracks on the specimen were recorded (Figure 5.22) and photographs were taken (Figures 5.23 and 5.24). Punching shear cracks on the top surface of the specimen are displayed in Figure 5.23, while Figure 5.24 shows large segments of concrete that spalled off of the bottom of the rectangular panel at failure.



Predominant Cracks on Top Surface of Specimen P30P3



Predominant Cracks on Bottom Surface of Specimen P30P3

*Bolded Lines Denote Concrete that Spalled at Failure

Figure 5.22 – Observed Cracks at Conclusion of Static Test of Panel A for Load Applied at Midspan of Square End

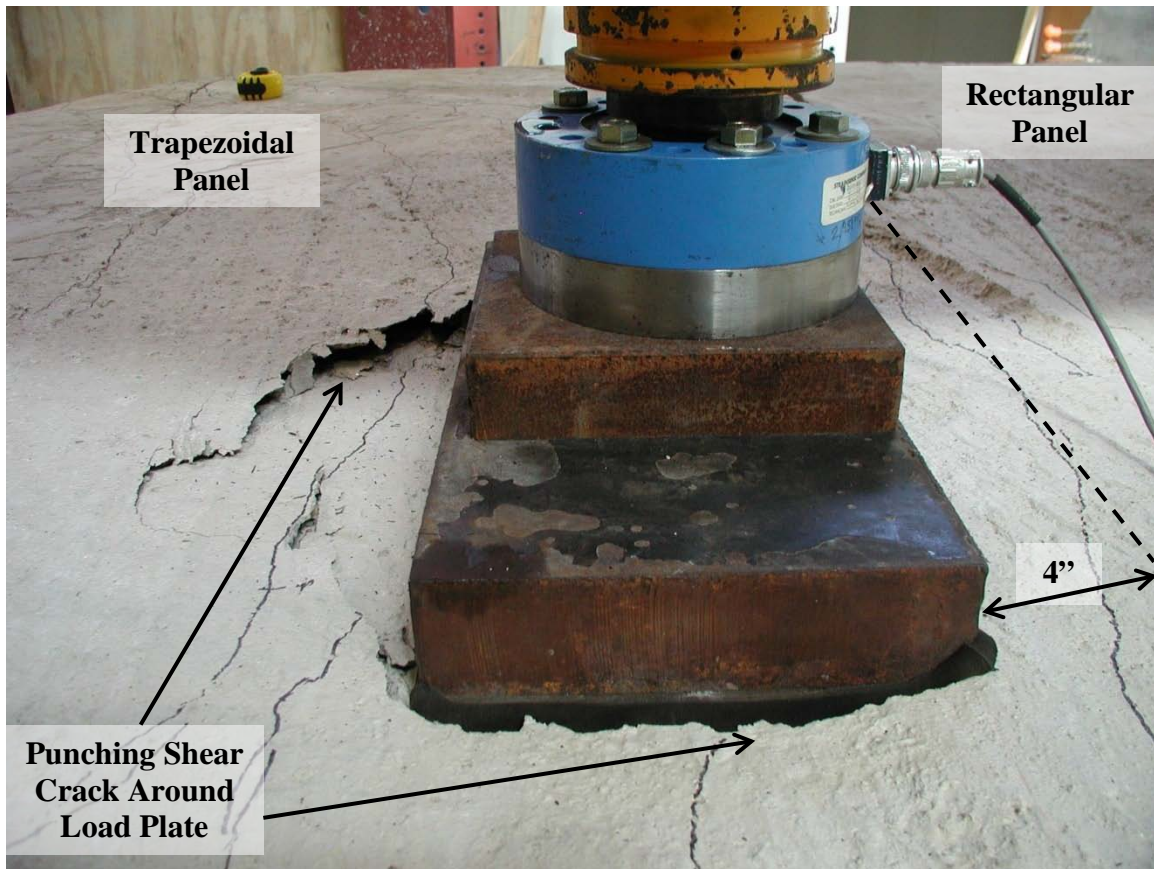
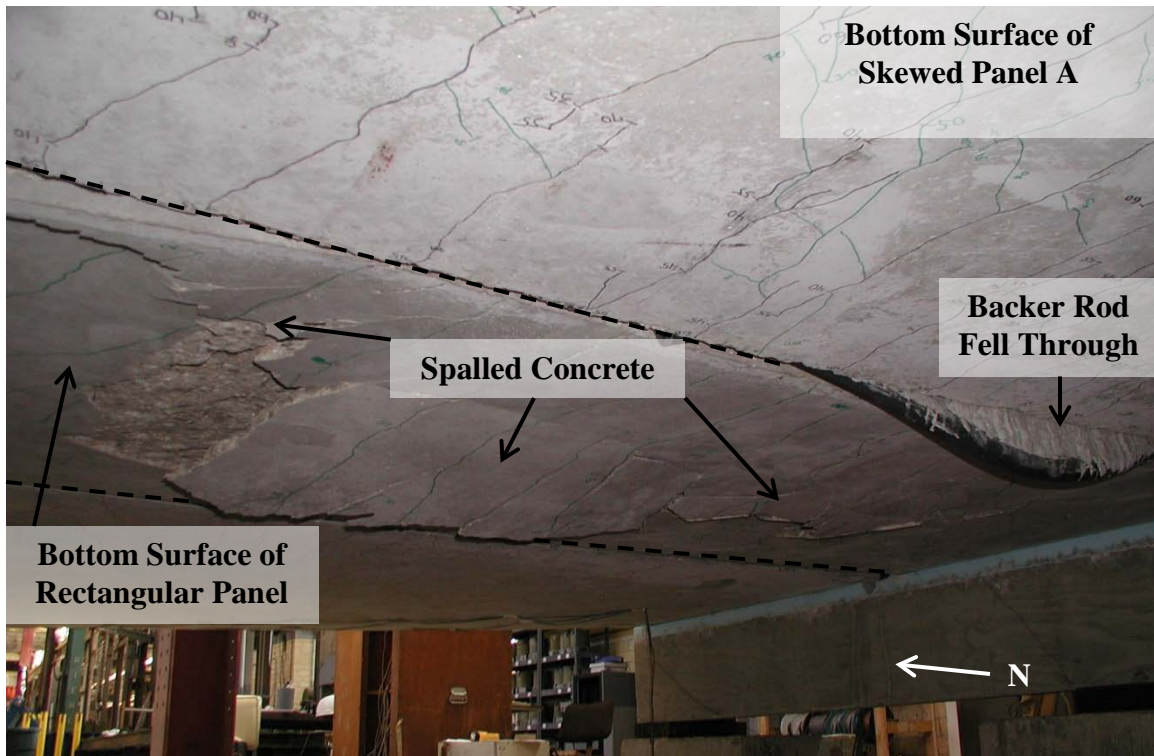
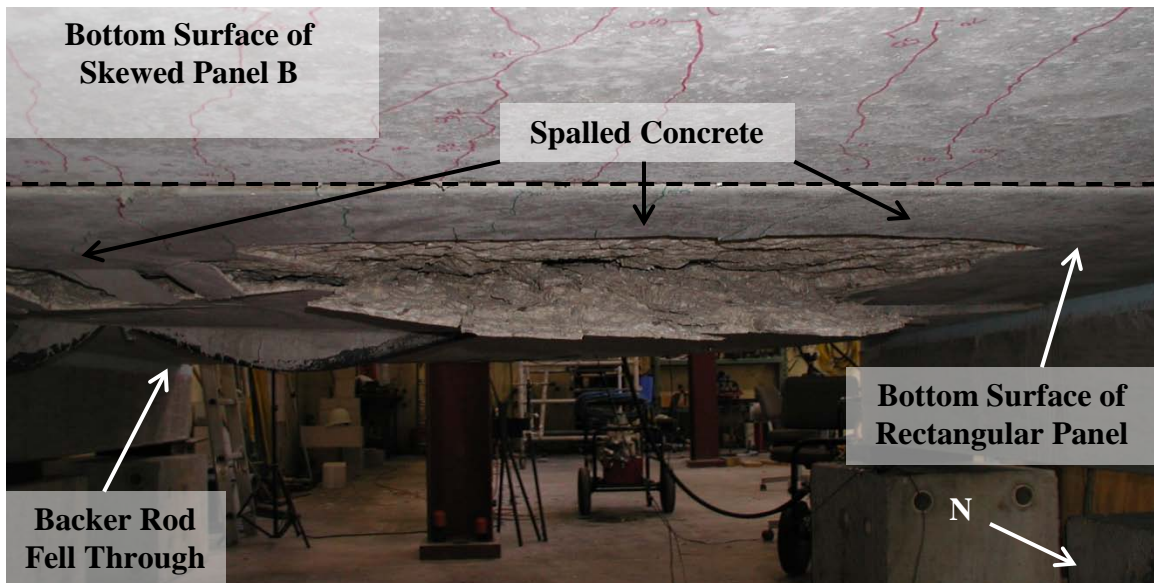


Figure 5.23 – Photograph of Punching Shear Failure under Load Applied at Midspan of the Square End of Panel A



(a) View of Underside of Specimen from South End



(b) View of Underside of Specimen from North End

Figure 5.24 – Photograph of Spalled Concrete at Conclusion of Test of Panel A for Load Applied at Midspan of Square End

5.4 SUMMARY

The response of the test specimen to loads applied at midspan of the skewed and square ends is summarized in Table 5.4. For comparison, a summary is also provided for the specimens tested by Boswell (2008) and Kreisa (2008) in Table B.7.

When load was applied at midspan of the skewed end, the cracking load for most specimens tested by Boswell (2008) and Kreisa (2008) was approximately 1.5 times the Design Wheel Load ($1.5P_L$). For the specimen tested in this phase of the investigation, the cracking load was slightly lower, approximately $0.9P_L$. This is likely due to the lower concrete compressive strength at testing, as well as a slightly thinner “bridge deck” of specimen P30P3, when compared to the specimens tested by Boswell (2008) and Kreisa (2008). For the previously tested specimens, the maximum applied load was about $4P_L$ for the 45° specimens and only $2.4P_L$ for the 30° specimens. The maximum load was believed to have been limited in the 30° specimens due to delamination of the precast panel from the cast-in-place topping slab. Tests conducted on the 30° specimen in this phase of the investigation resulted in a maximum applied load of $3.7P_L$, which better agrees with the capacities of previously tested specimens that did not experience delamination. Thus, delamination, and not the skew angle, was the limiting factor on specimen capacity.

For load applied at midspan of the square end, data implied a cracking load of approximately $1.5P_L$ to $2P_L$ for the specimens tested by Boswell (2008) and Kreisa (2008). In this phase of the investigation, panel A was tested at midspan of the square end and was shown to have a slightly lower cracking load of $1.2P_L$. For the previously tested specimens, the maximum applied load was $5.6P_L$ for the 45° specimens and $4P_L$ for the 30° specimens that experienced delamination. Panel A achieved a maximum applied load of $5.4P_L$ when loaded at the square end, which more closely resembles the capacities of previously tested specimens that did not fail in delamination.

Because delamination of the panel from the topping slab was avoided, only two failure modes were identified in the response of the specimen tested herein. Both 30°

panels failed in shear at the short side support when load was applied to midspan of the skewed end and punching shear failure occurred when panel A was loaded at midspan of the square end.

Table 5.4 - Summary of Response of Specimen P30P3

	Panel		
	A		B
	Test on Skewed End	Test on Square End	Test on Skewed End
Cracking Load, P_{CR} (kip)	20	25	18
P_{CR}/P_W	1.3	1.6	1.1
P_{CR}/P_L	0.9	1.2	0.8
P_{CR}/P_U	0.5	0.7	0.5
Maximum Applied Load, P_{MAX} (kip)	79	115	79
P_{MAX}/P_W	4.9	7.2	4.9
P_{MAX}/P_L	3.7	5.4	3.7
P_{MAX}/P_U	2.1	3.1	2.1

Chapter 6: Discussion of Results

6.1 INTRODUCTION

The experimental results presented in Chapter 5 are summarized and discussed in this chapter. Results from tests in which load was applied at midspan of the skewed end are considered first, followed by a discussion of the results from the test that applied load at midspan of the square end. Comparisons to the tests conducted by Boswell (2008) and Kreisa (2008), as well as those conducted by Agnew (2007), are made in Appendix B and are referenced throughout this chapter. Recommendations for the application of skewed precast panels in bridge deck construction are given last.

6.2 SUMMARY

To investigate the use of precast panels as stay-in-place formwork adjacent to expansion joints in bridge deck construction, TxDOT has funded two projects over the past nine years. The first project was TxDOT Project 0-4418, in which full-scale bridge decks were constructed using precast panels with a 0° skew. The results of testing indicated that using precast panels as stay-in-place formwork for a cast-in-place topping slab provided sufficient strength, reduced construction costs, and improved worker safety when compared with the traditional cast-in-place details at the expansion joint. Further discussion on Project 0-4418 can be found in Chapter 2.

The second project, TxDOT Project 0-5367, was completed in three phases. First, Agnew (2007) tested the precast panel system at the expansion joint in non-skewed bridges subjected to fatigue loading. Testing of the 0° specimens indicated that the performance of the precast panel system was more than adequate for service-level fatigue loading. In the next phase of the project, Boswell (2008) and Kreisa (2008) tested the response of the precast panel system at expansion joints in skewed bridges subjected to both static and fatigue loading. Using precast panels with 30° and 45° skews, five specimens were constructed and tested. All specimens were loaded at midspan of the

skewed end and some were also loaded at midspan of the square end, for a total of nine tests. Chapter 2 discusses the first two phases of Project 0-5367 in further detail.

In this investigation, the third phase of TxDOT Project 0-5367, tests were conducted on the precast panel system at expansion joints in skewed bridges subject to static loading. Due to the delamination experienced by the 30° specimens previously tested by Boswell (2008) and Kreisa (2008), the skew angle of 30° was again considered. Two panels, A and B, were included in specimen P30P3 and subjected to a total of three tests. Load was first applied at midspan of the skewed end of each panel, followed by loading at midspan of the square end of panel A. Response to loading of the skewed end is summarized in Section 6.2.1 and Section 6.2.2 summarizes the specimen response when load was applied at the square end.

6.2.1 Load Applied At Midspan of Skewed Ends

The deck exhibited similar responses when load was applied at midspan of the skewed ends. Relative load-displacement plots are provided in Figure 6.1 and significant observations from the skewed end response are listed below:

- The average relative deflection at midspan of the skewed end under the Design Wheel Load (P_L) was about 1/16 in., which corresponds to approximately $L/1800$ for a 9-ft clear span between girder flanges.
- Maximum applied loads were 3.7 times the Design Wheel Load, or $3.7P_L$. Recall that in previous testing of 30° specimens, the capacity was limited by delamination of the panels from the cast-in-place topping slabs, resulting in a maximum applied load of approximately $2.4P_L$ (Boswell 2008, Kreisa 2008). The capacity of the 30° specimen tested in this phase of the investigation was better correlated with those of the 45° specimens tested by Boswell (2008) and Kreisa (2008), which did not experience delamination and reached a maximum applied load of about $4P_L$ (Figure B.4).

- The surface roughness, as well as the moisture content, of the panels prior to placing the topping slab significantly improved the overall strength of the test specimen, when compared to previous tests conducted on 30° specimens. Whereas the 30° panels tested by Boswell (2008) and Kreisa (2008) had a rather smooth surface and were not wetted immediately prior to placement of the topping slab, the 30° specimen tested in this investigation had a very rough surface texture that was pre-wetted before the topping slab was placed. While the initial stiffnesses were comparable (Figure 6.2), the 30° specimens tested by Boswell (2008) and Kreisa (2008) failed in delamination at only $2.4P_L$. The pre-wetted, rough-textured 30° specimen tested herein failed in shear at $3.7P_L$, which better correlates with the ultimate strength and failure mode of previously tested 0° and 45° specimens (Figures B.2 and B.4).

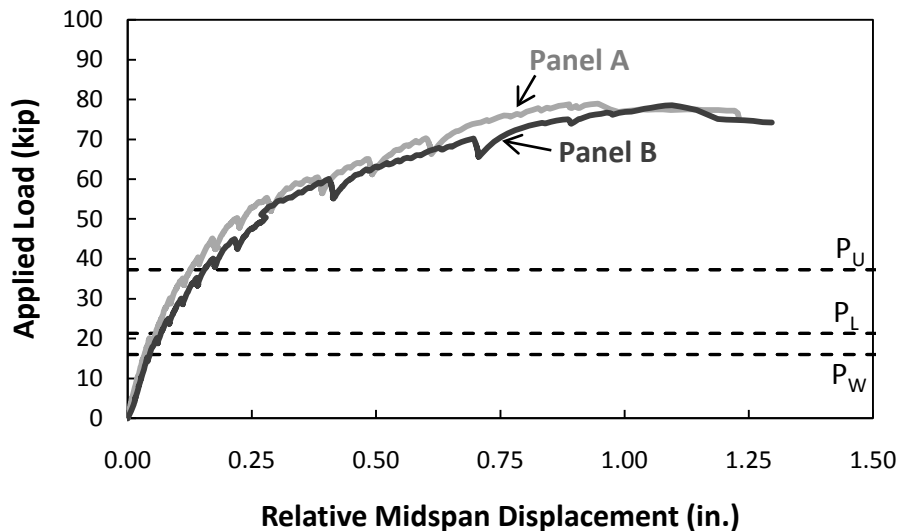


Figure 6.1 – Measured Displacement Response for Load Applied at Midspan of Skewed Ends of Specimen P30P3

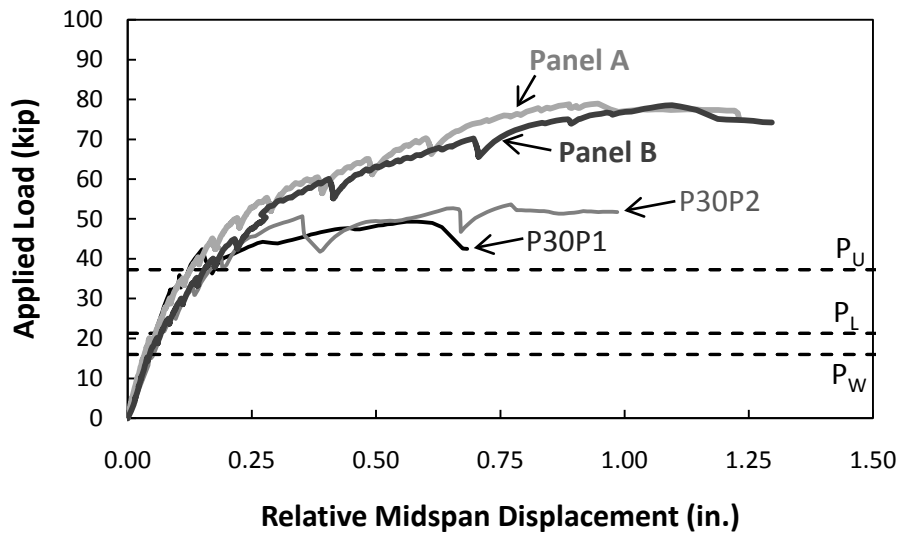


Figure 6.2 – Measured Displacement Responses of Specimen P30P3 Compared to Previously Tested 30° Specimens (Boswell 2008, Kreisa 2008)

A comparison of the compressive strains at midspan of the SEJ, for all 30° specimens tested to date, is provided in Figure 6.3. Much larger compressive strains were reached in the specimen that did not experience delamination.

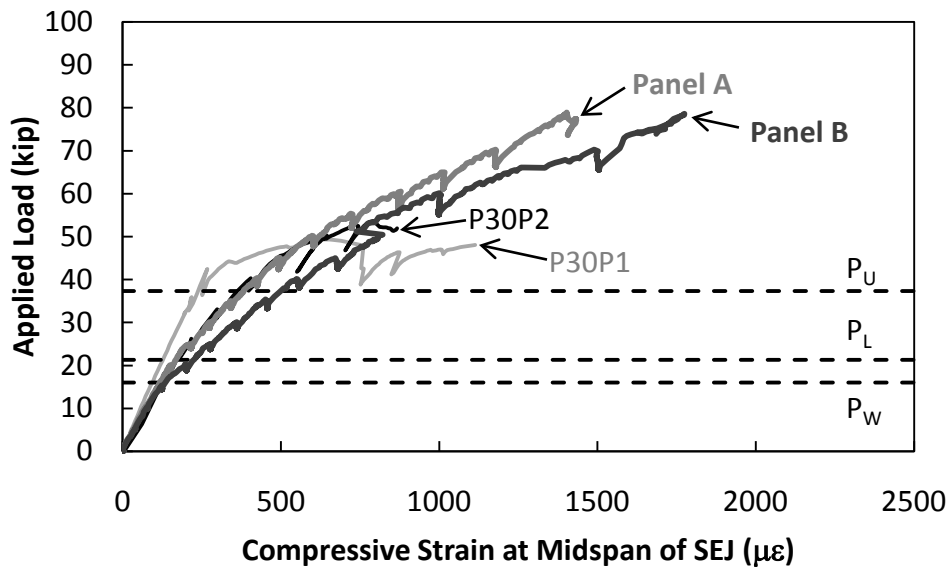


Figure 6.3 – Measured Compressive Strains in Specimen P30P3 at Midspan of SEJ Compared to Previously Tested 30° Specimens (Boswell 2008, Kreisa 2008)

The response of all 30° specimens tested to date is compared with the 0° specimens subjected to positive moment (Agnew, 2007) in Figure B.2. At failure, slightly greater loads and displacements were achieved in the 0° specimens, although the overall response is essentially the same for all specimens that did not experience delamination.

The compressive strains at midspan of the SEJ are provided for the previously tested 0° specimens and all of the 30° specimens tested to date in Figure B.3. The overall responses of the specimens were basically the same until delamination occurred in specimens P30P1 and P30P2. With the exception of specimen P30P1, the SEJ strains in the 30° specimens were slightly greater than the SEJ strains in the 0° specimens for a given level of axial load.

The relative displacement responses for specimen P30P3 are compared to those of all of the specimens tested by Boswell (2008) and Kreisa (2008) in Figure B.4. While the initial stiffness of all specimens is comparable, the strength of the 30° specimens that experienced delamination was significantly less than the other specimens. The response of panels A and B, in which delamination did not occur, was much better correlated with the 45° specimens. The compressive strains at midspan of the SEJ are compared to those of the 45° specimens in Figure B.5. Although the general response is similar, the 30° specimen tested herein underwent larger SEJ strains at a given axial load than the 45° specimens.

6.2.2 Load Applied At Midspan of Square End

After being loaded to failure at midspan of the skewed end, panel A was loaded at midspan of the square end. The relative displacement response is given in Figure 6.4 and important observations from the test are summarized below:

- Despite the damage induced during the previous test, the maximum applied load at midspan of the square end ($5.4P_L$) exceeded the capacity of the skewed end ($3.7P_L$). Recall that for the tests conducted by Boswell (2008) and Kreisa (2008), the capacities of the square ends

were $5.6P_L$ for the 45° specimen and only about $4P_L$ for the 30° specimens that failed in delamination (Table B.7). Figure B.6 provides a comparison of the square-end loading of panel A with the tests conducted by *Bowell (2008)* and *Kreisa (2008)* in which load was applied at midspan of the square end.

- The maximum applied load at midspan of the square end was limited by a punching shear failure. This was also true for all previously tested specimens loaded at midspan of the square end.
- Consistent with previous testing, the punching shear strength of panel A was not limited by the non-prestressed corner of the skewed panel.

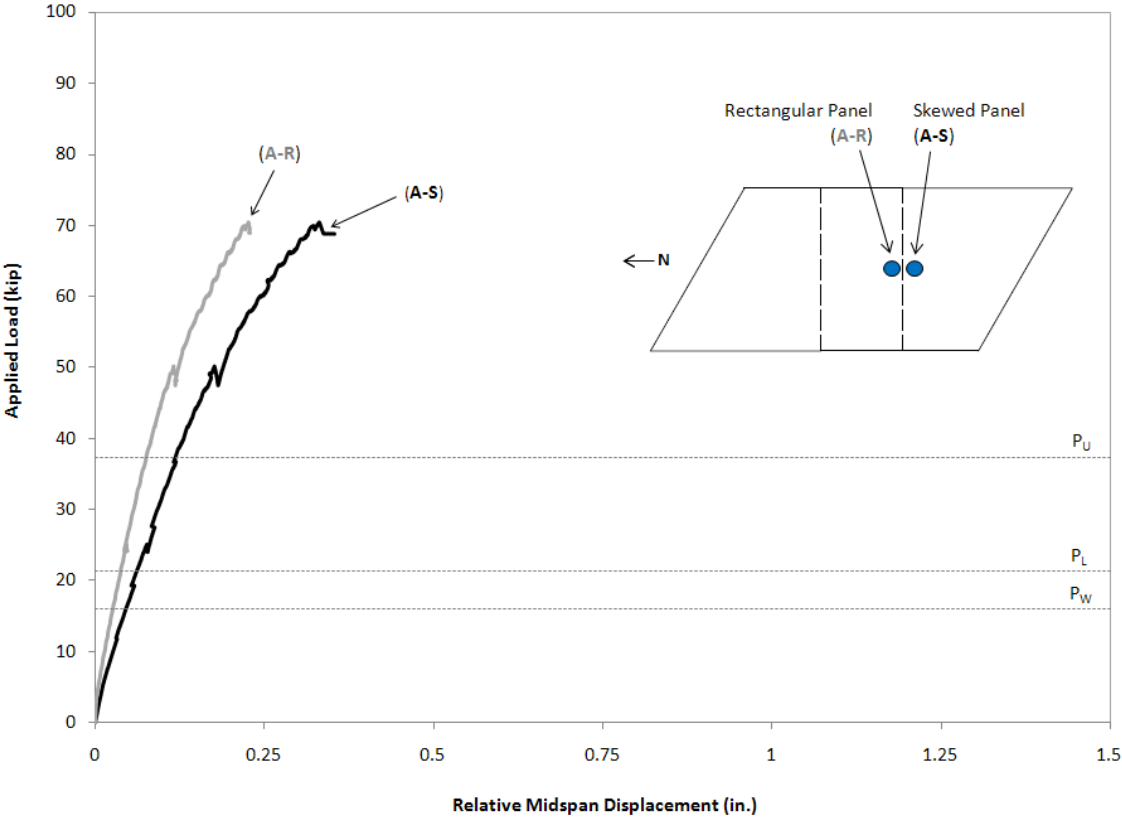


Figure 6.4 – Measured Displacement Response of Panel A for Load Applied at Midspan of Square End

6.3 RECOMMENDATIONS

The results of this and previously conducted research indicate that the precast panel system provides sufficient strength and stiffness for use adjacent to expansion joints in bridge deck construction. Furthermore, the response of skewed panels was similar to the response of non-skewed specimens when load was applied at midspan near the expansion joint. For current fabrication practices, trapezoidal precast panels are easier to produce in prestressing beds with the strands running parallel to the skewed end. While this results in a non-prestressed corner at the square edge, testing shows that neither strength nor stiffness is sacrificed. As prestressing beds have a standard width of 8 ft., production of trapezoidal panels with strands parallel to the skew is limited to a skew angle of 30°, although panels with a skew angle as large as 45° were tested in TxDOT Project 0-5367 and may be used with confidence.

While all tested specimens provided sufficient strength, the maximum load-carrying capacity of precast panel systems will be limited if the panels delaminate from the cast-in-place topping slab. True composite action of the bridge deck is necessary to achieve the designed behavior. Since composite action is only accomplished when horizontal shear forces can effectively be transferred between the topping slab and precast panel, it is crucial to ensure adequate surface roughness and moisture content on the precast panel surface prior to placing the topping slab. It is recommended that precast panels have a “rake” finish to achieve a ¼ in. typical surface roughness. To ensure this, it may be necessary to control flooding of the panels immediately after finishing, as is typically done to promote curing. Once the precast panels have been placed on site, it is also recommended that they be pre-wetted to a saturated, surface dry (SSD) condition prior to placement of the cast-in-place topping slab, in an effort to minimize the amount of water being pulled out of the fresh concrete by the otherwise dry panels.

Chapter 7: Conclusions and Recommendations

The results of testing were presented and discussed in Chapters 5 and 6, respectively, and are compared to previous testing in Appendix B. Concluding thoughts about the use of trapezoidal precast panels as stay-in-place forming adjacent to skewed expansion joints in bridge deck construction are presented in this chapter.

7.1 SUMMARY

For nearly three decades, TxDOT has used prestressed precast concrete panels as stay-in-place formwork for bridge deck production to speed up construction while reducing costs. At expansion joints, TxDOT has conventionally used a thickened bridge deck, known as the “IBTS” detail as a slab end diaphragm. This detail requires additional forming, which can become particularly complicated at skewed expansion joints, and creates a hazardous work environment for construction workers high above the ground. In the first two phases of TxDOT Project 0-5367, the response of rectangular and skewed precast panels adjacent to the expansion joint when subjected to static and fatigue loading was investigated. While testing of the 0° and 45° panels demonstrated that sufficient system stiffness and reserve capacity was provided, premature failure by delamination occurred during the testing of the 30° panels. It was thought that the delamination occurred due to the relatively smooth surface texture of the panels prior to placement of the topping slab, which limited the amount of horizontal shear stress that could be transferred from the topping slab to the precast panel. The purpose of this research was to reinvestigate the response of 30° skewed precast panels under static loading using panels with much rougher surface texture, in an effort to demonstrate that the lack of surface roughness, and not the skew angle, was the cause of the limited capacity in the delaminated specimens.

Representing the rear axle load from the HL-93 Design Truck, two precast panels (A and B) were subject to static point loads at midspan of the skewed end that generated positive moments in the bridge deck. Both panels were first loaded at midspan of the skewed end, which contained a sealed expansion joint (SEJ); panel A was then loaded at

midspan of the square end of the trapezoidal panel, which was adjacent to a rectangular panel.

7.2 CONCLUSIONS

Results of testing indicate that skewed precast panels used as stay-in-place forming adjacent to expansion joints provide ample stiffness and reserve capacity above design loads, provided that adequate precast panel surface roughness and surface moisture are provided prior to placement of the topping slab. Observations from this research are summarized as follows:

- Response of Specimens for Load Applied at Midspan of Skewed End
 - When sufficient panel surface roughness and moisture content was provided prior to placement of the topping slab, the skewed panels demonstrated stiffness and strength similar to previously tested rectangular panels, even though the unsupported end length was longer in the skewed specimens. To avoid premature failure in delamination, it is recommended that precast panel fabricators take care to ensure a surface texture of approximately ¼ in., which can be accomplished by applying a rake finish to the freshly placed panel concrete. It may also be necessary for the fabricator to forgo or postpone flooding of the prestressing bed to ensure that the surface texture remains intact. Once the precast panels are in place on site, TxDOT specifications require that they be wetted to a saturated surface dry condition to prevent the panels from drawing moisture out of the freshly placed topping slab.
 - Failing in diagonal shear at the short side support, specimens tested at midspan of the skewed end achieved ultimate loads that were 3.7 times greater than Design Wheel Load (P_L) for the HL-93 Design Truck.
- Response Under Load Applied at Midspan of Square End

- A larger ultimate load was reached in panel A when loaded at midspan of the square end ($5.4P_L$) than when loaded at midspan of the skewed end ($3.7P_L$). Whereas failure occurred in shear at the short side support when loaded at midspan of the skewed end, the maximum load was limited by punching shear failure when load was applied at midspan of the square end.
- The stiffness and ultimate punching shear strength at the square end was not limited by the non-prestressed corner of the square end of the skewed panel. Strands in the non-prestressed corner were debonded because they were too short to develop the prestressing force; the short strands resulted from fabrication of trapezoidal panels with strands running parallel to the skewed end.

Figure 7.1 provides the recommended trapezoidal precast panel for use adjacent to the expansion joint in bridge decks, as determined by the TxDOT report that summarized the testing and recommendations of Project 0-5367 (TxDOT Report No. FHWA/TX-09/0-5367-1: Recommendations for the Use of Precast Deck Panels at Expansion Joints, 2008). Further recommendations regarding panel fabrication and installation are outlined below:

- Precast Panel Fabrication Recommendations
 - Texture panel surface by applying a rake finish to provide a roughness of approximately $\frac{1}{4}$ in. Maintain the surface roughness during curing. Roughness may be reduced during flooding of the prestressing bed.
- Precast Panel Installation Recommendations
 - Support panel sides on bedding strips with a compressive strength of at least 60 psi prior to placement of the topping slab. Using material of adequate strength minimizes compression of

the bedding strips, which in turn helps ensure that concrete will flow under the sides of the panels and provide a uniform bearing surface for the composite deck after the topping slab is placed. The problem of crushing the bedding strips is most acute at the support of the short side of a trapezoidal panel. Care should also be taken to ensure proper consolidation of the topping slab concrete.

- Before placing the topping slab, wet the precast panels to a saturated surface dry condition to prevent the panels from drawing moisture out of the freshly placed topping slab.

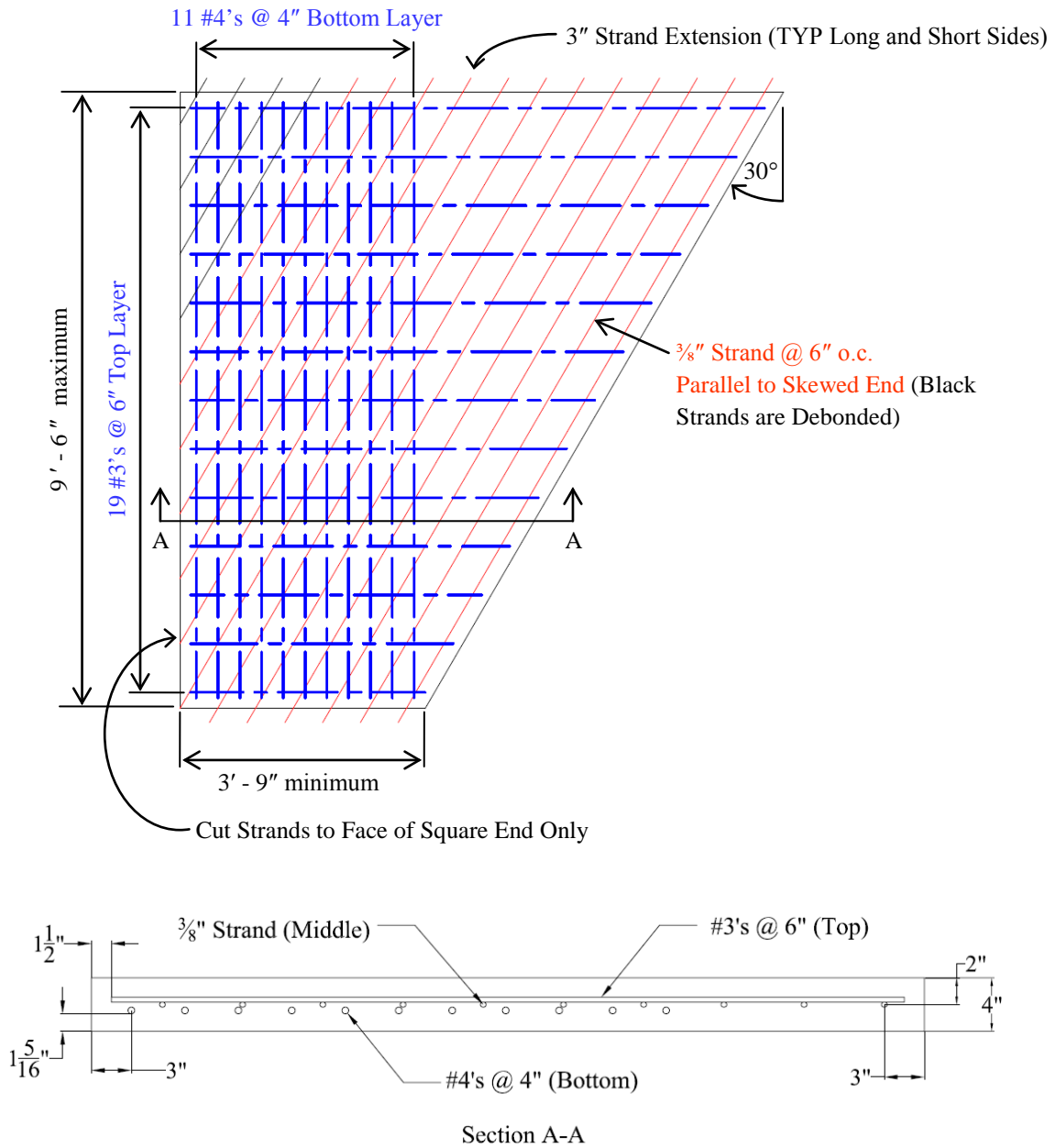


Figure 7.1 – Recommended 30° Skew Panel Ordinary Reinforcing Layout and Detail (modified from TxDOT Report No. FHWA/TX-09/0-5367-1: Recommendations for the Use of Precast Deck Panels at Expansion Joints, 2008)

Appendix A: Complete Set of Test Data

The measured responses of specimen P30P3 are summarized in Chapter 5. All of the measured data are plotted in this appendix, organized by panel.

A.1 PANEL A

Panel A was statically loaded, first at midspan of the skewed end and then at midspan of the square end. Data from the skewed end loading include displacements, tensile strains on the bottom of the precast concrete panel, and compressive strains on the top surface of the SEJ. After loading the skewed end to failure, the bottom surface of the panel was significantly cracked, thus the square end was not instrumented with strain gages for the second test. For this reason, the only data gathered during loading of the square end were the displacements. Data for load applied to the skewed end are provided first, followed by the data for load applied on the square end.

A.1.1 Load Applied at Midspan of Skewed End

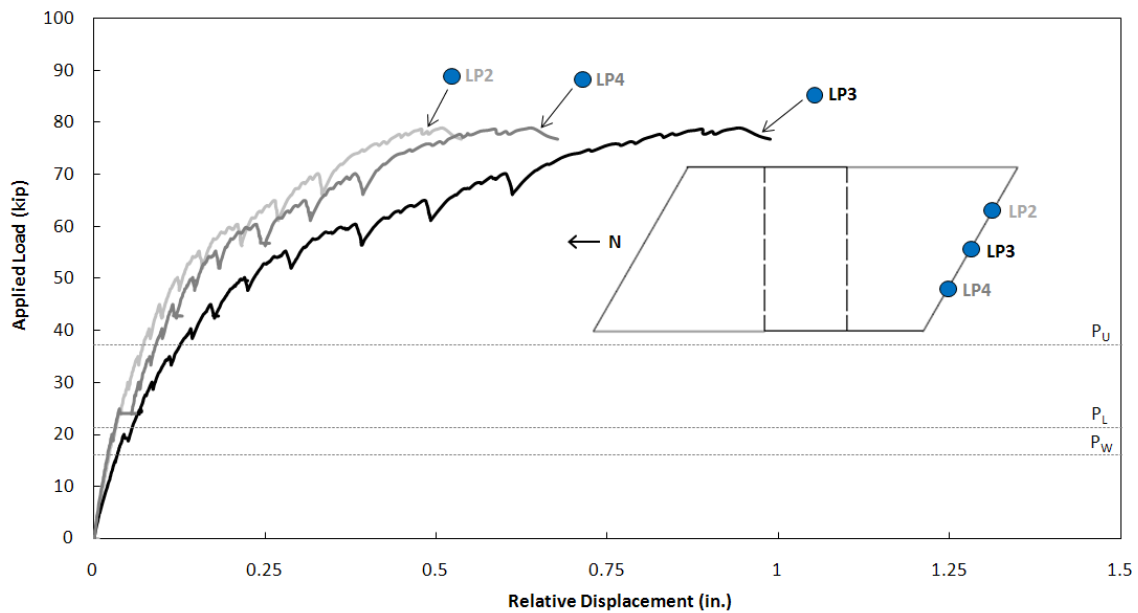


Figure A.1 – Measured Relative Displacements along Skewed End of Panel A

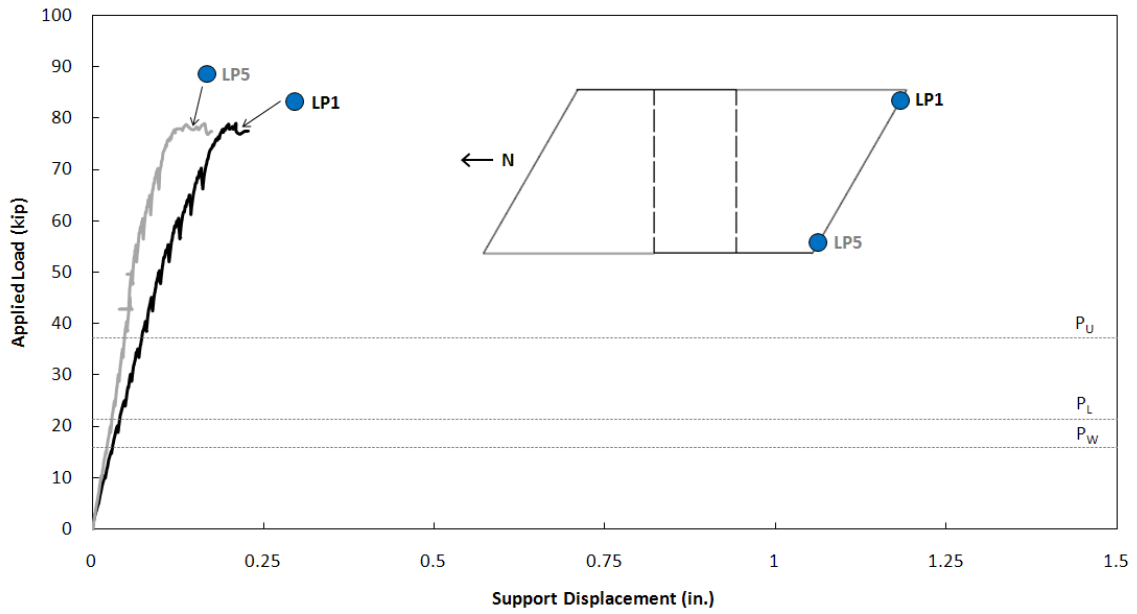


Figure A.2 – Measured Support Displacements of Panel A Loaded at Midspan of Skewed End

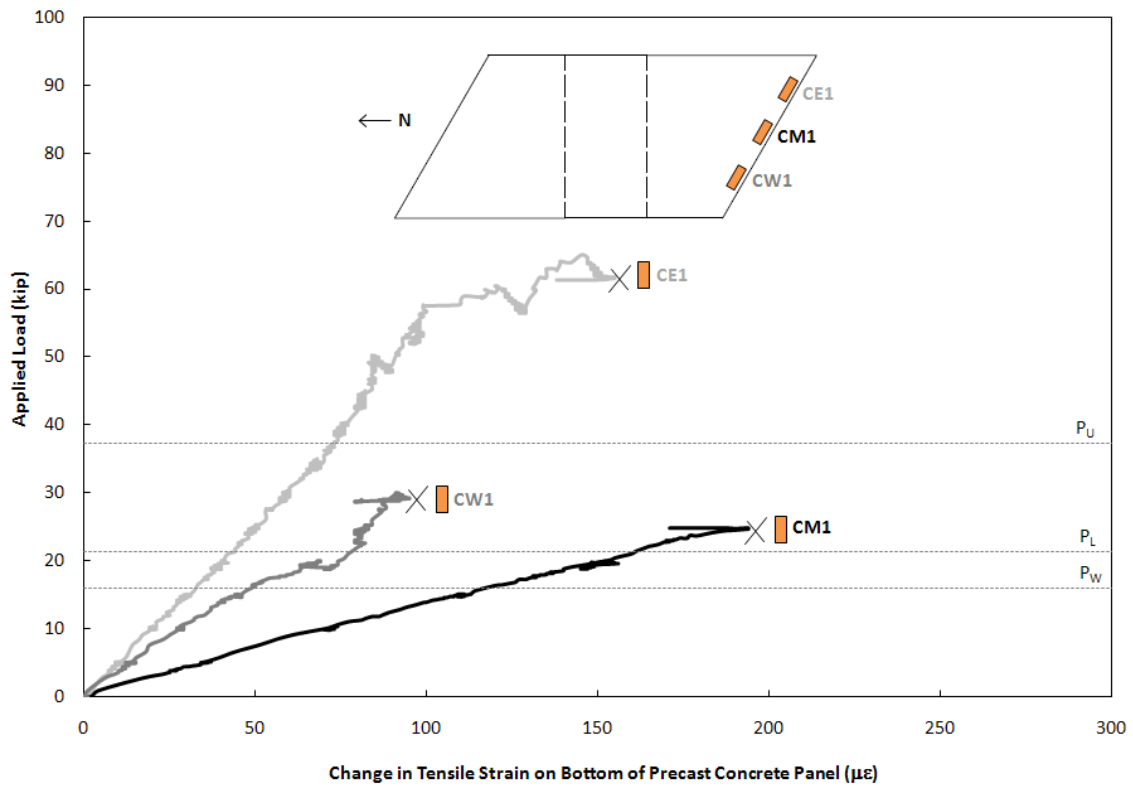


Figure A.3 – Measured Change in Tensile Strains on Bottom of Panel A for Load Applied at Midspan of Skewed End

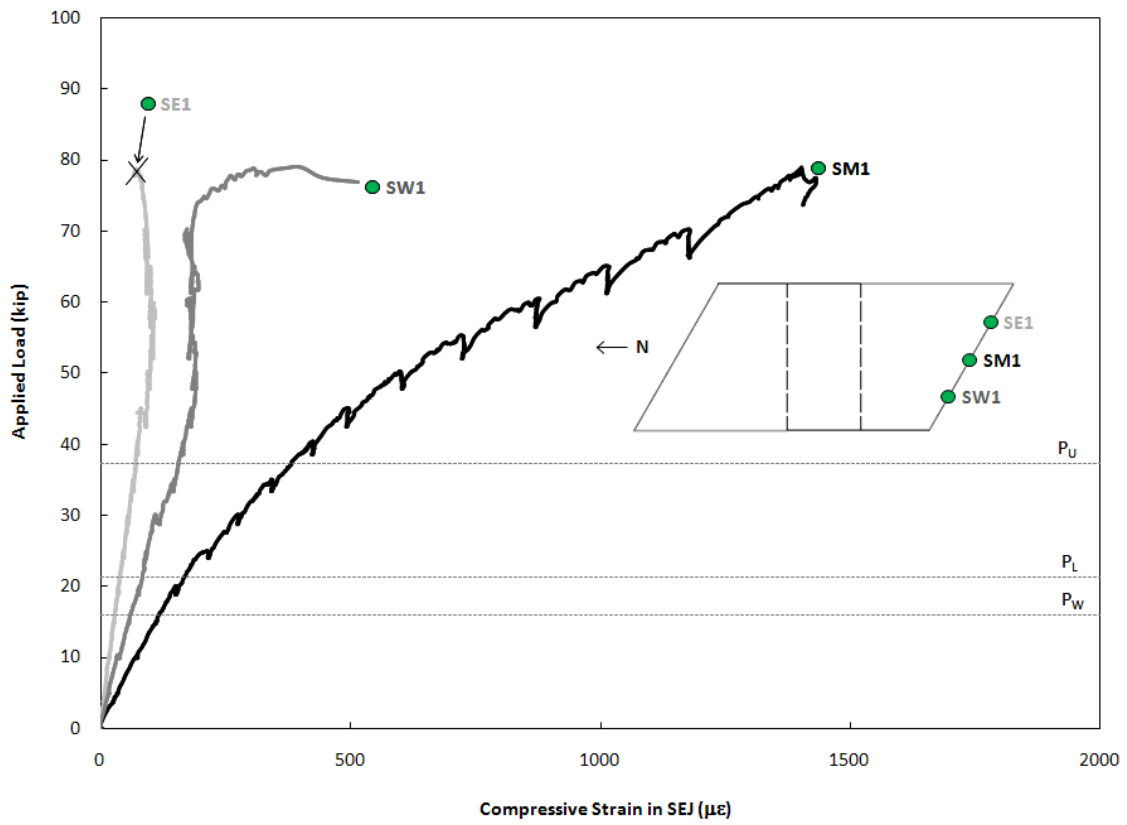


Figure A.4 – Measured Compressive Strains in SEJ of Panel A for Load Applied at Midspan of Skewed End

A.1.2 Load Applied at Midspan of Square End

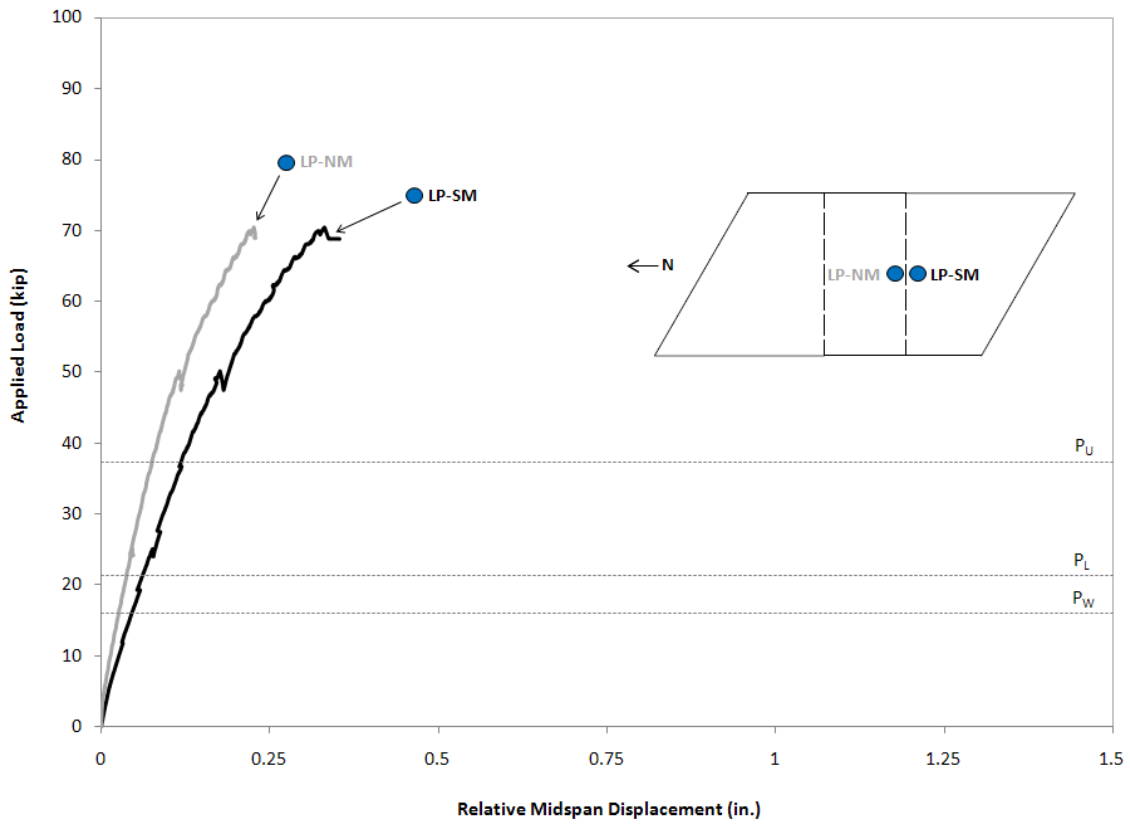


Figure A.5 – Measured Relative Displacements of Panel A for Load Applied at Midspan of Square End

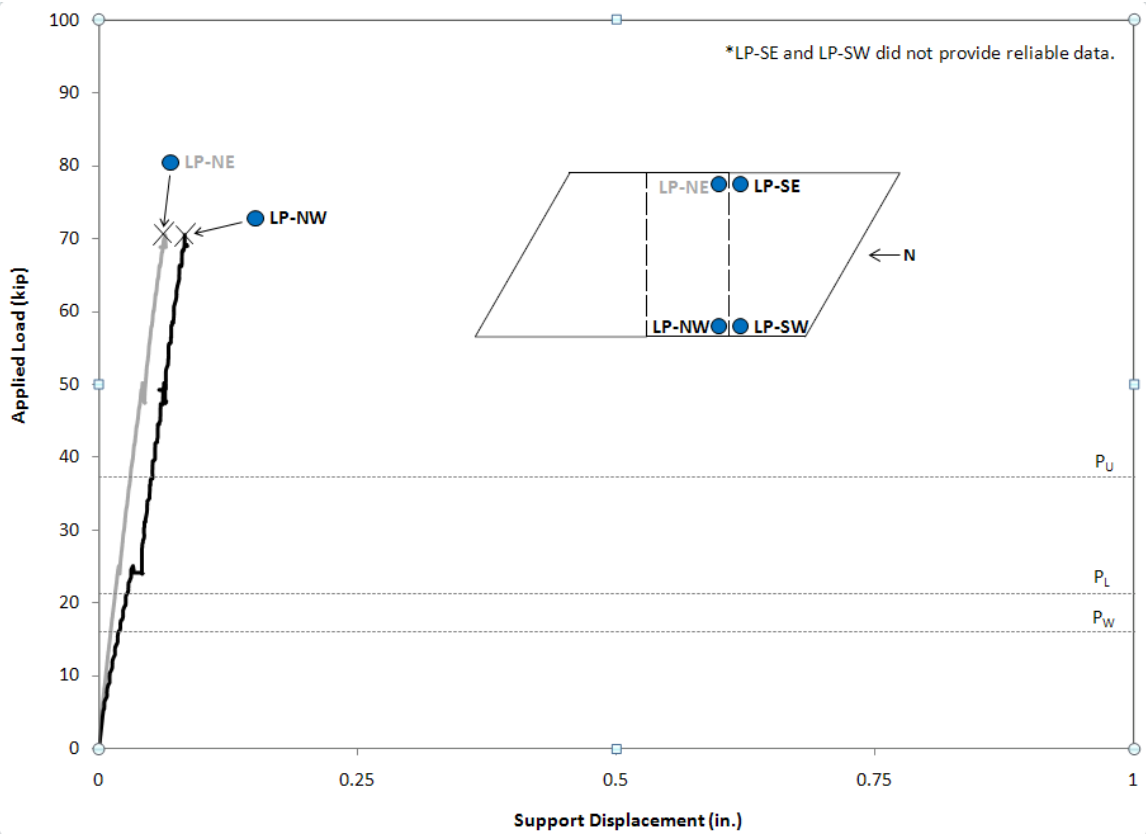


Figure A.6 – Measured Support Displacements of Panel A for Load Applied at Midspan of Square End

A.2 PANEL B

Panel B was statically loaded at midspan of the skewed end only. Data from this skewed end loading include displacements, tensile strains on the bottom of the precast concrete panel, and compressive strains on the top surface of the SEJ.

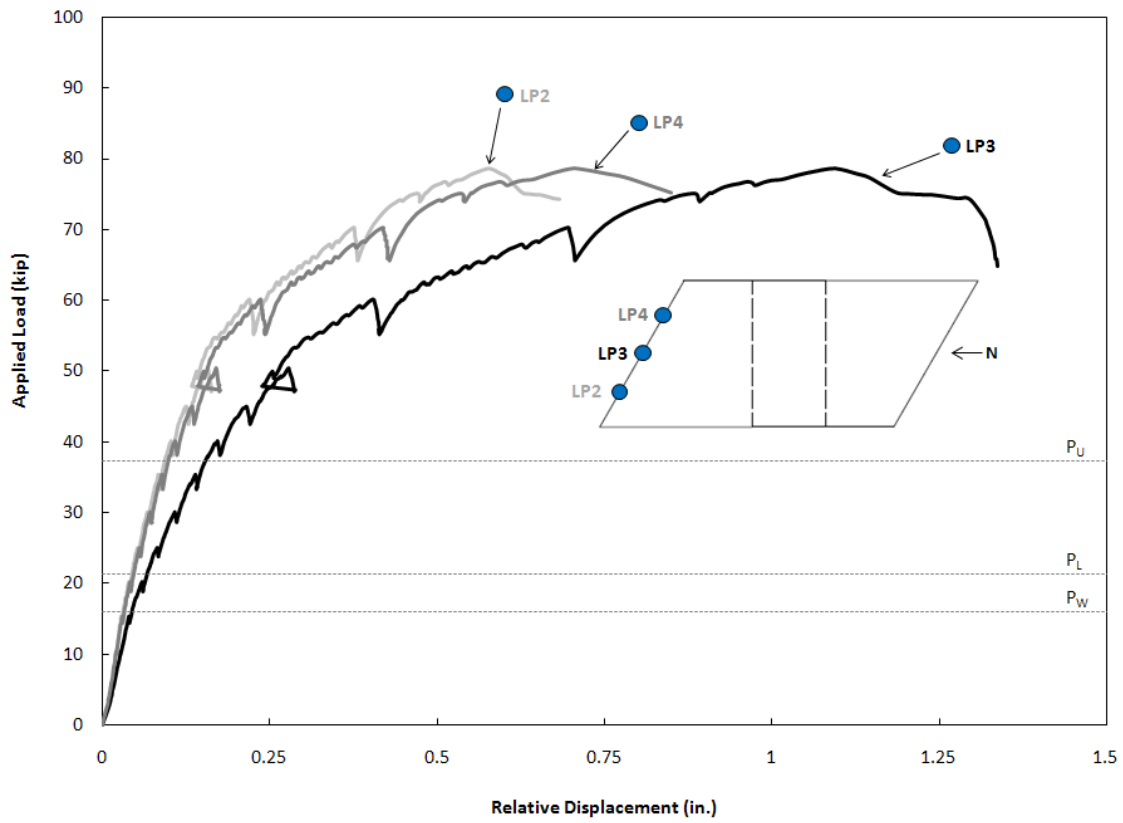


Figure A.7 – Measured Relative Displacements of Panel B for Load Applied at Midspan of Skewed End

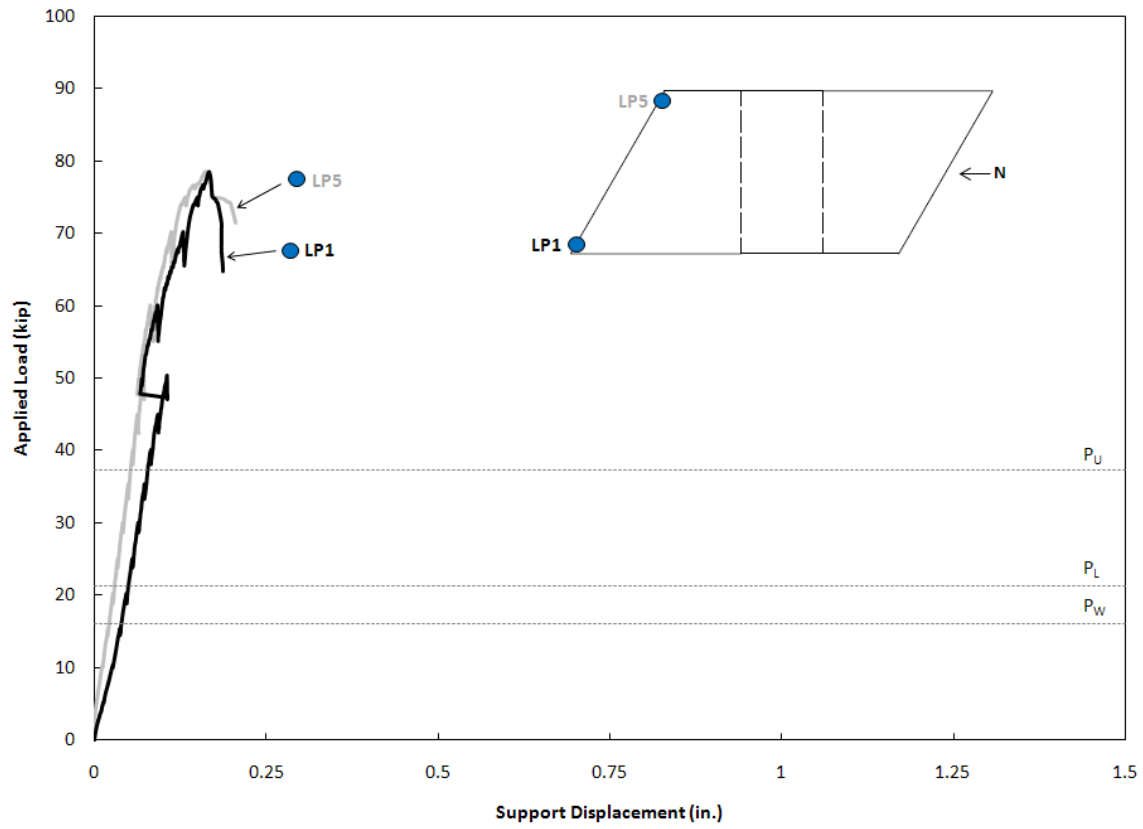


Figure A.8 – Measured Support Displacements of Panel B for Load Applied at Midspan of Skewed End

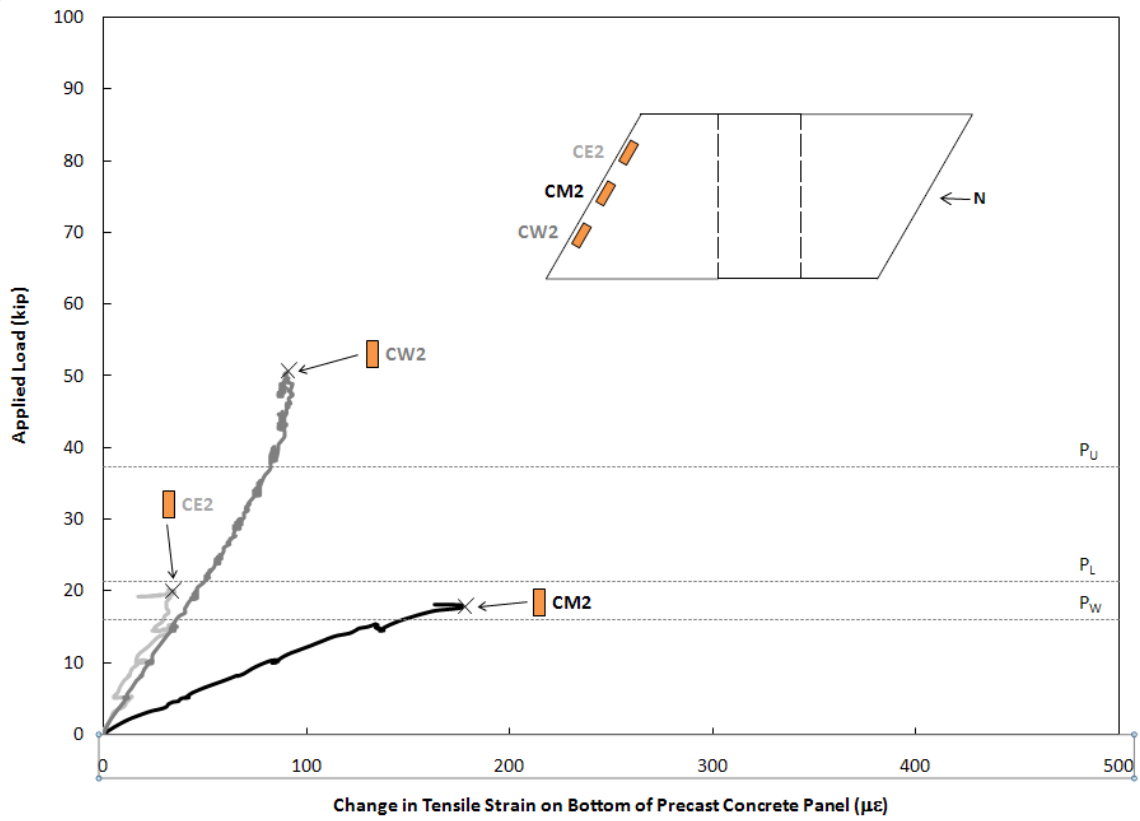


Figure A.9 – Measured Change in Tensile Strains on Bottom of Panel B for Load Applied at Midspan of Skewed End

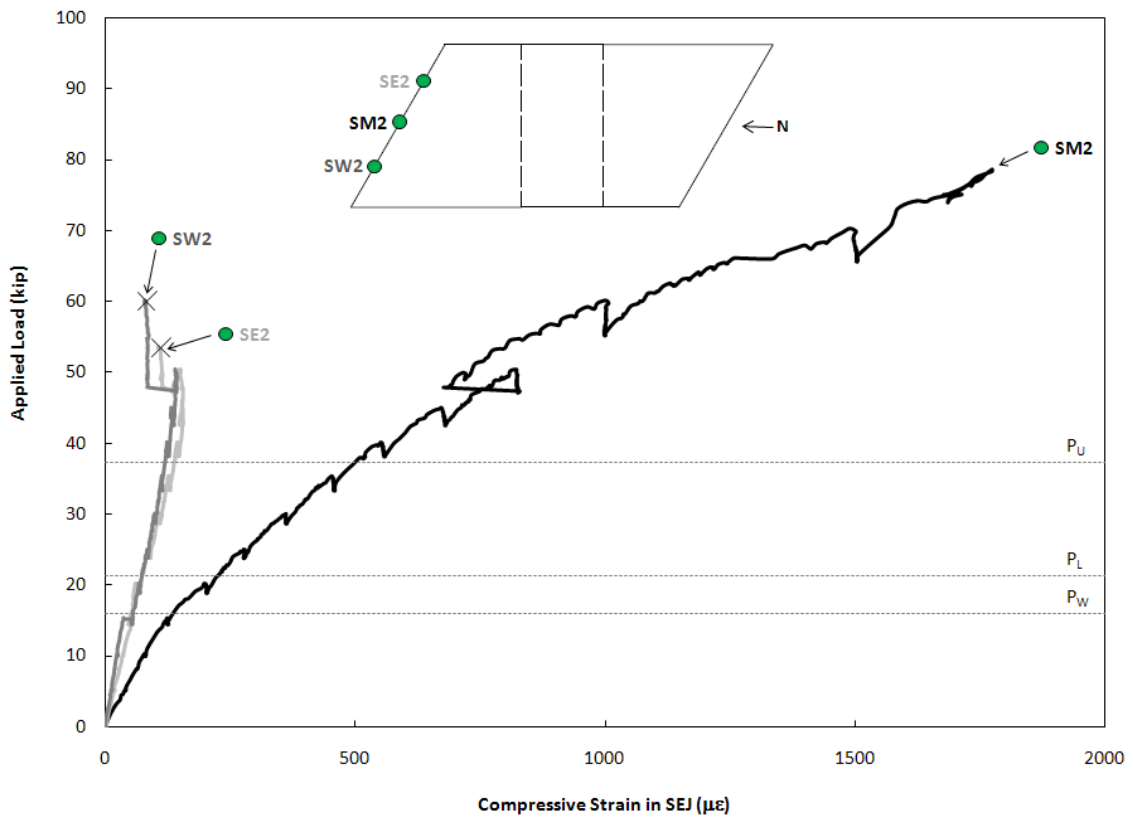


Figure A.10 – Measured Compressive Strains in SEJ of Panel B for Load Applied at Midspan of Skewed End

Appendix B: Summary of Specimens Tested in TxDOT Project 0-5367

In the first phase of TxDOT Project 0-5367, Agnew (2007) tested specimens with 0° skew to better understand the behavior of bridge deck construction that uses precast panels as stay-in-place forming. Boswell (2008) and Kreisa (2008) tested specimens with 45° and 30° skew ends for the second phase of Project 0-5367. The basis of this thesis is the third phase of Project 0-5367, in which a specimen with 30° skew ends was again considered. Because this phase of the investigation was initiated after delamination occurred in previously tested 30° specimens, this appendix provides information about the specimens tested by Boswell (2008) and Kreisa (2008) that can be compared to panels A and B tested in this phase of the project (Chapters 3 thru 6). A description of the previously tested specimens is presented first in Section B.1, followed by loading information in Section B.2, and the measured response of the tested specimens in Section B.3. Finally, a comparison of all of the specimens tested in Project 0-5367 is given in Section B.4.

B.1 DESCRIPTION OF SPECIMENS TESTED BY BOSWELL (2008) AND KREISA (2008)

A summary of the characteristics of the specimens tested in the second phase of Project 0-5367 is provided in Table B.1. Refer to Table 3.1 for the characteristics of panels A and B, tested in this phase of the investigation.

Table B.1 – Characteristics of Skewed Specimens Tested by Boswell (2008) and Kreisa (2008)

	Specimen				
	P45P1	P45P2	P45P3	P30P1	P30P2
Skew Angle	45°	45°	45°	30°	30°
No. of Panels	1	2	2	2	2
Skewed Panel Strand Pattern	Fanned	Parallel to Skew	Parallel to Skew	Parallel to Skew	Parallel to Skew
Skewed Panel Fabrication Site	FSEL	FSEL	FSEL	Off-Site	Off-Site
Long Beam Length	14' - 6"	18' - 6"	17' - 3"	13' - 3"	13' - 3"
Long Beam Cross Section	12" x 12"	12" x 12"	12" x 12"	16" x 12"	12" x 12"
Short Beam Length	5' - 0"	9' - 0"	7' - 9"	7' - 9"	7' - 9"
Short Beam Cross Section	12" x 12"	12" x 12"	12" x 12"	16" x 12"	12" x 12"
Beam Clear Spacing	9' - 0"	9' - 0"	9' - 0"	9' - 0"	9' - 0"
Bedding Strip Type	Foamular Rigid Foam Insulation	Dow Styrofoam Highload 40	Dow Styrofoam Highload 40	Dow Styrofoam Highload 40	Dow Styrofoam Highload 40
Bedding Strip Strength	25 psi	40 psi	40 psi	40 psi	40 psi

B.1.1 Material Properties

This section presents the material characteristics of the specimens tested by Boswell (2008) and Kreisa (2008), including the compressive strength of the topping slab at the time of testing and the amount of compression experienced by the bedding strips.

B.1.1.1 Concrete

For the specimens tested in the second phase of Project 0-5367, the compressive strength of the cast-in-place topping slab at the time of testing is provided in Table B.2 below. It should be noted that although the same concrete design mix was specified (Table 3.2), these strengths are higher than the compressive strength of the topping slab in specimen P30P3 (4880 psi).

Table B.2 – Concrete Cylinder Strengths for Topping Slabs at 21-days (Boswell 2008, Kreisa 2008)

	Specimen				
	P45P1	P45P2	P45P3	P30P1	P30P2
Topping Slab 21-Day Strength (psi)	5088	7236	NA	7316*	7316*

* Topping slabs for Specimens P30P1 and P30P2 were placed at the same time

B.1.1.2 Bedding Strip Material

Throughout Project 0-5367, there was an issue with excessive compression of the bedding strips under the weight of the precast panels, topping slab, and test loads. For the tests conducted by Bowell (2008) and Kreisa (2008), the type and compressive strength of the bedding strip was varied, although it was found that none of the materials provided sufficient compressive strength and in all cases, the bridge deck exceeded the design thickness of 8 in. once the topping slab was placed (Table B.3). For this phase of the investigation, specimen P30P3 was constructed using a bedding strip with a higher compressive strength than was previously used (Table 3.1), which resulted in the target bridge deck of 8 in.

Table B.3 – Average Overall Slab Depth at Midspan of Skewed End (Boswell 2008, Kreisa 2008)

	Specimen				
	P45P1	P45P2	P45P3	P30P1	P30P2
Overall Depth at Load Point	8-3/4"	8-3/4"	8-1/2"	8-1/4"	8-1/8"

B.1.2 Specimen Construction

This section provides information about the construction of specimens tested by Boswell (2008) and Kreisa (2008), including precast panel conditions prior to topping slab placement and a construction and testing timeline.

B.1.2.1 Precast Panel Conditions Prior to Topping Slab Placement

An important factor in the performance of a composite bridge deck is the condition of the precast panels prior to topping slab placement. This section provides a summary of the surface roughness and moisture content of the previously tested precast panels immediately before the cast-in-place topping slab was placed (Table B.4). As delamination occurred in the 30° specimens tested by Boswell (2008) and Kreisa (2008), special care was taken to ensure adequate surface roughness and moisture content for the precast panels used in specimen P30P3 for this phase of Project 0-5367. A general timeline for construction and testing of the specimens investigated by Bowell (2008) and Kreisa (2008) is also provided in Table B.5.

Table B.4 – Panel Surface Roughness and Wetness before Topping Slab Placement
(Boswell 2008, Kreisa 2008)

	Specimen				
	P45P1	P45P2	P45P3	P30P1	P30P2
Relative Panel Surface Roughness	Rough	Rough	Rough	Smooth	Smooth
Panel Surface Moisture Content	Dry	Wet	Wet	Dry	Dry

Table B.5 – Timeline of Specimen Construction and Testing
(Boswell 2008, Kreisa 2008)

	Specimen				
	P45P1	P45P2	P45P3	P30P1	P30P2
Date Panel Cast	9/7/2007	1/10/2008	1/31/2008	11/6/2007	11/6/2007
Date Deck Cast	9/20/2007	1/29/2008	2/20/2008	11/27/2007	11/27/2007
Date of First Test	10/12/2007	2/26/2008	3/19/2008	12/18/2007	12/19/2007
Date of Second Test	N/A	2/26/2008	4/17/2008	12/18/2007	12/19/2007

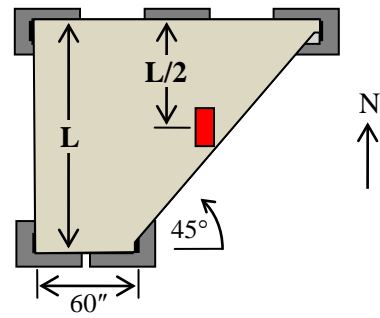
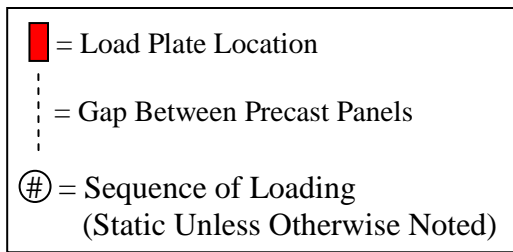
B.2 LOADING INFORMATION FOR SPECIMENS TESTED BY BOSWELL (2008) AND KREISA (2008)

This section provides a summary of the loading type and sequence of loading for the specimens tested by Boswell (2008) and Kreisa (2008) in Table B.6 and Figure B.1. It should be noted that fatigue loading of specimen P45P3 did not significantly affect the

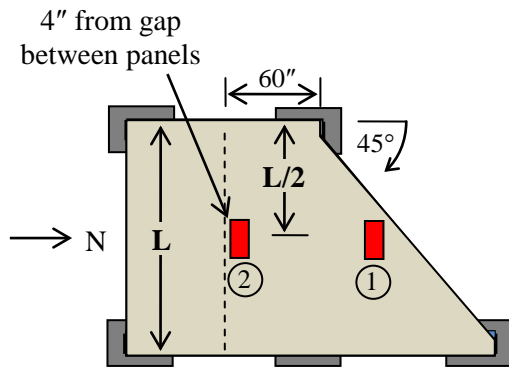
stiffness of the specimen. For this reason, specimen P30P3 was only subjected to monotonically increasing static loads (Table 4.1 and Figure 4.3).

Table B.6 – Applied Loads to Specimens Tested by Boswell (2008) and Kreisa (2008)

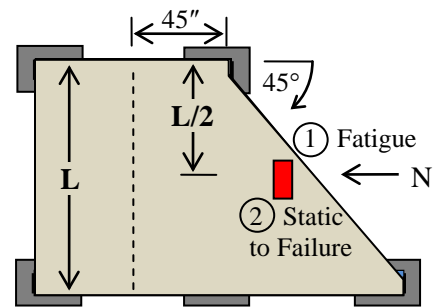
	Specimen				
	P45P1	P45P2	P45P3	P30P1	P30P2
No. of Tests	1	2	2	2	2
Test 1 Location	Skewed End	Skewed End	Skewed End	Skewed End	Skewed End
Test 1 Type	Static	Static	Fatigue	Static	Static
Test 2 Location	N/A	Square End	Skewed End	Square End	Square End
Test 2 Type	N/A	Static	Static	Static	Static
Test 3 Type	N/A	N/A	N/A	N/A	N/A
Date of Test 1	10/12/2007	2/26/2008	3/19/2008	12/18/2007	12/19/2007
Date of Test 2	N/A	2/26/2008	4/17/2008	12/18/2007	12/19/2007



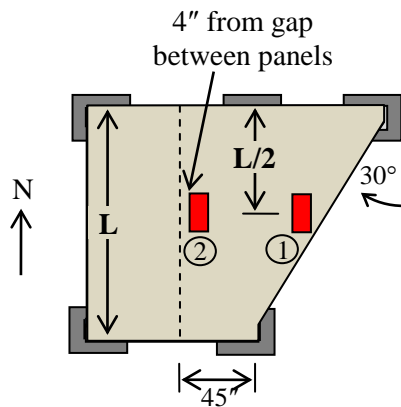
Specimen P45P1
(Fanned Strands)



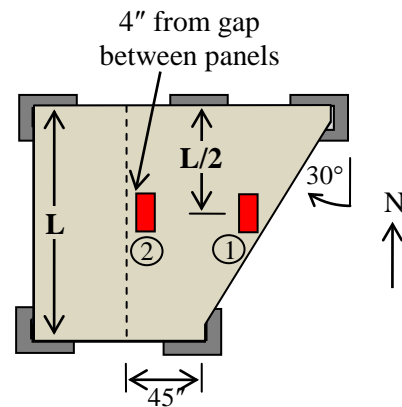
Specimen P45P2
(Parallel Strands)



Specimen P45P3
(Parallel Strands)



Specimen P30P1
(Parallel Strands)



Specimen P30P2
(Parallel Strands)

Figure B.1 – Location of Load Plates and Order of Loading for Specimens Tested by Boswell (2008) and Kreisa (2008)

B.3 MEASURED RESPONSE OF SPECIMENS TESTED BY BOSWELL (2008) AND KREISA (2008)

For the specimens tested in the second phase of Project 0-5367, a summary of the specimen response to test loads is provided in Table B.7. A comparison can be made to specimen P30P3 by referring to Table 5.4.

Table B.7 - Summary of Response of Specimens Tested by Boswell (2008) and Kreisa (2008)

		Specimen				
		P45P1	P45P2	P45P3	P30P1	P30P2
Skewed End	Cracking Load, P_{CR} (kip)	33	32	32	32	26
	P_{CR}/P_W	2.1	2.0	2.0	2.0	1.6
	P_{CR}/P_L	1.5	1.5	1.5	1.5	1.2
	P_{CR}/P_U	0.9	0.9	0.9	0.9	0.7
	Maximum Applied Load, P_{MAX} (kip)	83	89	81	49	54
	P_{MAX}/P_W	5.2	5.6	5.1	3.1	3.4
	P_{MAX}/P_L	3.9	4.2	3.8	2.3	2.5
	P_{MAX}/P_U	2.2	2.4	2.2	1.3	1.4
Square End	Cracking Load, P_{CR} (kip)	-	40	-	27	45
	P_{CR}/P_W	-	2.5	-	1.7	2.8
	P_{CR}/P_L	-	1.9	-	1.3	2.1
	P_{CR}/P_U	-	1.1	-	0.7	1.2
	Maximum Applied Load, P_{MAX} (kip)	-	120	-	87	84
	P_{MAX}/P_W	-	7.5	-	5.4	5.3
	P_{MAX}/P_L	-	5.6	-	4.1	3.9
	P_{MAX}/P_U	-	3.2	-	2.3	2.3

B.4 COMPARISON OF ALL SPECIMENS TESTED IN TXDOT PROJECT 0-5367

This section presents a comparison of all of the specimens tested throughout the duration of Project 0-5367, including the specimens with 0° skew tested by Agnew (2007), the specimens with 45° and 30° skew tested by Boswell (2008) and Kreisa (2008), and the 30° specimen tested in this phase of the investigation.

B.4.1 Load Applied At Midspan of End Adjacent to SEJ

Figure B.2 provides a comparison of the load-displacement responses of the 0° and 30° specimens subjected to load at midspan of the end with the sealed expansion joint (SEJ). For the 30° specimens, the end adjacent to the SEJ was skewed, whereas this end was square in the 0° specimens. Note that specimens P30P1 and P30P2, tested by Boswell (2008) and Kreisa (2008) experienced delamination and failed at much lower loads than panels A and B. Specimen P30P3 demonstrated behavior very similar to the rectangular specimens tested by Agnew (2007).

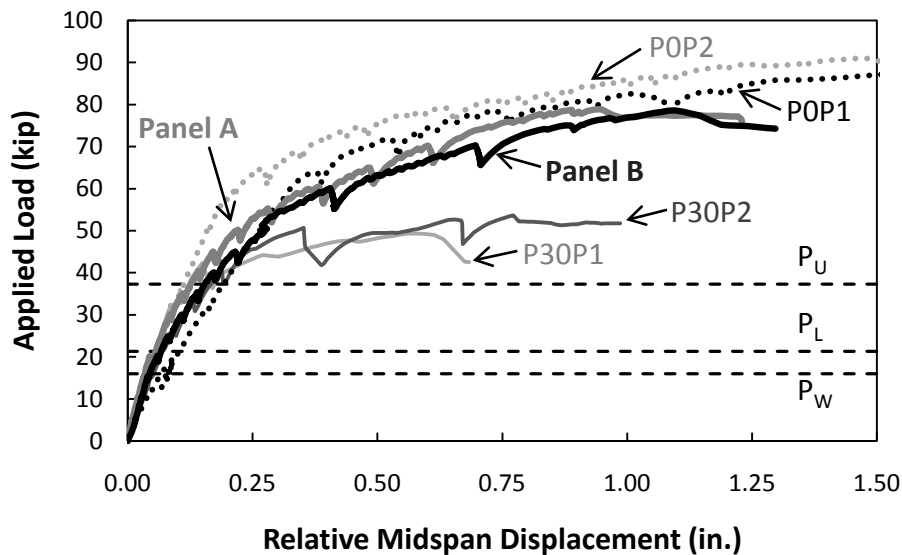


Figure B.2 – Measured Displacement Responses of Specimen P30P3 Compared to Previously Tested 0° (Agnew 2007) and 30° Specimens (Boswell 2008, Kreisa 2008)

The delamination failure experienced by the 30° specimens tested previously is also reflected in the load-SEJ strain plot provided in Figure B.3. Panels A and B did not experience delamination and were able to achieve compressive strains in the SEJ that were much closer to those achieved in the rectangular specimens.

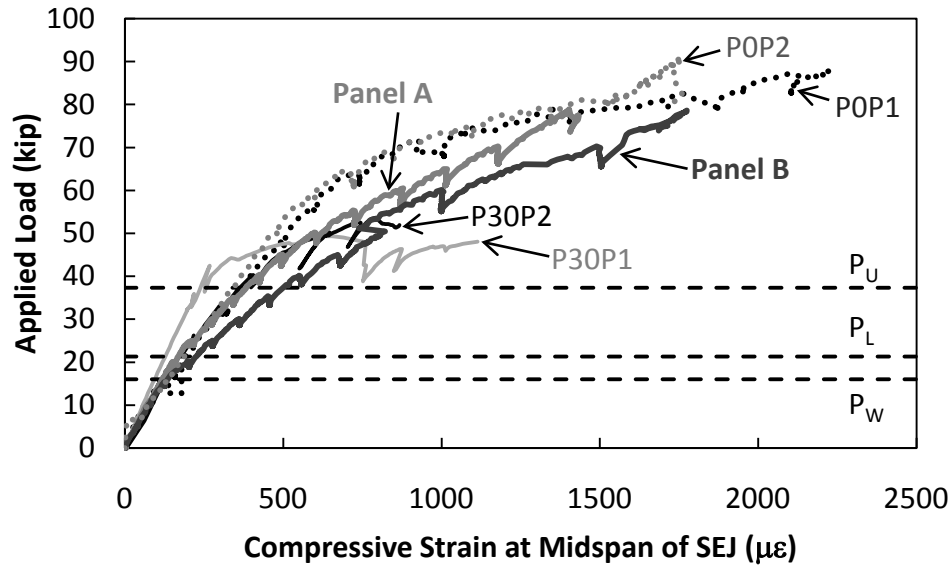


Figure B.3 – Measured Compressive Strains in Specimen P30P3 at Midspan of SEJ Compared to Previously Tested 0° (Agnew 2007) and 30° Specimens (Boswell 2008, Kreisa 2008)

Comparing the load-displacement responses of all specimens tested in the second and third phases of Project 0-5367 (Figure B.4) further illustrates that fact that delamination, and not skew angle, was the factor that limited capacity for the 30° specimens tested by Boswell (2008) and Kreisa (2008). Although the specimens that failed by delamination failed at loads slightly greater than the factored wheel load (P_U), the reserve capacity is much greater in the specimens that did not fail prematurely due to delamination. Systems with greater reserve capacity are always preferred in conservative design. Load-SEJ strain responses are also provided for panels A and B, tested in this phase of the project, and the 45° specimens tested previously, in Figure B.5. Overall, panels A and B were able to achieve SEJ strains similar to the 45° specimens.

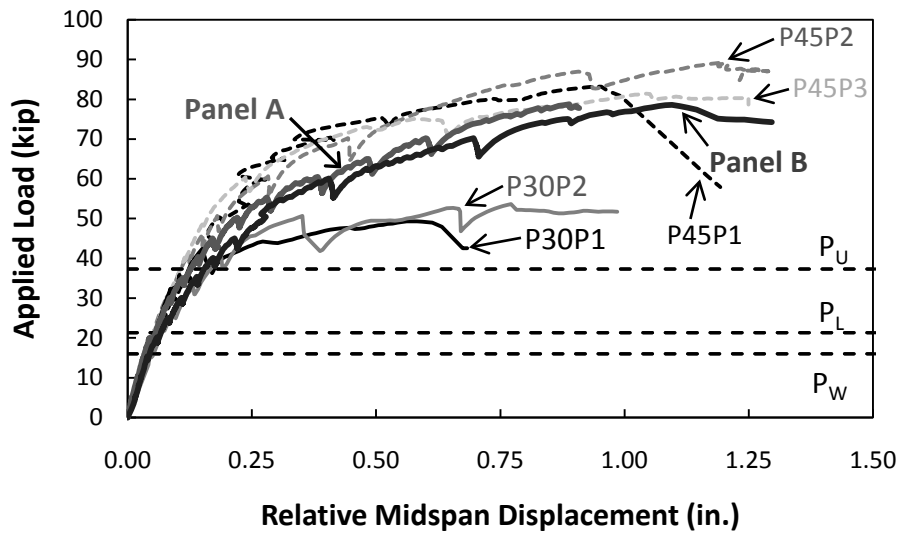


Figure B.4 – Measured Displacement Responses of Specimen P30P3 Compared to Previously Tested 45° and 30° Specimens (Boswell 2008, Kreisa 2008)

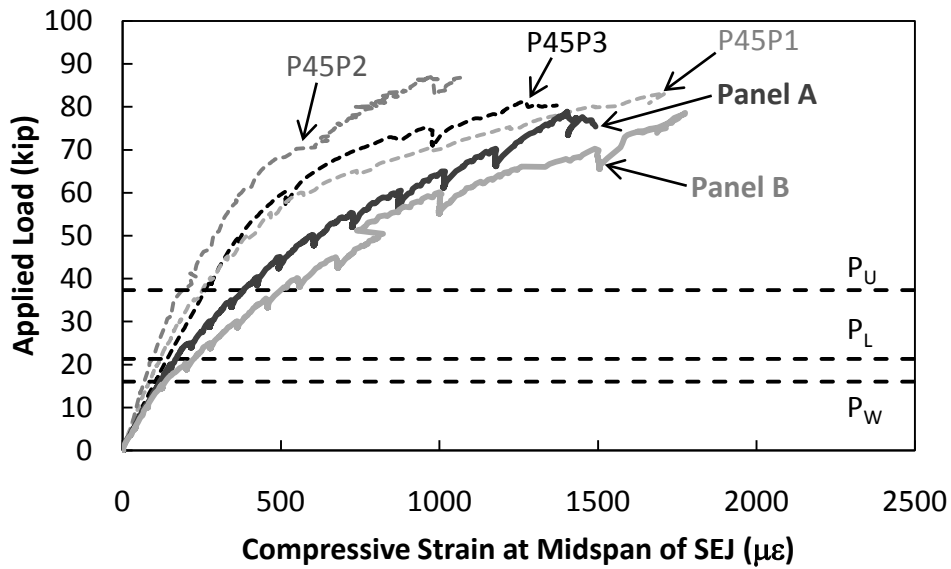


Figure B.5 – Measured Compressive Strains in Specimen P30P3 at Midspan of SEJ Compared to Previously Tested 45° Specimens (Boswell 2008, Kreisa 2008)

B.4.2 Load Applied At Midspan of Square End of Skewed Specimens

This section compares the responses of skewed specimens when loaded at midspan of the square end, which did not contain a sealed expansion joint. All of the specimens loaded at midspan of the square end were first loaded to failure at midspan of the skewed end. Due to the significant cracking caused by the previous loading of panel A at midspan of the skewed end, the response of the square end of the skewed panel (A-S) was less stiff than the response of the rectangular panel (A-R), as shown in Figure B.6. For all specimens loaded at midspan of the square end, the response was generally similar (Figure B.7) and failure always occurred in punching shear at load levels of at least 3.9 times the design wheel load ($3.9P_L$). The 30° panels that had previously failed in delamination at the skewed end were only able to achieve $3.9P_L$ to $4.1P_L$ when loaded at the square end, whereas panel A achieved $5.4P_L$ before failing in punching shear at the square end. This better correlates to the $5.6P_L$ achieved by specimen P45P1 when loaded at midspan of the square end.

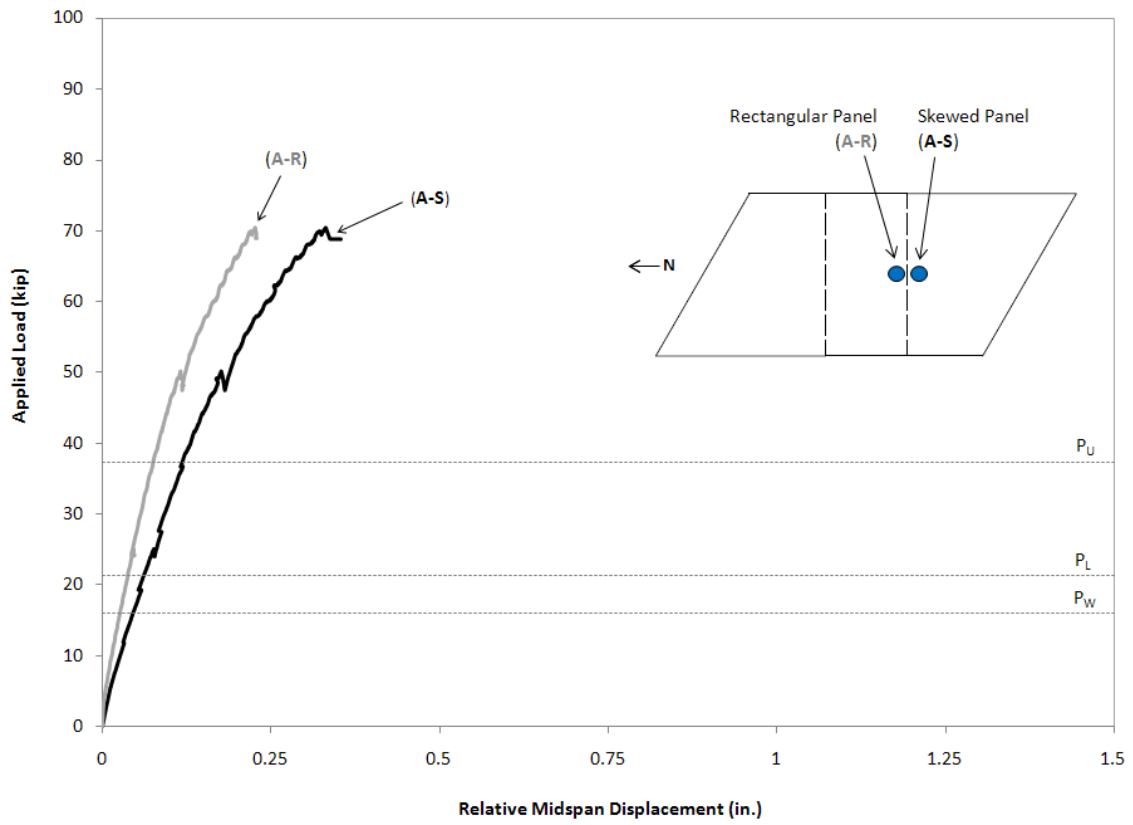


Figure B.6 – Measured Displacement Response of Panel A for Load Applied at Midspan of Square End

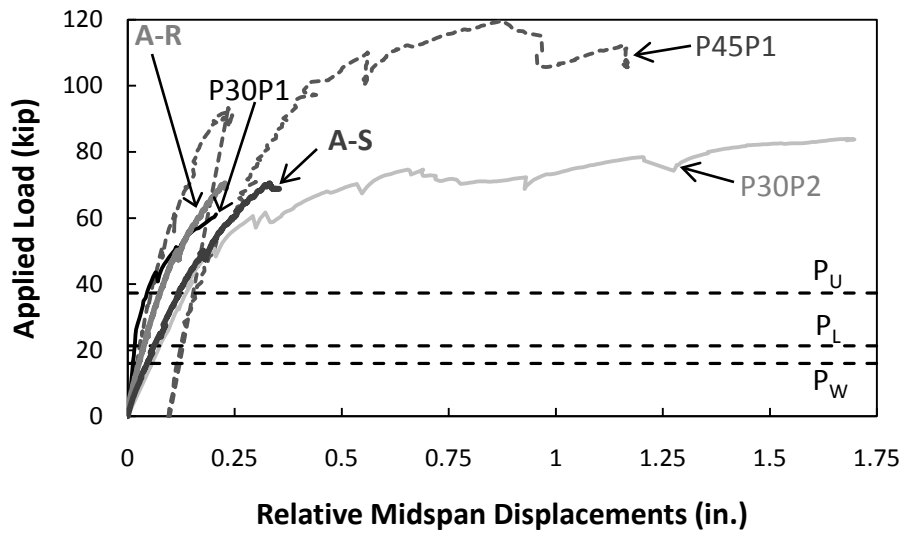


Figure B.7 – Measured Displacement Responses of All Skewed Specimens Loaded at Midspan of Square End

References

Abendroth, R. E. (1994). Deformations in Composite Prestressed Concrete Bridge Deck Panels. *Journal of Structural Engineering* , Vol. 120, No. 11.

Agnew, L. S. (2007). *Evaluation of the Fatigue Behavior of Bridge Decks with Precast Panels at Expansion Joints*. Austin, TX: The University of Texas at Austin.

Barker, J. M. (1975). Research, Application, and Experience with Precast Prestressed Bridge Deck Panels. *PCI Journal* , Vol. 20, No. 6.

Boswell, C. A. (2008). *Simple Design Details using Precast Concrete Panels at Skewed Expansion Joints*. Austin, TX: The University of Texas at Austin.

Coselli, C. J. (2004). *Behavior of Bridge Decks with Precast Panels at Expansion Joints*. Austin, TX: The University of Texas at Austin.

Dowell, R. K., & Smith, J. W. (2006). Structural Tests of Precast, Prestressed Concrete Deck Panels for California Freeway Bridges. *PCI Journal* , March-April, 2-13.

Kreisa, A. R. (2008). *Constructability of Prestressed Concrete Panels for Use at Skewed Expansion Joints*. Austin, TX: The University of Texas at Austin.

Merrill, B. D. (2002). *Texas' Use of Precast Concrete Stay-in-Place Forms for Bridge Decks*. Austin, TX: Texas Department of Transportation.

Ryan, J. L. (2003). *Zero-Skew Bridge Deck Behavior at Expansion Joints*. Austin, TX: The University of Texas at Austin.

TxDOT. (2008, May). "Prestressed Concrete Panels". *Detail of Standard Drawings* . Retrieved from:
<ftp://ftp.dot.state.tx.us/pub/txdot-info/cmd/cserve/standard/bridge/pcpstde1.pdf>.

TxDOT. (2008, November). "TxDOT Report No. FHWA/TX-09/0-5367-1". *Recommendations for the Use of Precast Deck Panels at Expansion Joints*. Austin, TX: Center for Transportation Research.

Van Landuyt, D. (2006, September). "Survey of Skew Angles of TxDOT Bridges". Austin, TX: Results presented at research project meeting.